

Abteilung Molekulare Botanik

(Leiter: Prof. Dr. Axel Brennicke)

Universität Ulm

**The role of Cyclic Nucleotide-Gated Channels  
(CNGC) in plant development and stress  
responses in *Arabidopsis thaliana***

**Dissertation**

zur Erlangung des akademischen Grades (Dr. rer. nat.)

an der Fakultät für Naturwissenschaften

der Universität Ulm

vorgelegt von  
Sabine Frietsch  
aus Schramberg

2006

Amtierender Dekan der Fakultät für Naturwissenschaften:

Prof. Dr. Klaus-Dieter Spindler

Erstgutachter:

PD Dr. Stefan Binder, Abteilung Molekulare Botanik, Universität Ulm

Zweitgutachter:

Prof. Dr. Axel Brennicke, Abteilung Molekulare Botanik, Universität Ulm

Drittgutachter:

Prof. Dr. Jeffrey F. Harper, Department of Biochemistry, University of Nevada,  
Reno, USA

Datum der Promotion: 24. April 2006

# Contents

<b>1</b>	<b>Introduction .....</b>	<b>1</b>
1.1	The family of Cyclic Nucleotide-Gated Channels (CNGCs).....	1
1.2	Ion signaling during fertilization in plants.....	3
1.3	Objective of the study.....	4
<b>2</b>	<b>Material and Methods.....</b>	<b>5</b>
2.1	Plant material .....	5
2.2	Bacterial strains.....	5
2.3	Vectors .....	5
2.4	Oligonucleotides.....	5
2.5	Plant growth conditions .....	8
2.5.1	Standard MS media (half strength).....	8
2.5.2	Modified plant growth media for phenotypic analysis .....	9
2.6	Solutions and buffers.....	10
2.6.1	Pollen germination media (Fan et al., 2001).....	10
2.6.2	Alexander staining solution .....	11
2.6.3	Solutions for $\beta$ -glucuronidase activity staining.....	11
2.7	Microscopy .....	12
2.8	Software and websites used .....	13
2.9	Molecular biological standard methods .....	14
2.10	Isolation of T-DNA insertion lines .....	14
2.11	Phenotypic analysis of homozygous T-DNA insertion lines.....	14
2.12	Plasmid constructs and transformation .....	15
2.13	Characterization of a male gametophytic phenotype.....	16
2.13.1	Basta spray-application for selection of plants grown in soil .....	16
2.13.2	Complementation of <i>cngc18-1</i> plants transformed with <i>gCNGC18</i> (ps# 632) or <i>ACA9promoter::i-GFP-CNGC18</i> (ps# 855) .....	17
2.13.3	Pollen tube germination and imaging of pollen expressing GFP constructs.....	17
2.13.4	Histochemical pollen viability staining .....	18
2.14	Histochemical staining of a promoter::GUS activity.....	18
2.15	Inductively coupled plasma spectroscopy (ICP).....	19
<b>3</b>	<b>Results .....</b>	<b>20</b>
3.1	Phenotypic analysis under abiotic and biotic stress conditions .....	20
3.2	CNGC18 is essential for pollen tube growth.....	22
3.2.1	<i>cngc18</i> gene disruptions result in male sterility .....	22
3.2.2	Complementation .....	24
3.2.3	CNGC18 is expressed in pollen .....	25
3.2.4	CNGC18 is essential for directional pollen tube growth <i>in vitro</i> .....	27
3.2.5	<i>cngc18</i> pollen tubes cannot enter the transmitting tract .....	30
3.2.6	CNGC18 localizes to the plasma membrane at the growing pollen tube tip .....	31

---

3.3	Hypersensitivity responses of <i>cngc9-2</i> to Ca <sup>2+</sup> stress .....	36
3.3.1	Phenotypic analysis of <i>cngc9-2</i> plants .....	36
3.3.2	Different CNGC9 expression levels in two independent T-DNA disruption lines causes different Ca <sup>2+</sup> sensitivity .....	39
3.3.3	<i>cngc9-2</i> plants accumulate more Ca <sup>2+</sup> when grown under high Ca <sup>2+</sup> conditions.....	41
3.3.4	Expression pattern of CNGC9.....	43
<b>4</b>	<b>Discussion .....</b>	<b>44</b>
4.1	Is CNGC9 a Ca <sup>2+</sup> permeable channel involved in plant hormone signaling? .....	44
4.2	CNGC18 is essential for polarized tip growth.....	46
4.3	<i>cngc18</i> defines a unique pollen tube growth phenotype.....	46
4.3.1	A calcium signaling CNGC paradigm .....	48
4.3.2	Asymmetric subcellular localization of CNGC18 .....	49
4.3.3	A model for CNGC18 in polarized tip growth.....	50
<b>5</b>	<b>Summary.....</b>	<b>54</b>
<b>6</b>	<b>Future outlook .....</b>	<b>56</b>
6.1	What is the ion conductivity of a plant CNGC?.....	56
6.2	The function of other CNGC isoforms expressed in pollen.....	59
6.3	Structure function studies using the male sterile phenotype of <i>cngc18</i> .....	60
<b>7</b>	<b>References .....</b>	<b>63</b>
<b>8</b>	<b>Acknowledgements.....</b>	<b>69</b>
<b>9</b>	<b>Appendix .....</b>	<b>70</b>
9.1	Abbreviations .....	70
9.2	Isolated T-DNA disruption lines .....	72
9.3	Plasmid maps and sequences .....	74
9.3.1	Maps of selected constructs.....	74
9.3.2	Sequence information of the CNGC18 plasmids used provided as a fasta format text file .....	76
9.3.3	Sequence information of the CNGC9 plasmids provided as a fasta format text file.....	82
9.4	Publications.....	876
9.4.1	Publications .....	876
9.4.2	Oral presentations .....	876
9.4.3	Posters .....	876
9.5	Deutschsprachige Zusammenfassung .....	887

# 1 Introduction

Signaling through ion channels is a key feature in excitable and non-excitable cells in all eukaryotes. For example, calcium fluxes are one of the major regulatory mechanisms involved in signal transduction of key physiological processes (Sanders et al., 2002). In plants, ion dynamics have been studied in several single cell models such as guard cells, root hairs and pollen tubes (Very and Davies, 2000; Schroeder et al., 2001; Hepler et al., 2001). Regulatory functions of  $H^+$ ,  $K^+$ ,  $Ca^{2+}$ , and  $Cl^-$  fluxes are well established in these systems (Barbier-Brygoo et al., 2000; Schroeder et al., 2001; Very and Sentenac, 2002). However, the identification of specific ion transporters and their biological functions remain a challenging question. While our understanding about  $K^+$  channels (such as KAT1 and AKT1) and  $H^+/Ca^{2+}$  ATPases increased over the recent years (Sanders et al., 2002; Cherel, 2004), the knowledge about other transporters such as  $Ca^{2+}$  channels is still very limited. Indirect evidence from recent studies in pollen tubes, leaf guard cells and mesophyll cells suggest that Cyclic Nucleotide-Gated Channels (CNGCs) might be one of the potential  $Ca^{2+}$  permeable channels involved in cell signaling (Malho et al., 2000; Lemtiri-Chlieh and Berkowitz, 2004).

## 1.1 The family of Cyclic Nucleotide-Gated Channels (CNGCs)

Cyclic Nucleotide-Gated Channels (CNGCs) are Shaker-like cation channels with 6 predicted trans-membrane domains and a regulatory cytosolic domain at the C-terminus (Fig. 1). The regulatory domain consists of an overlapping cyclic nucleotide binding pocket and a  $Ca^{2+}/CaM$  binding site suggesting antagonistic functions of these two signaling components. Based on the structure of the fourth transmembrane domain, CNGCs are expected to be only weakly voltage gated. Several studies have demonstrated activation of a plant CNGC by either cAMP or cGMP, while binding of  $Ca^{2+}/CaM$  closes the channel (Schuurink et al., 1998; Leng et al., 1999; Arazi et al., 1999; Kohler and Neuhaus, 2000; Arazi et al.,

2000; Leng et al., 2002; Balague et al., 2003; Hua et al., 2003a). Heterologous expression in yeast and initial electrophysiological analyses suggest that CNGCs are permeable to  $\text{Ca}^{2+}$ ,  $\text{K}^+$  and in some cases  $\text{Na}^+$  (Leng et al., 1999; Arazi et al., 1999; Leng et al., 2002; Balague et al., 2003; Hua et al., 2003a; Gobert et al., 2006). However, electrophysiological characterization, especially of the potential  $\text{Ca}^{2+}$  current remains a challenge.

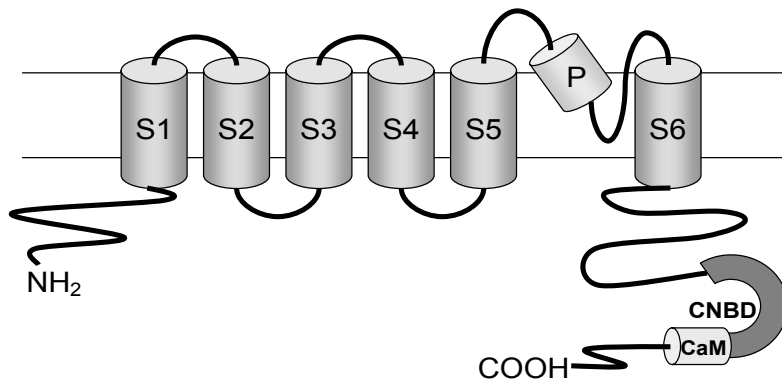


**Figure 1: Predicted protein structure of a plant CNGC.** A typical CNGC consists of 6 transmembrane domains (S1-S6), a pore region (P), and a cyclic nucleotide binding domain (CNBD) overlapping with a  $\text{Ca}^{2+}$ /CaM binding site (CaM).

The model plant *Arabidopsis thaliana*, encodes 20 CNGCs that can be clustered in 5 different subgroups (Fig. 2) (Maser et al., 2001; Talke et al., 2003). Despite expression in almost every tissue (Talke et al., 2003), the knowledge about the physiological role of CNGCs in plants is still fragmented. Mutation of CNGC2 and CNGC4 results in strong dwarfism, spontaneous lesions and a loss of hypersensitive response, while CNGC1 and 10 are involved in heavy metal uptake and resistance (Arazi et al., 1999; Clough et al., 2000; Sunkar et al., 2000; Balague et al., 2003; Li et al., 2005). Recent studies suggest that CNGC11 and 12 are positive regulators of responses to pathogens (Yoshioka et al., 2006). Despite severe mutant phenotypes, presently none of the CNGCs have been shown to be essential for a plants life cycle.

For further insights in the role of CNGCs in plant development and responses to abiotic stress, the phenotypes of several CNGC T-DNA disruption lines have been investigated in the course of this thesis, thereby identifying a crucial role of CNGC18 in pollen tube growth and fertilization.

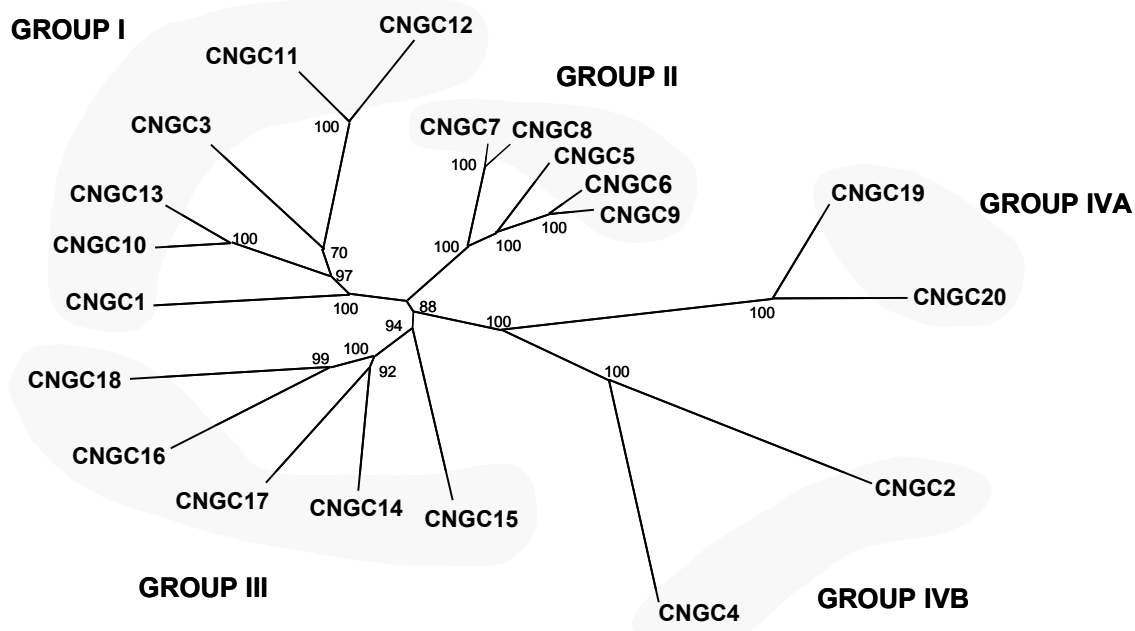


**Figure 2: Phylogenetic tree of the 20 *Arabidopsis* CNGCs adapted after Maeser et al. (Maser et al., 2001).** CNGCs are grouped in 5 different subclasses (Group I, II, III, IVA and IVB). Values indicate the number of times (in percent) that each branch topology was found during bootstrap analysis.

## 1.2 Ion signaling during fertilization in plants

Fertilization in flowering plants requires that pollen tubes grow long distances inside the pistil in search of fertile ovules (Franklin-Tong, 1999). Upon contact of a pollen grain with the stigma, it takes up water and salts before germinating a pollen tube which grows into the transmitting tract to double fertilize the ovule and the central cell (Johnson and McCormick, 2001). This journey is not a process of random growth, but rather involves a directional growth mechanism in which the pollen tube tip perceives guidance signals and alters growth accordingly. Ion

fluxes resulting in local ion gradients are an essential regulatory element of this process (Messerli and Robinson, 2003; Griessner and Obermeyer, 2003; Holdaway-Clarke and Hepler, 2003; Feijo et al., 2004). For example, a tip-focused oscillating  $\text{Ca}^{2+}$  gradient reaching 3-10  $\mu\text{M}$  at the extreme tip and dropping sharply to basal levels of 150-300 nM within 20  $\mu\text{m}$  from the apex has been found to be essential for pollen tube growth and orientation (Pierson et al., 1994; Malho and Trewavas, 1996; Holdaway-Clarke et al., 1997; Messerli and Robinson, 1997). Indirect studies using vibrating probes and  $\text{Ca}^{2+}$  indicators have identified the plasma membrane as the main source of the apical  $\text{Ca}^{2+}$  gradient (Pierson et al., 1994), but the involved channels remain elusive.

### **1.3 Objective of the study**

The driving hypothesis of the following research is that a subset of CNGCs act as  $\text{Ca}^{2+}$  permeable channels involved in cell signaling during plant development and responses to abiotic stresses.

The starting point for my analysis of the *Arabidopsis* CNGC protein family is the isolation of CNGC-TDNA disruption lines followed by phenotypic analyses of these mutants. In the main part of this thesis, a combination of physiology, cell and molecular biology allow a precise molecular dissection of the role of CNGC18 in pollen tube growth and orientation. As a contingency project, a potential role of CNGC9 in plant hormone signaling is investigated.

The analysis of the gene disruption lines of CNGC9 and 18 will not only contribute to our understanding of the physiological role of CNGCs in plants, but will also provide the first genetic evidence for the involvement of a cyclic nucleotide regulated channel in the calcium dependent pollen tube growth and orientation.

## 2 Material and Methods

### 2.1 Plant material

*Arabidopsis thaliana*, var. Columbia and var. Wassilewskija-2

### 2.2 Bacterial strains

*Escherichia coli*, strain K12 DH5α and TB1 for cloning

*Agrobacterium tumefaciens*, strain GV3101 for plant transformation

### 2.3 Vectors

pGEM®-T Easy vector (Promega Corp., Madison, Wisconsin, USA)

pGreen and pSOUP (Hellens et al., 2000)

pBI101 / pBI101.2 / pBI101.3 (BD Clontech, Heidelberg, Germany)

### 2.4 Oligonucleotides

Name	Oligonucleotide Sequence 5' -3'	Gene/AGI	TM (°C)
680a	aagctcgagATGAATTCCGACAAAGAGAAG	CNGC1, At5g53130	49
680b	catcactagtccacccatCATCACTGTTGAAATCTGG	CNGC1, At5g53130	49
930	CTGTATTATAGAGTTAGAATTATGACATCTCC	CNGC2, At5g15410	57
797a	gaggcgcgcgtgtATGCCCTCTCACCCCAACTT	CNGC2, At5g15410	54
797b	gggctagccccTTCGAGATGATCATGCGGTC	CNGC2, At5g15410	52
798a	aagctcgagATGAATCCCCAAAGAAACAA	CNGC3, At2g46430	46
798b	gggcctaggccGGTTTCATCCATAGGAAACT	CNGC3, At2g46430	48
865a	ggcgcgccATGGCCACAGAACAGAACATTACAC	CNGC4, At5g54250	56
865b	ctaactagtccgcctccATAATCATCAAATCGTCGGGATTG	CNGC4, At5g54250	53
794	CGGGACCCTTGAAACCGTGTAGCCATGTA	CNGC5, At5g57940	64
681a	aaaggcgcgcgtcgacATGGCAGGGAAAAGAGAAAAC	CNGC5, At5g57940	50
681b	accacctaggccacccGTCAGCAGTGAAATCAGGCTC	CNGC5, At5g57940	54
703e	GAATCTGTTCTAACGTCAG	CNGC5, At5g57940	49
796a	aagctcgagATGGCATCAAGGTACTCGCA	CNGC6, At2g23980	52
796b	catcactagtccacccGTTGATCTTCAGCAGAGAAAAT	CNGC6, At2g23980	48
854a	GTAGAAGCGGATTCTACAACCGGA	CNGC6, At2g23980	57
854b	CGTATGGAAACCACTTGCTAGGC	CNGC6, At2g23980	57
929	GATTATGGTAACCAACTTCACAACGGTCC	CNGC7, At1g15990	60
682a	aaaggcgcgcgtcgacATGATGATGCAGAGAAACTGT	CNGC7, At1g15990	49
682b	accacctaggccacccTTCAGCATCAAATCAGGTTC	CNGC7, At1g15990	49

Name	Oligonucleotide Sequence 5' -3'	Gene/AGI	TM (°C)
960a	gtctcgagATGTCATCTAATGCTACGGGAATGAAG	CNGC8, At1g19780	57
960b	cgtctagacccgcGCCGTTCAAGTCATCTGTATCAAGAGCC	CNGC8, At1g19780	56
900	GGACCGAGTCCTTAATATGAAGCTGATG	CNGC9, At4g30560	60
962	GATGCTTCGGAGACGCCGATTGG	CNGC9, At4g30560	61
679a	aaaggcgcgcactcgacATGTTAGACTGTGGAAAAAGC	CNGC9, At4g30560	52
679b	accacctaggccacccACTAGTATCATCAGCAGAGAA	CNGC9, At4g30560	49
846a	GCAAGTTAGGATTTGCTGCTTG	CNGC9, At4g30560	54
846b	CACACTTGCACCTTAGAGATG	CNGC9, At4g30560	53
883a	cctcgaggATCGAAGAGCAAGGTCTGTGAAACCAGAGC	CNGC9, At4g30560	63
883b	gtcgacACCGCCTCCGCTTTCTGTGACTCAACTCATGAAT CCCCAAC	CNGC9, At4g30560	63
883d,r	GAAAGAAGTTACACGCCAAATCAGAC	CNGC9, At4g30560	56
883e	CATCTGTGAAACCGACTTCGTCCTCC	CNGC9, At4g30560	57
884g	GGCTGGTGCAGCTTATTACTTGCTACTC	CNGC9, At4g30560	61
884,h,r	TCGATGATGCATCCACTGTTCTGAATCAC	CNGC9, At4g30560	61
884,i	GTTATATTCTCCATAGCACTTGCCATTGCTG	CNGC9, At4g30560	62
884,j,r	CAAGTGCCTCATGTCAAAGCTCTCC	CNGC9, At4g30560	61
884a	gtcgacggcgaggATGTTAGACTGTGGAAAAAGCAGTCAAATCAC	CNGC9, At4g30560	61
884b	tctagacctccgcACTAGTATCATCAGCAGAGAAATCAGGTTCTG	CNGC9, At4g30560	60
884c	cctaggTCAACTAGTATCATCAGCAGAGAAATCAGGTTCTG	CNGC9, At4g30560	61
884d,r	CGCATCAATTACTGTCCGCAGCGTTG	CNGC9, At4g30560	60
884e	CTGTGGATCCGCTCTTCTTGATCTTCC	CNGC9, At4g30560	60
884f,r	CAAACCTGGTCCAGCATCCATTATAACG	CNGC9, At4g30560	60
884k	GTCGGCTTGAGAGTGTGACCAACC	CNGC9, At4g30560	61
962	GAT GCT TTC GGA GAC GCC GAT TGG	CNGC9, At4g30560	61
839a	aagctcgagATGATTGTTAGGTTCAAAGATGAAG	CNGC10, At1g01340	53
839b	ctactctagaccgcctcAGGGTCAGTTGATGATTGGCGGTGAAG	CNGC10, At1g01340	61
855a	GAGAAGATCTCTCCCCTGGCAT	CNGC10, At1g01340	59
855b	GAGTGAGATGTTGTTGGAGATTAGC	CNGC10, At1g01340	56
795	GAGACTGCAGAGCCCCCACCGTAGACGAC	CNGC11, At2g46440	69
678a	aagctcgagATGAAAACACTCGAAAATCTGG	CNGC11, At2g46440	49
678b	catcaactgtccacctcc CGCATAATCGCAGCACCTAA	CNGC11, At2g46440	52
718a	aaaggcgcgcactcgacATGGGAGTTGATGGAAAATTGA	CNGC12, At2g46450	49
718b	catcaactgtccacctcc TGCTTCAGCCTTGCAAACACTCGAG	CNGC12, At2g46450	57
762a	aagctcgagATGGCTTTGGCCGAACAATCGT	CNGC13, At4g01010	57
762b	gggtctagaccgcctcAGGGTTCCGGAGACTGAAATCAGG	CNGC13, At4g01010	57
674a	aaaggcgcgcactcgagATGAAACAAGAAGTACTCCCA	CNGC14, At2g24610	49
674b	accacctaggccacccATCATCCACTGAGAAATCCGG	CNGC14, At2g24610	52
998a	ATGGAGTTCAAGAGAGACAATACTGTC	CNGC14, At2g24610	57
998b	GTTGATTGCTAGAAGATACTTGAGATCG	CNGC14, At2g24610	57
998c	CTCTCTCATCTTGTGTTACGTAAAG	CNGC14, At2g24610	58
879	GTCTCAATTGCTTAGTATGTTAGTC	CNGC15, At2g28260	52
675a	aagctcgagATGGGTTATGGTAACCTCAAGA	CNGC15, At2g28260	49
675b	catcaactgtccacctcc TTCACTAGAAAAATCTGGCTC	CNGC15, At2g28260	49
676a	aagctcgagATGAGCAACCTCCACCTCTAC	CNGC16, At3g48010	54
676b	catcaactgtccacctcc GAAGAATCCTGGATCCTCTGG	CNGC16, At3g48010	54
785a	TACTCGAGCTTGAGCTTGAGCTTCTCTA	CNGC17, At4g30360	60
785b	GTCAGCTCTCTCTGGTTACATCAG	CNGC17, At4g30360	60
864	GCTAGTAATTCCAGGGGCCAC	CNGC18, At5g14870	56
877	GTCTTGGTGGGGTTAAGAAATC	CNGC18, At5g14870	54
961	GTGTGAAAGGATTCTGTGACAAGAG	CNGC18, At5g14870	56
885a	cctcgaggCCATTGATGGTTGTATCTAAAGATCAAAGGAAT	CNGC18, At5g14870	60
885b	gtcgacACCGCCTCCCTCCATGGCGGATCCGGTAAATCG	CNGC18, At5g14870	63
885d,r	GATCAATCAAATCGGCCTAGTGTG	CNGC18, At5g14870	56
885e	GATTGTGTCGAAATTACGTAAAGATC	CNGC18, At5g14870	55

Name	Oligonucleotide Sequence 5' -3'	Gene/AGI	TM (°C)
885f,r	GGGTTTGAGAGTTGGAGAGGATG	CNGC18, At5g14870	57
885g	GTTTGTGATAGTACCAAGAGATTCTC	CNGC18, At5g14870	56
885h,r	CTTGAGAACATAACATTACGTGTCCTC	CNGC18, At5g14870	56
885i	GGGAACCTTGCATCTTCATAAATG	CNGC18, At5g14870	56
885j,r	GATTATGATAACTTAACTAACATATGTGAC	CNGC18, At5g14870	54
885k	GTATTCTAGATCCATGAATTAGTTGGAG	CNGC18, At5g14870	56
885l,r	CATTAACCCGTAATTCAATTATACTGTC	CNGC18, At5g14870	54
885m	GTGGTAGCGCTGCTTCTATATAC	CNGC18, At5g14870	56
886a	gtcgacggcgaggatGAATAAAATCCGGTCTCTCCGCTGCC	CNGC18, At5g14870	61
886b	cctaggccgcctccAACGTCTTCTTATCTAGAGAAATCAGGCTCATC	CNGC18, At5g14870	61
886c	cctaggTTAACGTCTTCTTATCTAGAGAAATCAGGCTCATC	CNGC18, At5g14870	61
886d,r	GCTATTGGCATGATTAGCAGTTCC	CNGC18, At5g14870	56
886e	GATTGCTATGAGATACTGAAGACAG	CNGC18, At5g14870	55
886f,r	CAAATTGTTACAGAACAAAGGTCTCG	CNGC18, At5g14870	55
886g	GTGTCCAAGTACTGTATTGCTTTG	CNGC18, At5g14870	55
886h,r	AGGCCATGTAAGAAGTTCTCCC	CNGC18, At5g14870	57
886i	GAGGACAATAGAGAGCTAACACAC	CNGC18, At5g14870	56
886k	GTTGCTAAGAACATCTATTGTGGGCAG	CNGC18, At5g14870	58
886l	GATCAATGTTAAAAATCGTTAGGCGGTAGC	CNGC18, At5g14870	60
886m	ATAATTAGGGAGTTCCCTAACTATTTACCATC	CNGC18, At5g14870	57
988a	ATGCAAAACCCCCAAAAACAAAAATC	CNGC18, At5g14870	51
988b	ATGGCCCTCTCTCAGTTTCC	CNGC18, At5g14870	55
988c	ATGCAAAACGTGTGCTGTTTGAG	CNGC18, At5g14870	54
991a	TTGGTGGAAAGTCTCTGCAATCG	CNGC18, At5g14870	58
991b	CCTCTTCGTGTCGCCGCAAAT	CNGC18, At5g14870	59
691a	aagctcgagATGGCTCACACTAGGACTTC	CNGC19, At3g17690	52
691b	catcaactgtccacctccACGGTTGGAATTGGAGTGAGC	CNGC19, At3g17690	54
938a	cgctcgagATGGCTTCCCACAACGAAAACGATGATATTG	CNGC20, At3g17700	60
938b	gcggatccgcctccaAAGGCTATAACTAGACTGAGGAGTGC	CNGC20, At3g17700	58
79-1	TCGACCGGCCGCTCAATCAGTCAGAACATT(T) <sub>17</sub>	oligo d(T) <sub>17</sub>	65
792	GTGATGGTTCACGTAGTGGGCCATCG	SALK LBa1	58
791	CTCTTGTCCAAACTGGAACAAACACTC	SALK LBa2	63
247	TGGGAAAACCTGGCGTTACCCAACTTAAT	SALK RB	60
248	TGGCGAATGAGACCTCAATTGCGAGCTT	SALK RB	62
638	GCCTTTCAGAAATGGATAAAATGCCTTGCTTCC	Syngenta LB1	62
639	GCTTCCTATTATATCTTCCCAAATTACCAATACA	Syngenta LB2	58
640	TAGCATCTGAATTTCATAACCAATCTCGATACAC	Syngenta LB3	60
635	CAAACCTAGGATAAAATTATCGCGCGCGGTGTCA	Syngenta QRB1	63
636	GGTGTCTATGTTACTAGATCGGGATTGA	Syngenta QRB2	61
637	CGCCATGGCATATGCTAGCATGCATAATT	Syngenta QRB3	62
958	ATATTGACCATCATACTCATTGC	GABI LB, o8409	50
959	CGCCAGGGTTTCCCAGTCACGACG	GABI RB, o2588	64
35S 5'	GTCAACATGGTGGAGCACGACACAC	CaMV 35S primer	61
35S 3'	CACTGACGTAAGGGATGACG	CaMV 35s primer	54
EF1α_fwd	GGCCACGTCGATTCTGGAAA	Elongation factor 1 α	58
EF1α_rev	GGCTGGTTGGAGTCATCTT	Elongation factor 1 α	55

**Table 1: List of the oligonucleotides used including the corresponding gene name and AGI (if applicable), as well as the annealing temperature.** Linkers and restriction sites are in lower case. The annealing temperature was calculated for standard condition using the Oligo-Analyzer 3.0 from Integrated DNA Technologies (IDT), Coralville, Iowa, USA (<http://www.idtdna.com/analyzer/Applications/OligoAnalyzer/Default.aspx>).

## 2.5 Plant growth conditions

Plants used for the experiments presented in this thesis were grown at 22°C, 70% humidity with a 16-h-light/8-h-dark photoperiod regime at ~70  $\mu\text{mol m}^{-2} \text{s}^{-1}$ . Only the plants grown for the initial phenotype screen were grown with a 8-h-light/16-h-dark photoperiod to slow down the development.

### 2.5.1 Standard MS media (half strength)

½ x Murashige Skoog Salts including Gamborg B5 vitamins (M0404), Sigma-Aldrich Corp., St. Louis, Missouri, USA

0.5 g MES

0.5% (w/v) sucrose

1% (w/v) agar (A-4550), Sigma-Aldrich Corp., St. Louis, Missouri, USA

pH 5.7 (adjusted with KOH)

For segregation analysis, mutant isolation and selection of transgenic plants the media contained the following antibiotics/herbicides as appropriate:

10  $\mu\text{g/ml}$  glufosinate-ammonium (basta), (45520), Sigma-Aldrich Corp., St. Louis, Missouri, USA

11.25  $\mu\text{g/ml}$  sulfadiazine, sodium salt (S6387), Sigma-Aldrich Corp., St. Louis, Missouri, USA

25  $\mu\text{g/ml}$  hygromycin B from *Streptomyces hygroscopicus* (H9773), Sigma-Aldrich Corp., St. Louis, Missouri, USA

50  $\mu\text{g/ml}$  kanamycin sulfate from *Streptomyces kanamyceticus* (K4378), Sigma-Aldrich Corp., St. Louis, Missouri, USA

### 2.5.2 Modified plant growth media for phenotypic analysis

The growth media used for the phenotypic analysis in this thesis is based on the standard MS media that was supplement as follows. Media with lower K<sup>+</sup> or Ca<sup>2+</sup> contents meets standard condition for the other component. Media supplemented with abscisic acid contains ¼ strength MS media and phytagel (P8169), Sigma-Aldrich Corp., St. Louis, Missouri, USA, as gelling agent.

Final concentration of supplements:

50-125 mM NaCl

50 or 100 mM KCl

10-50 mM CaCl<sub>2</sub>

200 mM mannitol

10 mM LaCl<sub>3</sub>

0.5 mM PbAc

1 or 5 mM CeCl<sub>3</sub>

50 or 100 µM CdCl<sub>2</sub>

0–1.0 µM abscisic acid (ABA), (A1049), Sigma- Aldrich Corp., St. Louis, Missouri, USA

Media with low K<sup>+</sup> content:

10.4 mM NH<sub>4</sub>NO<sub>3</sub>

0.75 mM MgSO<sub>4</sub>

616 µM NaH<sub>2</sub>PO<sub>4</sub>

1.5 mM CaCl<sub>2</sub>

10 or 100 µM KCl

50 ml/l Murashige Skoog Basal Salt Micronutrient Solution, 10x, (M0529), Sigma-Aldrich Corp., St. Louis, Missouri, USA

Media with low Ca<sup>2+</sup> content:

10.4 mM NH<sub>4</sub>NO<sub>3</sub>

0.75 mM MgSO<sub>4</sub>

616 µM NaH<sub>2</sub>PO<sub>4</sub>

150 µM CaCl<sub>2</sub>

2 mM KCl

50 ml/l Murashige Skoog Basal Salt Micronutrient Solution, 10x, (M0529), Sigma-Aldrich Corp., St. Louis, Missouri, USA

## 2.6 Solutions and buffers

### 2.6.1 Pollen germination media

1 mM KCl

0.8 mM MgSO<sub>4</sub>

1.5 mM H<sub>3</sub>BO<sub>3</sub>

10 mM CaCl<sub>2</sub>

5 mM MES

16.6% (w/v) sucrose

4% (w/v) sorbitol

10 µg/ml myo-inositol (optional)

0.5-1% (w/v) low gelling temperature agarose (A-9414 and A-6560) Sigma-Aldrich Corp., St. Louis, Missouri, USA

pH 5.8 adjusted with TRIS

Media was heated for 20-40 sec in the microwave to melt the agarose. After cooling, 500 µl of the media is evenly spread on a microscope glass slide with a razor blade.

### **2.6.2 Alexander staining solution**

For pollen viability staining, the following stock was diluted to a 1:50 working solution:

10 ml 95% (v/v) ethanol,

5 ml of a 1% (w/v) malachite green solution (95% (v/v) ethanol), (M-9015), Sigma-Aldrich Corp., St. Louis, Missouri, USA

5 ml of a 1% (w/v) acid fuchsin solution (water), (F-8129) Sigma-Aldrich Corp., St. Louis, Missouri, USA

0.5 ml of a 1% (w/v) orange G solution (water), (O-7252), Sigma-Aldrich Corp., St. Louis, Missouri, USA

50 ml distilled water

25 ml glycerol

5 g phenol

2 ml glacial acetic acid

### **2.6.3 Solutions for $\beta$ -glucuronidase activity staining**

Basic sodium phosphate GUS-buffer:

11.54 ml of 0.5 M Na<sub>2</sub>H(PO<sub>4</sub>)

8.46 ml of 0.5 M NaH<sub>2</sub>(PO<sub>4</sub>)

0.1% (v/v) Triton

0.5 mg/ml 5-bromo-4-chloro-3-indolyl  $\beta$ -D-glucuronide cyclohexylamine salt (X-Gluc) dissolved in N,N-Dimethylformamide (DMF).

ad 100 ml ddH<sub>2</sub>O

GUS-Buffer for pollen grain and *in planta* pollen tube staining:

Pollen germination media (without agar)

0.1% (v/v) Triton

0.5 mg/ml 5-bromo-4-chloro-3-indolyl  $\beta$ -D-glucuronide cyclohexylamine salt (X-Gluc) dissolved in N,N-Dimethylformamide (DMF).

## 2.7 Microscopy

Fluorescence imaging of GFP and YFP proteins expressed in pollen was done by spinning-disc confocal microscopy (at room temperature) using a QLC100 confocal scanning unit (Solamere Technology Group, Salt Lake City, UT, USA) attached to a NIKON Eclipse TE 2000-U bright field microscope containing a 40x/0.95 and a water immersion 60x/1.20 NIKON Plan Apo objective (Nikon, Tokyo, Japan). An argon laser was used to excite at a wavelength of 488 nm (500 M Select, Laserphysics, West Jordan, UT, USA). For filtering the emission wavelength, emitter HQ525/50 at 500-550 nm was used (Chroma Technology Corp., Rockingham, VT, USA). Images were captured with a CCD-camera (CoolSnap-HQ, Photometrics, Tucson, AZ, USA) using Metamorph software (Universal Imaging, Downingtown, PA, USA).

Changes in CFP and YFP emission of a cameleon protein as response to changes in cytosolic  $\text{Ca}^{2+}$  levels were visualized using a Nikon Eclipse TE300 microscope equipped with a Plan Fluor 40x/1.30 oil immersion objective, a Plan Fluor 10x/0.30 objective and a 75 W xenon light source (Nikon, Tokyo, Japan). The excitation wavelength was filtered through a 440 $\pm$ 10 nm bandpass filter (CFP excitation) and a 455 DCLP dichroic mirror (Chroma Technology Corp., Rockingham, VT, USA). CFP and YFP emissions were filtered with an emitter at 485 $\pm$ 20 nm (CFP) and 535 $\pm$ 15 nm (YFP) respectively and captured by a Orca digital camera (model: C4742-95, Hamamatsu, Tokyo, Japan) using the MetaFluor software (Universal Imaging, Downingtown, PA, USA). MetaFluor allowed automatic control of the microscope shutters and emission filter wheel

(Ludl Electronic Products Ltd, Hawthorne, New York, USA) in order to acquire a new set of images every 5 sec. The fluorescent intensity changes documented with MetaFluor was analyzed using Microsoft Excel.

The same microscope setups as well as a Leica MZ 9 stereomicroscope equipped with a Leica D3 300 camera (Leica Microsystems AG, Wetzlar, Germany) controlled by Adobe Photoshop (Adobe Systems, San Jose, California, USA) was used for darkfield and differential interference contrast microscopy.

## 2.8 Software and websites used

Microsoft Windows, XP and Office XP (Microsoft Corporation, Redmond, Washington, USA)

Macromedia FreeHand 9.0 (Adobe Systems, San Jose, California, USA)

Reference Manager 9.5 (Thomson ISI ResearchSoft, Philadelphia, Pennsylvania, USA)

Adobe Photoshop and Write (Adobe Systems, San Jose, California, USA)

Image J (National Institute of Health (NIH), Bethesda, Maryland, USA)

Jellyfish (LabVelocity, Los Angeles, California, USA)

MetaMorph and MetaFlour version 5.3 (Universal Imaging, Downingtown, Pennsylvania, USA)

<http://signal.salk.edu/cgi-bin/tdnaexpress>

<http://www.arabidopsis.org/>

<http://www.idtdna.com/analyizer/Applications/OligoAnalyzer/Default.aspx>

<http://plantst.genomics.psu.edu/>

<http://prodes.toulouse.inra.fr/multalin/multalin.html>

<https://www.genevestigator.ethz.ch/>

<http://www.tigr.org>

## 2.9 Molecular biological standard methods

All molecular standard methods used in this thesis have been implemented after protocols of Sambrook et al. (Sambrook et al., 1989). If commercially available kits were used, the manufacturer's protocols were followed.

## 2.10 Isolation of T-DNA insertion lines

To isolate homozygous T-DNA insertion lines, seeds were germinated and grown  $\frac{1}{2}$  MS plant growth media including the appropriate selection marker. DNA was extracted from leaves of 10-14 day old seedling following transfer to soil. The genotype of the plants was determined by PCR analysis using the primers listed in Table 1.

## 2.11 Phenotypic analysis of homozygous T-DNA insertion lines

To test for differences in the phenotype of mutant and wild-type plants, seeds of side-by-side grown plants were sterilized and plated on  $\frac{1}{2}$  MS media supplemented with the following salts, hormones or heavy metal (compare section 2.5.2). The plants were germinated and grown under an 8-h-light/16-h-dark photoperiod regime.

Control condition	Stress condition
$\frac{1}{2}$ MS standard media including sucrose	100 mM NaCl, 50 and 100 mM KCl, 20 and 30 mM CaCl <sub>2</sub> 50 and 100 $\mu$ M CdCl <sub>2</sub> 0.1 mM NiCl <sub>2</sub>
$\frac{1}{2}$ MS standard media including sucrose, agar replaced by agarose	10 and 100 $\mu$ M KCl (1.5 mM CaCl <sub>2</sub> ) 150 $\mu$ M CaCl <sub>2</sub> (2 M KCl)
$\frac{1}{2}$ MS standard media excluding sucrose	150 and 200 mM mannitol
$\frac{1}{2}$ MS standard media including sucrose, pH 4.7	0.1 mM PbAc
$\frac{1}{4}$ MS standard media excluding sucrose, including 500 $\mu$ l ETOH	0.3 and 0.5 $\mu$ M abscisic acid (ABA)

Table 2: Conditions tested in the phenotype screen.

The experiments were performed in duplicates with 12 mutant and 12 wild-type seeds per plate. To randomize possible shading or temperature differences the position were altered between the plates as illustrated in Figure 3. After scoring the germination rate, plant growth was observed and monitored every 1-2 days using a stereomicroscope attached to a camera.

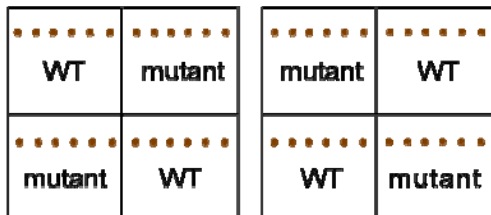


**Figure 3: Plating scheme for phenotype screen.**

## 2.12 Plasmid constructs and transformation

Plants were transformed with *Agrobacterium* (GV3101) containing the helper plasmid pSoup using the floral dip method (Clough and Bent, 1998; Hellens et al., 2000). All transgene constructs were cloned in a pGreen II transformation vector (Hellens et al., 2000) providing kanamycin resistance in bacteria (50 µg/ml) and hygromycin resistance in plants. All PCR derived constructs were first TA-cloned in a pGEM®-T Easy vector (Promega Corp., Madison, WI, USA) and verified by DNA sequencing. The complete construct sequences are provided in the appendix (Fig. A3-A11).

Plasmid *gCNGC18* (ps# 632) contains a 6.88 kb genomic fragment subcloned as a *Kpn* I and *Xho* I fragment from the Bacterial Artificial Chromosome *T9L3* (Choi et al., 1995) (Fig. A1, A3). Representative transgenic *cngc18-1* plants expressing this vector are ss# 761-765.

Plasmid CNGC18-promoter::*GUS* (ps# 827) is a plant expression vector containing a  $\beta$ -glucuronidase gene (*GUS* reporter) under the control of a 3.35 kb CNGC18 promoter (Fig. A4). This promoter was amplified using primers 885a

and 885b. Representative transgenic plants expressing this construct are ss# 766 and 767.

Plasmid *ACA9promoter::i-GFP-CNGC18* (ps# 855) is a plasmid encoding a *GFP-CNGC18* fusion construct under the control of the *ACA9* promoter (Fig. A1, A5) (Schiott et al., 2004). The *CNGC18* cDNA was amplified from a cDNA library using primers 886a and 886c, based on the open reading frame predicted from cDNA clone NM\_121491.2 (GI:30685090). To reduce toxicity issues from leaky expression in *Agrobacterium*, the plant transformation vector contained an upstream untranslated leader sequence with an intron. Representative transgenic lines showing complementation are ss# 673-678.

Plasmid *gCNGC9* (ps# 633) contains a 5.27 kb genomic fragment subcloned as a *Hind* III fragment from the Bacterial Artificial Chromosome *F17I23* (Mozo et al., 1998) (Fig. A2, A8).

Plasmid *CNGC9-promoter::GUS* (ps# 826) is a plant expression vector containing a  $\beta$ -glucuronidase gene (*GUS* reporter) under the control of a 1.09 kb *CNGC9* promoter (Fig. A9). This promoter was amplified using the primers 883a and 883b.

Plasmid *N-TAP-GFP-CNGC9* (ps# 790) and *CNGC9-GFP-TAP* (ps# 776) are plasmids encoding a cDNA of *CNGC9* with a N- and C-terminal *GFP-TAP*-tag fusion construct under the control of the *CaMV-35S* promoter (Fig. A2, A510, and A11). The *CNGC9* cDNAs encoded in ps# 776 and ps# 855 were amplified from a cDNA library using primers 884a and 884b/884c respectively, based on the open reading frame predicted by The Institute for Genomic Research (TIGR) (<http://www.tigr.org>).

## **2.13 Characterization of a male gametophytic phenotype**

### **2.13.1 Basta spray-application for selection of plants grown in soil**

A 0.7% Finale solution (Farnam Companies Inc., Phoenix, Arizona, USA) was applied by spraying 3-4 week old plants (4-6 leaves) that have been germinated

on soil. Plants that do not encode the *bar* gene conferring basta (glufosinate) resistance died within a few days. WT plants were included as a negative control to insure proper selection.

### **2.13.2 Complementation of *cngc18-1* plants transformed with *gCNGC18* (ps# 632) or *ACA9promoter::i-GFP-CNGC18* (ps# 855)**

*Agrobacterium tumefaciens* mediated transformation of *Arabidopsis thaliana* rather transforms the ovule than the pollen (Ye et al., 1999). Therefore complementation of a male sterile phenotype can be tested at the earliest in the T2 generation after transformation.

After *Agrobacterium* mediated transformation of *cngc18-1* plants with *gCNGC18* (ps# 632) or *ACA9promoter::i-GFP-CNGC18* (ps# 855), T1 and T2 plants were selected on media containing 25 µg/ml hygromycin. *cngc18-1* mutants containing the transgene were subsequently isolated by basta spray-application. Complementation was investigated by basta segregation and PCR analysis.

### **2.13.3 Pollen tube germination and imaging of pollen expressing GFP constructs**

*Arabidopsis* pollen tube germination has been found to be highly variable and dependent on many factors such as perfect “health condition” of the plants (Johnson-Brousseau and McCormick, 2004). Pollen has a rather short live span of 2-3 days (Johnson-Brousseau and McCormick, 2004). Therefore, pollen of flowers in stage 14 (youngest open flower) (Smyth et al., 1990) was applied directly to the germination media by brushing the anthers carefully over the surface. For some experiments flowers were harvested a few hours or the evening before the experiment to ensure complete desiccation of the anthers. To enhance the germination frequency, pistil and stamen of the flower were placed in proximity to the pollen on the germination media. However, no experimental

data is available yet to confirm a possible positive effect of guidance factors and other substances from the pistil (Johnson-Brousseau and McCormick, 2004).

After 30 min to 6h after incubation at 26°C in a petridish containing a wet paper towel (to ensure high humidity), pollen tube germination was analyzed by differential interference contrast or fluorescent microscopy. The localization of GFP-CNGC18 was analyzed in complemented *cngc18-1* plants in the *quartet* background that were segregating for *GFP-CNGC18*. Tetrads of these plants expressed *GFP-CNGC18* in only two pollen grains which allowed simultaneous analysis of pollen grains with and without GFP fluorescence. For analysis of ACA9-YFP expression in the pollen grain, WT and *aca9-1* pollen complemented with ACA9-YFP were mixed on the germination media again allowing simulations analysis.

#### **2.13.4 Histochemical pollen viability staining**

To test for pollen viability, *cngc18-1* and wild-type pollen tetrads were incubated for 12h in modified Alexander staining solution according to Johnson-Brousseau and McCormick (Alexander, 1969; Johnson-Brousseau and McCormick, 2004). Alexander solution stains the cytoplasma of viable pollen in a purple-red color and the cell wall of the aborted pollen grains in green. The analysis was carried out in *cngc18-1* plants in the *quartet* background allowing simultaneous analysis of all four meiotic products.

#### **2.14 Histochemical staining of a promoter::GUS activity**

The expression pattern of a promoter:: $\beta$ -glucuronidase (GUS) construct was studied after 30 min incubation in 80% acetone followed by washing and final incubation in GUS staining solution (X-Gluc-solution) for 3-24 h at 37°C in the dark (Jefferson et al., 1987; Johnson et al., 2004). To ensure better tissue penetration of the GUS staining solution, a light vacuum was applied for the first 30 min-1 h of the incubation.

To examine *lat52*-promoter::*GUS* expression in pollen tubes *in vivo* (Fig. 9), pistils manually fertilized with *cngc18-1* (ss# 578) pollen were mounted with medical adhesive and stained as described above. As control, pistils fertilized manually pollinated with wild-type and positive control that contain a T-DNA harboring a *lat52*::*GUS* reporter in a phenotypically silent location, were analyzed in parallel (*cngc11-2*, ss# 189).

## 2.15 Inductively coupled plasma spectroscopy (ICP)

To determine the ion accumulation profile, mutant and wild-type plants were grown side by side on  $\frac{1}{2}$  MS plant growth media supplemented with 0, 10, and 20 mM CaCl<sub>2</sub>. After 3 weeks the root and shoot material of 10 plants each were collected and digested with concentrated nitric acid. The digestion procedure involved placing the plant tissue in 15ml poly-propylene centrifuge tubes and the volume is adjusted by adding 1ml HNO<sub>3</sub>. The tubes are capped and allowed to sit over night.

The solutions are then heated in a convection oven to approximately 90°C for 2 to 3 hours, or until only trace amounts of residual plant tissue remains. After the tubes are allowed to cool, the final volume is adjusted to 5 ml with ddH<sub>2</sub>O for ICP analysis. The samples are diluted 1:10 prior to ICP analysis. Three standards are used for ICP calibration. Two are custom standards from SPEX Certiprep®, Metuchen, New Jersey, USA: Mix A containing: Ag, As, Ba, Cd, Ca, Ce, Cr, Co, Cu, Fe, Gd, K, La, Li, Mg, Mn, Na, Ni, Pb, Rb, Se, V, Zn, and Mix B containing: B, Mo, P, S, Si, W. A third (Mix C) containing Ca, K, and Na is prepared from salts. The standards are diluted to the following concentrations for calibration: Mix A) 0.01, 0.05, 0.1, 0.5, 1, 10, 25 ppm; Mix B) 0.01, 0.05, 0.1, 0.5, 1, 10, 100 ppm; Mix C) 0.2, 1, 10, 100, 250 ppm. Standards and samples are loaded into a Varian® SP5 auto sampler and run concurrently on a Varian® Vista ICP controlled by Varian® ICPExpert© software (Varian, Palo Alto, California, USA). The current analysis involves 3 replicate reads of 5 seconds with a total up-take volume of approximately 2.5 ml.

### 3 Results

Despite recent studies providing first evidence for a role of CNGCs in responses to biotic and abiotic stresses (Talke et al., 2003), little is known about the function and specificity of most members of the plant CNGC family. As a starting point of studying the physiological role of CNGCs, an initial set of 16 CNGC T-DNA disruption lines were tested under abiotic and biotic stress conditions. Based on the observed phenotypes, the T-DNA disruptions in CNGC9 and 18 were chosen to study the physiological role of these CNGCs in plant development.

In the course of this thesis, homozygous *Arabidopsis* T-DNA insertion lines were isolated for every CNGC, except for CNGC18 which has been found to be essential for a plants life cycle. For many CNGCs multiple mutant alleles were isolated. All 39 isolated *cngc* mutant lines are listed in Table A1 of the Appendix of this thesis. Seven of these 39 gene disruption lines have been isolated by Lisbeth Rosager prior to this thesis, three lines have been isolated by Dr. Nadia Robert (University of California San Diego, USA) and one mutant line was provided by Dr. Catherine Chan (University of Wisconsin-Madison, Wisconsin)(Chan et al., 2003).

#### 3.1 Phenotypic analysis under abiotic and biotic stress conditions

To study the role of CNGCs in plant development and in stress responses, the first set of isolated T-DNA disruption lines was studied under abiotic and biotic stress conditions. Due to the time requirement of the screen, the phenotypic analysis was split in two rounds with slightly different conditions. In round one, germination and growth were monitored over a period of 8 days for *cngc2-3*, *cngc6-1*, *cngc11-1*, *cngc11-3*, *cngc17-2*, and *cngc19-2* on plant growth media containing physiologically high and low levels of various cations, heavy metals as well as the plant stress hormone abscisic acid (ABA): 100 mM NaCl, 10 and 100

$\mu$ M KCl, 50 and 100 mM KCl, 150  $\mu$ M and 30 mM CaCl<sub>2</sub>, 200 mM mannitol, 100  $\mu$ M CdCl<sub>2</sub>, 0.5 mM PbAc , low pH (4.7), as well as 0.3 and 0.5  $\mu$ M ABA. In round two, germination and growth were observed over 12 days for *cngc3-2*, *cngc6-2*, *cngc9-2*, *cngc10-1*, *cngc11-2*, *cngc13-1*, and *cngc13-2* on media containing: 100 mM NaCl, 10  $\mu$ M and 100 mM KCl, 150  $\mu$ M and 20 mM CaCl<sub>2</sub>, 150 mM mannitol, 50  $\mu$ M CdCl<sub>2</sub>, 0.1 mM NiCl<sub>2</sub>, 0.5 mM PbAc , low pH (4.7), as well as 0.5  $\mu$ M ABA. The phenotypes discovered under these conditions are summarized in Table 3.

No homozygous plants were identified for *cngc18-1* and *cngc18-2*. Therefore a genetic analysis has been carried out to determine the developmental defect in these mutants (compare section 3.2).

Name	AGI	T-DNA number	condition and phenotype
<i>cngc2-3</i>	At5g15410	SALK_018387	100 mM NaCl: late germination
<i>cngc3-1</i>	At2g46430	SALK_056832	10 $\mu$ M K <sup>+</sup> : longer roots than WT, slight late germination
<i>cngc3-2</i>	At2g46430	SALK_066634	10 $\mu$ M K <sup>+</sup> : longer roots than WT, slight late germination
<i>cngc6-1</i>	At2g23980	SALK_042207	no phenotype under tested conditions
<i>cngc6-2</i>	At2g23980	SALK_064702	no phenotype under tested conditions
<i>cngc9-2</i>	At4g30560	SAIL_736_D02	20-50 mM Ca <sup>2+</sup> : curly roots and callus; 150 mM mannitol: longer roots than WT
<i>cngc10-1</i>	At1g01340	SALK_015952	0.5 mM Ca <sup>2+</sup> , plant smaller than WT +retarded
<i>cngc11-1</i>	At2g46440	JP72_0E08L	late germination
<i>cngc11-2</i>	At2g46440	SAIL_165_A02	late germination, 150 mM mannitol, shorter and less branched roots
<i>cngc13-1</i>	At4g01010	SALK_013536	100 mM NaCl: smaller shoot than WT
<i>cngc13-2</i>	At4g01010	SALK_060826	100 mM NaCl: smaller shoot than WT
<i>cngc17-2</i>	At4g30360	SALK_041923	no phenotype under tested conditions
<i>cngc18-1</i>	At5g14870	SAIL_191_H04	male sterile
<i>cngc18-2</i>	At5g14870	GABI_052_H11	male sterile
<i>cngc19-2</i>	At3g17690	SALK_007105	no phenotype under tested conditions

**Table 3: Phenotypes identified in CNGC T-DNA gene disruption lines.** The phenotypic analysis of this initial set of mutants revealed an altered phenotype for 11 of the 16 tested lines.

Apart for the observed phenotypes of *cngc9-2* and *cngc18* mutants which were chosen for in depth analysis, the late germination phenotypes of *cngc11-1* and *11-2* are of special interest because they indicate a potential defect in seed

dormancy, gibberlic acid, or abscisic acid regulation of seed germination. Further studies are necessary to investigate the role of CNGC11 in seed germination.

### 3.2 CNGC18 is essential for pollen tube growth

#### 3.2.1 *cngc18* gene disruptions result in male sterility

Two independent *cngc18* T-DNA gene disruption lines, *cngc18-1* (SAIL\_191\_H04) (McElver et al., 2001) and *cngc18-2* (GABI\_052\_H11) (Rosso et al., 2003) were identified by PCR diagnostics. Both insertions were found to disrupt the coding sequence in exons 5 and 1 of CNGC18 (At5g14870), respectively (Fig. 4), as shown by DNA sequencing of the insertion sites adjacent to the T-DNA left border. Mutants harboring the *cngc18-1* and *18-2* alleles were backcrossed twice with wild-type pollen to segregate away possible second site T-DNA insertions and insure co-segregation between the T-DNA encoded selectable marker and the CNGC18/TDNA border.

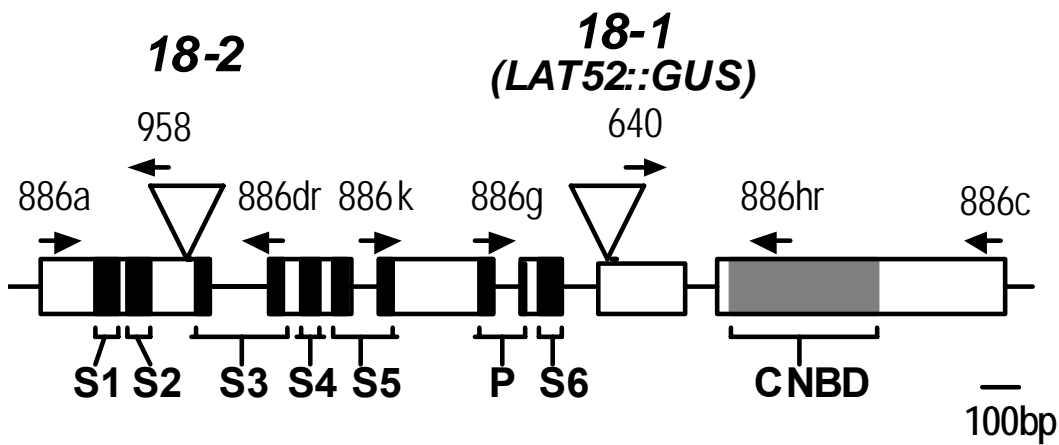


**Figure 4: Diagram showing CNGC18 T-DNA disruptions.** The diagram displays the genomic structure of CNGC18 (At5g14870). The T-DNA insertion sites in *cngc18-1* and *cngc18-2* are indicated as triangles 1555 bp and 435 bp downstream of the start codon, respectively. The *cngc18-1* T-DNA encodes the pollen expressed *LAT52*-promoter::*GUS*.

□ = exons, - = introns, ■ = trans-membrane domains (S1-6) and pore domain (P), ■ = cyclic nucleotide binding domain (CNBD), → = position of the primers.

When plants heterozygous for either *cngc18-1* or *18-2* (-/+) were allowed to self-fertilize, a segregation distortion of the T-DNA encoded selectable marker was evident. Instead of the expected 3:1 segregation ratio (resistant/sensitive) for Mendelian segregation of the T-DNA encoded selectable marker, a 1:1 ratio was observed. Statistical analysis did not only exclude a Mendelian segregation pattern but also a 1:2 segregation ratio that would have indicated a sporophytic lethality. Moreover, within 251 resistant plants that were genotyped by PCR analysis, no homozygous plant was isolated implying a defect in the female or male gametophyte.

	parent female x male	Segregation of T-DNA			
		total	exp	observ	transm
<b>A</b>	<i>cngc18-1</i> , selfed	802	602	426 <sup>a,b,c</sup>	53%
	<i>cngc18-2</i> , selfed	300	225	143 <sup>a,b,c</sup>	48%
<b>B</b>	WT x <i>cngc18-1</i>	37	19	0	0%
	<i>cngc18-1</i> x WT	20	10	10	50%
	<i>ms1-1</i> x <i>cngc18-1</i>	120	60	0	0%
<b>C</b>	<i>gCNGC18</i> , selfed	437	328	349 <sup>d</sup>	79.9%
	<i>GFP-CNGC18</i> , selfed	873	655	626 <sup>d</sup>	71.7%

**Table 4: Segregation analysis of the T-DNA in *cngc18* mutants.** Comparison of observed resistance conferred by a T-DNA encoded selectable marker gene (observ) with an expected Mendelian segregation (exp = 75% resistance) of: (A) Self-fertilized *cngc18* mutants (*cngc18*, selfed) (B) reciprocal crosses with WT and *male sterility1* (*ms1-1*) plants (Van der Veen and Wirtz P., 1968) and (C) self-fertilized F2 progeny of *cngc18-1* plants complemented with a genomic construct (*gCNGC18*, selfed) or the *GFP*-tagged cDNA of *CNGC18* (*GFP-CNGC18*, selfed). Statistical significance was determined by Pearson  $\chi^2$ - test. The transmission (transm) of the T-DNA to the next progeny was calculated as (total/100)\*observed resistance.

<sup>a</sup> significantly different from Mendelian segregation ratio 3:1 ( $\chi^2$ ,  $P < 0.01$ )

<sup>b</sup> significantly different from segregation ratio 2:1 ( $\chi^2$ ,  $P < 0.01$ )

<sup>c</sup> not significantly different from segregation ratio 1:1 ( $\chi^2$ ,  $P > 0.01$ )

<sup>d</sup> not significantly different from Mendelian segregation ratio 3:1 ( $\chi^2$ ,  $P > 0.01$ )

To distinguish between lethality in the male or female gametophyte, reciprocal crosses between *cngc18-1* (-/+) and wild-type plants were conducted, as well as out-crossing pollen from *cngc18-1* to *male sterility 1* plants (*ms1-1*) (Van der Veen and Wirtz P., 1968) (Tab. 4B). While the transmission through the female gametophyte was not affected (ratio 1:1, n=20), transmission through the male gametophyte never occurred (0 transmission, n= 157). Together, the genetic analyses support the contention that both *cngc18-1* and *18-2* mutations result in sterile pollen, with no indication of a defect in the female gametophyte.

### 3.2.2 Complementation

To provide confirmation that *cngc18-1* male sterility resulted from a loss-of-function mutation, complementation was tested in *cngc18-1* (-/+) plants transformed with a 6.88 kb fragment of genomic DNA (*gCNGC18*) containing the *CNGC18* open reading frame as well as a 3.4 kb upstream and 0.9 kb downstream region. Within this genomic fragment, *CNGC18* is predicted to be the only complete gene, according to annotation by The Institute for Genomic Research TIGR (<http://www.tigr.org>, as of 8/1/2005).

Since *Agrobacterium* transformation targets the ovules but not the pollen (Ye et al., 1999), complementation of *gCNGC18* was verified by a segregation analysis of the *cngc18-1* encoded resistance marker (*basta*) in the second generation of transgenic plants (T2). In 6 of 6 transgenic lines analyzed, the *cngc18-1* allele was found to segregate in a normal Mendelian fashion (Tab. 4C). A PCR diagnostic analysis of 33 hygromycin (transgene selectable marker) and *basta* (T-DNA encoded marker) selected plants confirmed that the complementation construct allowed pollen transmission of *cngc18-1* leading to the production of 11 plants homozygous for the *cngc18-1* T-DNA disruption. As described later, complementation was also observed using a GFP-tagged *CNGC18* cDNA expressed under the control of a pollen specific promoter (Tab. 4C). In this case, PCR analysis of 41 hygromycin and *basta* selected plants

identified 15 homozygous *cngc18-1* plants, confirming the previously observed Mendelian segregation pattern.

### 3.2.3 CNGC18 is expressed in pollen

To determine the developmental and tissue specific expression pattern of CNGC18 *in planta*, the 3.35 kb upstream region of CNGC18 (including the 5' untranslated region) was fused to the reporter gene  $\beta$ -glucuronidase (*GUS*) (Jefferson et al., 1987) and transformed into *Arabidopsis* plants (Clough and Bent, 1998). Histochemical staining demonstrated GUS activity in the anthers and pollen grains starting late in flower stage 12 (Fig. 5A-C). Leaves, trichomes, roots and root hairs of young seedlings did not show any GUS activity indicating that CNGC18 is predominantly expressed in anthers and pollen (Fig. 5D-G).

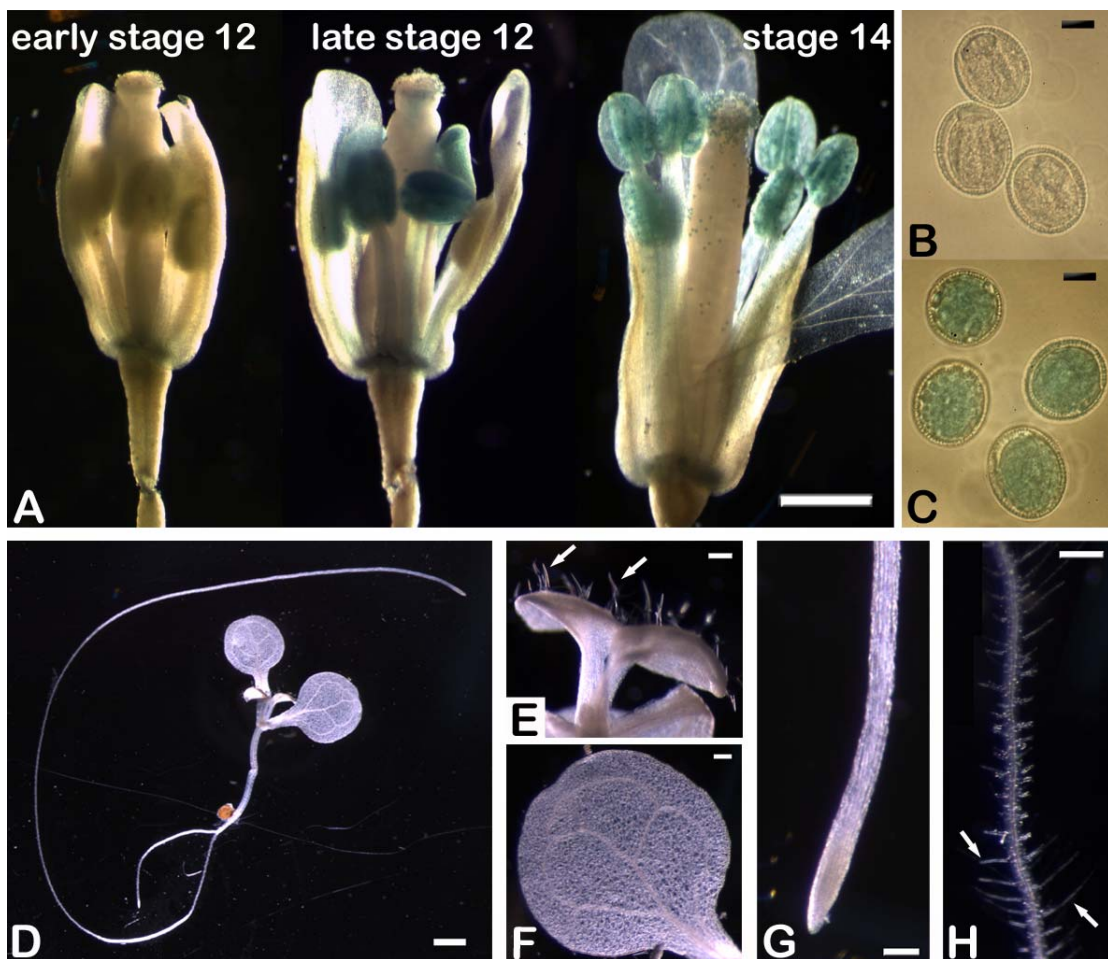


**Figure 5: Histochemical staining documenting pollen expression of a CNGC18-promoter::GUS reporter.** (A) Histochemical staining of GUS activity in flowers of the same inflorescence in stage 12 and 14, (B) WT control pollen, and (C) pollen expressing CNGC18-promoter::GUS. No GUS activity was detected in (D) young seedlings, (E) trichomes, (F) leaves, (G) roots and (H) root hairs. The size marker equals to 1 mm in A and D, 10 µm in B and C, and 200 µm in E-H.

Over 2190 publicly available microarray datasets, that were collected and processed through searchable Genevestigator database (Zimmermann et al., 2004), make it possible to perform a broader analysis and examine the expression of CNGC18 including different organs, developmental stages as well as stress conditions. The Digital Northern algorithm, which shows the expression level on each single microarray experiment and the Meta-Analyzer program, which groups the microarray profiles by tissue type were used to study the expression pattern of CNGC18 based on Gene Chip experiments. The analysis confirms the experimentally observed expression pattern with strong expression of CNGC18 in pollen, stamen and flowers, while vegetative tissues and stress samples show only background levels of CNGC18 transcripts (Fig. 6).

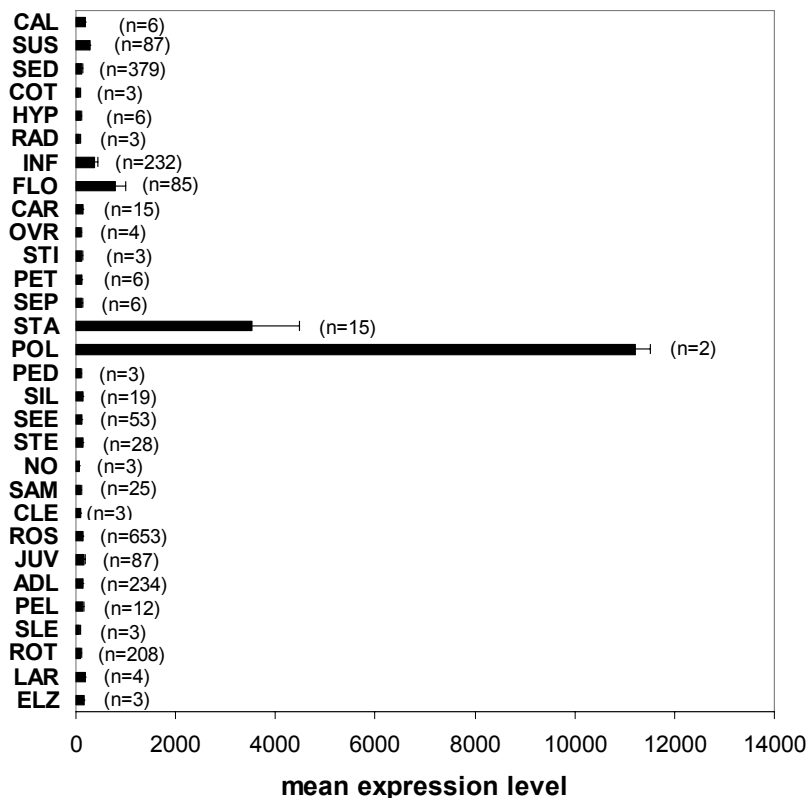


**Figure 6: Tissue specific expression of CNGC18.** The analysis was performed using the Meta-Analyzer algorithm from the Genevestigator database. Meta-Analyzer groups the expression profile of 2190 publicly available microarray data sets into tissue specific expression (n= number of microarray datasets per tissue type).

Abbreviations: CAL= callus, SUS= cell suspension culture, SED= seedling, COT= cotyledons, HYP= hypocotyls, RAD= radicle, INF= inflorescence, FLO= flower, CAR= carpel, OVR=ovary, STI= stigma, PET= petal, SEP= sepal, STA= stamen, POL= pollen, PED= pedicle, SIL= siliques, SEE= seeds, STE= stem, NO= node, SAM= shoot apical meristem, CLE= cauline leaf, ROS= rosette, JUV= juvenile leaf, ADL= adult leaf, PEL= petiole, SLE= senescent leaf, ROT= root, LAR= lateral root, ELZ= elongation zone.

### 3.2.4 CNGC18 is essential for directional pollen tube growth *in vitro*

As a starting point of testing which aspect of pollen development is compromised in *cngc18* mutants, the seed set in mature siliques was evaluated. A full seed set was observed for *cngc18-1* (-/+) (Fig. 7). This indicates that mutant pollen did not compete with and block fertilization by wild-type pollen, as observed in some classes of male sterile mutants (e.g. *aca9*, Schiott et al., 2004).

Additional pollen viability and growth studies were done with pollen tetrads produced from *cngc18-1* (-/+) plants. The *cngc18-1* allele was originally isolated in a *quartet* background (*qrt*) (McElver et al., 2001). In the *qrt* background, four pollen grains, representing all four male meiotic products, remain attached through their cell walls as a tetrad allowing simultaneous analysis (Preuss et al., 1994; Johnson-Brousseau and McCormick, 2004).

To test for defects in pollen maturation, pollen tetrads of heterozygous *cngc18-1* plants were subjected to Alexander viability staining (Alexander, 1969). Alexander solution stains the cytoplasm of viable cells in a purple-red color, while the cell walls of aborted pollen grains appear in green (Robertson et al., 2004). The results of the Alexander staining shown in Figure 7D demonstrate that all 4 pollen grains were equally stained in red and therefore are viable. Thus, CNGC18 does not appear to be required for the development of mature pollen grains.

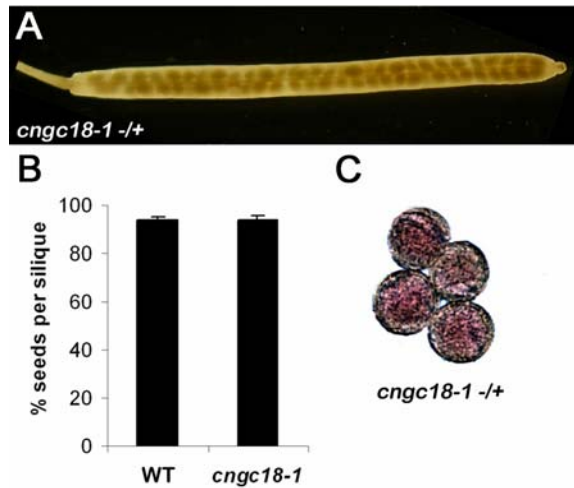


**Figure 7: Histochemical staining and seed set analysis demonstrate that *cngc18-1* pollen is normally developed and does not disrupt fertilization through wild-type pollen. (A)** Siliques of *cngc18-1* (-/+) plants have full seed set. (B) Quantification of the seed set in WT (n=5) and *cngc18-1* (n=9) siliques. (C) Representative example of a pollen tetrad of a heterozygous *cngc18-1* (-/+) plant in the *qrt* background stained with Alexander solution (Alexander, 1969).

As a next step, defects in pollen germination on agar were tested by comparing the germination frequency of control tetrads from the parental *qrt* background with those from heterozygous *cngc18-1* (-/+) plants. If the *cngc18-1* mutation blocked germination, an up to 2-fold reduction in germination frequency compared to the control should be evident. In the analysis of tetrads competent for germination (i.e. tetrads showing at least one germinated pollen grain), the base-line frequency of pollen grain germination in the *qrt* parental background was 52% (n = 2940 pollen grains). These finding are consistent with previous studies which indicate that the *qrt* mutation itself causes a reduction of *in vitro* germination frequencies (Golovkin and Reddy, 2003). Similar to the *qrt* parent, pollen grains from *cngc18-1* (-/+) showed a germination frequency of 46% (n=2848 pollen grains). The nearly identical germination frequencies indicate that the *cngc18-1* mutation did not significantly disrupt pollen germination.

While viability and germination were not affected in *cngc18-1* pollen, *in vitro* growth assays provided evidence for a cell autonomous pollen tube growth defect. In comparison to tetrads from *qrt* controls, which produced up to four normally developed pollen tubes (Fig. 8A), *cngc18-1* tetrads developed “kinky”,

short and often thin pollen tubes with high frequency (Fig. 8B-D). The “kinky” pollen tubes only grew a short distance with non-directional growth, often prematurely terminating with a bursting event.

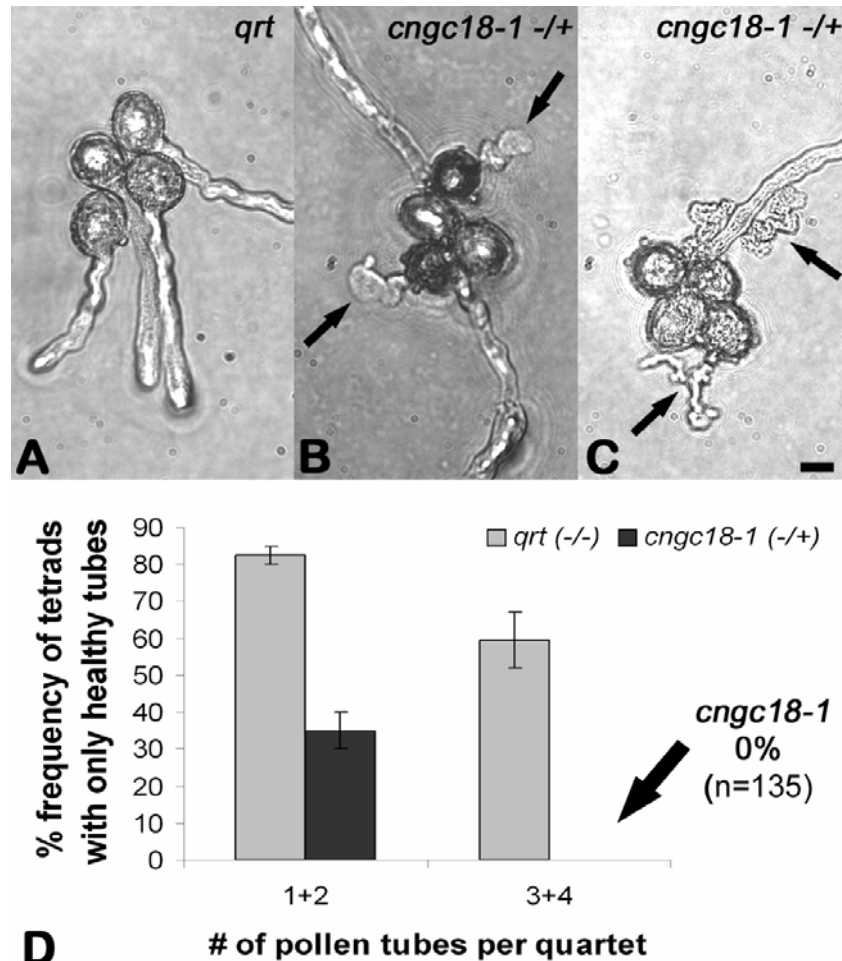


**Figure 8: *In vitro* germination of *cngc18* pollen tubes.** (A) A germinated tetrad from a *qrt* control line showing 4 normal and healthy pollen tubes. (B,C) Representative pollen tetrads from heterozygous *cngc18-1* plants (ss# 130) with two aberrant and one/two normally developed pollen tubes. The size marker corresponds to 10  $\mu\text{m}$ . (D) Frequency of tetrads in which all the germinated pollen grains produced normally developed (healthy) pollen tubes. Pollen tubes were considered aberrant if they had kinky morphologies or failed to grow more than 50  $\mu\text{m}$ . The graph shows the frequency of tetrads consisting of one or two tubes (1+2) with normal/healthy morphology, (*qrt*: n = 520, *cngc18-1*: n = 577) versus three or four pollen tubes (3+4) (*qrt*: n = 215, *cngc18-1*: n = 135). The analysis was done in three independent experiments with similar germination frequencies in each analysis. An arrow indicates that no *cngc18-1* tetrads were observed with more than two healthy tubes.

To evaluate the pollen tube growth defect, 735 wild-type and 712 *cngc18-1* tetrads were individually scored for normal/"healthy" or aberrant pollen tube morphologies. Again, the *qrt* background of *cngc18-1* plants allowed simultaneous examination of all four meiotic products, consisting of two wild-type and two mutant pollen grains. Figure 8E shows the frequency of mutant and *qrt* control tetrads that developed only normal/"healthy" pollen tubes (i.e. no aberrant morphologies). In cases where tetrads only germinated 1 or 2 pollen tubes (category 1+2), the mutant tetrads showed a dramatic reduction (approximately two-fold) in the frequency of tetrads with only "healthy" pollen tubes. This is consistent with the expectation that 50% of these tubes are segregating as mutant pollen. In the 135 cases in which the mutant tetrads produced more than 2 visible tubes (category 3+4), tetrads with more than 2 "healthy" tubes were never observed. Thus, these results demonstrate that the *cngc18* null mutation results in a pollen tube growth defect when grown *in vitro*.

### 3.2.5 *cngc18* pollen tubes cannot enter the transmitting tract

The *in vitro* pollen tube growth defect of *cngc18* was corroborated *in vivo* by histochemical staining of *cngc18-1* pollen growing in pistils of WT plants. The T-DNA of *cngc18-1* contains a  $\beta$ -glucuronidase gene (*GUS*) under the control of the pollen promoter *LAT-52* (Fig. 4) (McElver et al., 2001). This linked molecular marker makes it possible to specifically stain mutant pollen, thus differentiating between mutant and wild-type pollen tubes of heterozygous *cngc18-1* plants.

24h after manual fertilization of wild-type pistils with *cngc18-1* pollen, the pollinated pistils (flower stage 14) were dissected and stained with GUS solution (Jefferson et al., 1987; Johnson et al., 2004). For a positive control, a parallel pollination was carried out with pollen from a homozygous *cngc11-2* plant (ss# 189) that also carries the *lat52-promoter::GUS* encoding T-DNA but does not display a pollen defect. All 20 pistils that were crossed with pollen of *cngc11-2* showed GUS activity in pollen tubes growing into the transmitting tract. In contrast, none of the 10 pistils with *cngc18-1* pollen showed GUS-activity

corresponding to a pollen tube entering the transmission tract despite equal staining time and similar GUS intensity of the pollen grains (Fig. 9B, C). Instead GUS activity was only observed in the stigma area or wherever a pollen grain had fallen during the experiment. These findings are consistent with the *in vitro* observation indicating that *cngc18* pollen tube growth defect results in pollen tubes that never enter the transmitting tract.

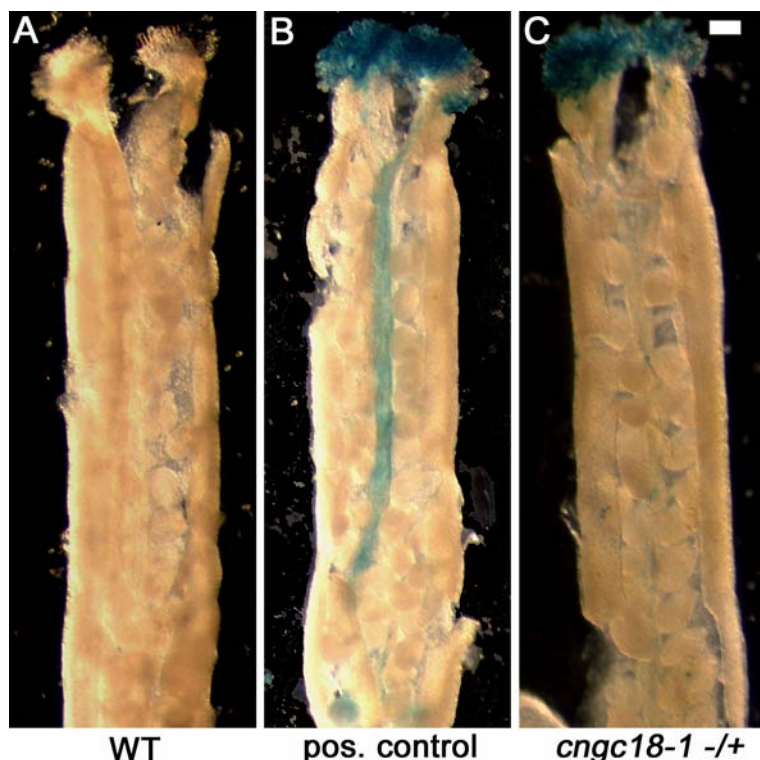


**Figure9: Histochemical staining for a T-DNA-encoded GUS-reporter demonstrates that mutant pollen never enter the transmitting tract.** Representative example of GUS-stained pistils fertilized with pollen from (A) wild-type (WT), (B) the positive control *cngc11-2* (pos. control), and (C) *cngc18-1* (-/+ ) plants (ss# 578). The T-DNA of the phenotypically silent *cngc11-2* and the male sterile *cngc18-1* plants encode the pollen specific *LAT-52::GUS* (McElver et al., 2001). Size marker for all images identifies 0.1 mm.

### 3.2.6 CNGC18 localizes to the plasma membrane at the growing pollen tube tip

The potential subcellular localization of CNGC18 was investigated in *cngc18* plants expressing a transgene encoding an N-terminal GFP-tagged CNGC18 (*GFP-CNGC18*) under the control of the pollen specific promoter of the  $\text{Ca}^{2+}$ -

pump ACA9 (Schiott et al., 2004) (Fig. A1, A5). This promoter was chosen because the frequently used CaM-35S promoter does not initiate transcription in pollen and the native CNGC18 promoter was expected to provide insufficient expression for fluorescent microscopy. To avoid possible expression in bacteria, a short non-coding sequence requiring *in planta* splicing was inserted between the promoter and the GFP open reading frame. The CNGC18 cDNA was amplified from a cDNA library according to the cDNA clone NM\_121491.2 (GI:30685090). A three Glycin-linker was added to the 5' end of the CNGC18 cDNA.

*GFP-CNGC18* restored Mendelian segregation in the T2 generation in 41 of 42 *cngc18-1* lines. Complementation of the male sterile phenotype by *GFP-CNGC18* was confirmed through PCR analysis with primers (886k, 886c, and 640) that do not amplify the cDNA. The GFP fluorescence level was analyzed simultaneously in pollen of wild-type and all 41 *cngc18-1* lines complemented with *GFP-CNGC18*. Wild-type pollen did not show fluorescence at the GFP filter settings while 12 of the 41 complemented lines displayed detectable GFP fluorescence.

To investigate the potential subcellular localization, pollen of complemented *cngc18-1* plants expressing *GFP-CNGC18* were germinated *in vitro* and analyzed by confocal microscopy imaging. Pollen expressing GFP and ACA9-YFP were germinated and analyzed in parallel as markers for the cytosol and plasma membrane respectively (Fig. 10A, B). In comparison to these controls, *GFP-CNGC18* predominantly localizes in the cell perimeter of the growing pollen tube consistent with a tip-focused plasma membrane localization. In addition, small fluorescent vesicles that move with the cytoplasmic streaming were evident.

The localization of *GFP-CNGC18* was also observed during initiation of pollen tube germination. While early staged hydrated pollen grains displayed a diffuse *GFP-CNGC18* pattern that could not be attributed to any specific compartment (Fig. 11B-F) later stages showed a polarized *GFP-CNGC18* localization

consistent with the plasma membrane at the emerging bulge, the presumed point of pollen tube emergence (Fig. 10F and 11G-N). This asymmetric localization at the growing tip became even more evident in later stage when a short pollen tube emerged and in comparison to the ACA9-YFP localization at the plasma membrane of the entire pollen grain and tube (Fig. 10 E, G). Focal section through the entire pollen grain confirmed that the observed localization pattern is indeed asymmetric and not an imaging artifact (Fig. 11).

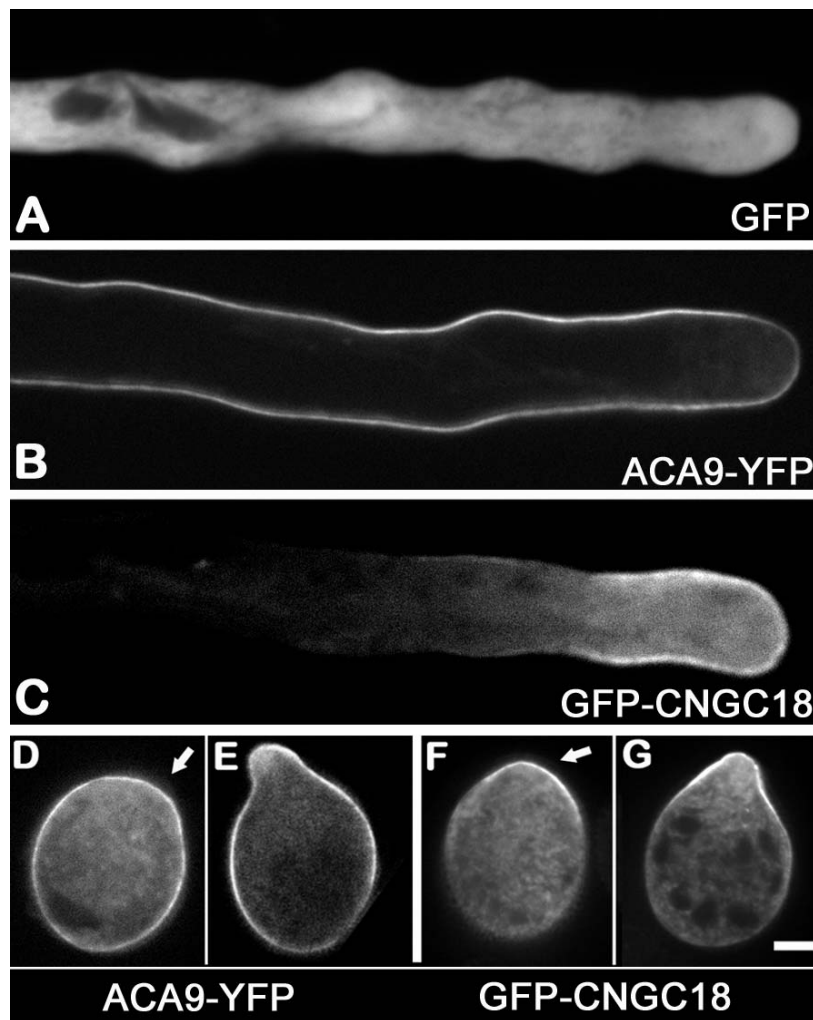


**Figure 10: Confocal fluorescence images showing polarized tip-localization of GFP-CNGC18.** Pollen were germinated *in vitro* and analyzed in parallel: (A) WT pollen expressing GFP, (B, D, and E) *aca9-1* mutant pollen complemented with ACA9-YFP (Schrott et al., 2004) and (C, F, and G) *cngc18-1* pollen complemented with GFP-CNGC18. Three developmental stages were analyzed: (A-C) fully grown pollen tubes (D, F) pollen grains with initial germination bulge, and (E, G) pollen grains with emerging tip. To exclude possible background auto-

fluorescence, WT pollen was imaged side-by-side with identical camera and microscope settings. Exposure times in the images shown are: A: 0.5 sec; B: 3 sec; C-G: 6 sec. Size markers correspond to 5  $\mu$ m.

In conclusion, the correlation between the pollen tube growth defect of *cngc18* mutants and the localization of CNGC18 at the tip of growing pollen tubes suggest that CNGC18 functions in regulation of directional pollen tube growth.

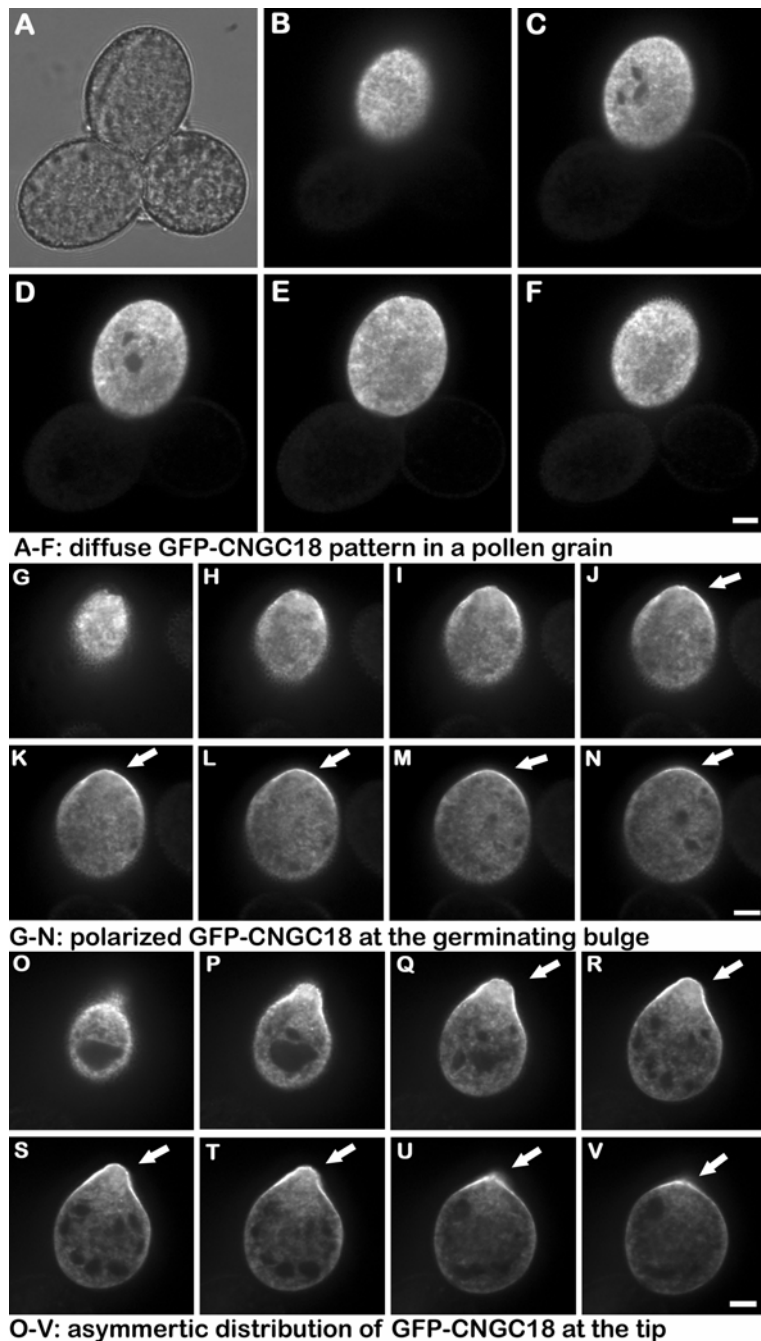


**Figure 11: Different focal sections through pollen grains with asymmetric localization of GFP-CNGC18 at the germinating tip.** (A) Differential Interference Contrast (DIC) image of a pollen tetrad (fourth grain below focal plane). (B-F) Fluorescent images of the pollen tetrad shown in (A) with one GFP-CNGC18 expressing (top) and two wild-type pollen grains (bottom two). (G-N) Fluorescent images showing polarized localization of GFP-CNGC18 at the site of tip formation (indicated by arrow). (O-V) Fluorescent images showing tip localization of GFP-CNGC18 in an emerged pollen tube. Exposure time is 6 sec in all fluorescent images. All size markers equal 5  $\mu\text{m}$ .

### 3.3 Hypersensitivity responses of *cngc9-2* to Ca<sup>2+</sup> stress

During the phenotypic analysis of the responses of several *cngc* mutants to abiotic and biotic stress (compare chapter 3.1), a hypersensitivity response of *cngc9-2* to elevated CaCl<sub>2</sub> levels in the plant growth media was observed. Since characterization of male sterile *cngc18* mutants was the main focus of this thesis, only initial studies to investigate the *cngc9-2* (SAIL\_736\_D02) were undertaken providing first leads for future in depth analyses.

#### 3.3.1 Phenotypic analysis of *cngc9-2* plants

When *cngc9-2* plants were tested under abiotic and biotic stress conditions in the initial phenotype screen, altered responses in comparison to wild-type to osmotic and Ca<sup>2+</sup> stress were observed. While *cngc9-2* plants appeared to be less sensitive to high concentrations of mannitol as evident by significantly longer roots (Fig. 12, p-value: 5.27E-08), elevated levels of CaCl<sub>2</sub> resulted in a stunted growth of *cngc9-2* seedlings, as well as wavy looking, more branched roots (Fig. 13A, C). After 18 days of growth on 20 mM CaCl<sub>2</sub>, some plants developed callus-like structures in the shoot that could be attributed to any organ leading to eventual death of the plant (Fig. 13E). Rescue efforts by transferring the plants to standard ½ MS media were not successful. Other abiotic stresses such as 100 mM NaCl or KCl did not result in a similar phenotype.

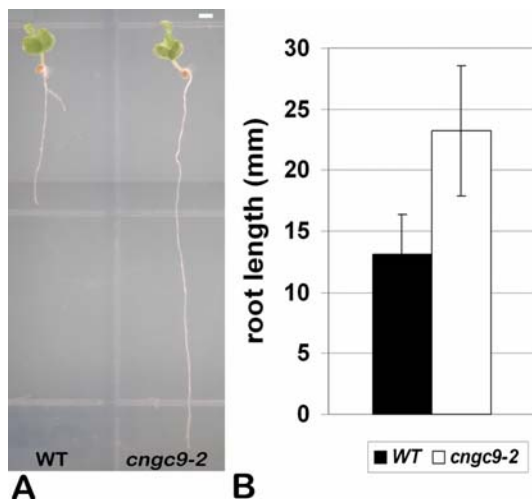


**Figure 12: Root length of *cngc9-2* plants germinated on growth media containing 150 mM mannitol.** A: representative example a 2 week old wild-type and *cngc9-2* seedling grown under an 8-h/16-h-dark regime. Due to the length of the root of the *cngc9-2* plant two photos were taken and later combined in Adobe Photoshop. The size marker equals 1 mm. B: Average root length of WT and *cngc9-2* seedlings ( $n=24$ , each). Error bars indicate the standard deviation.

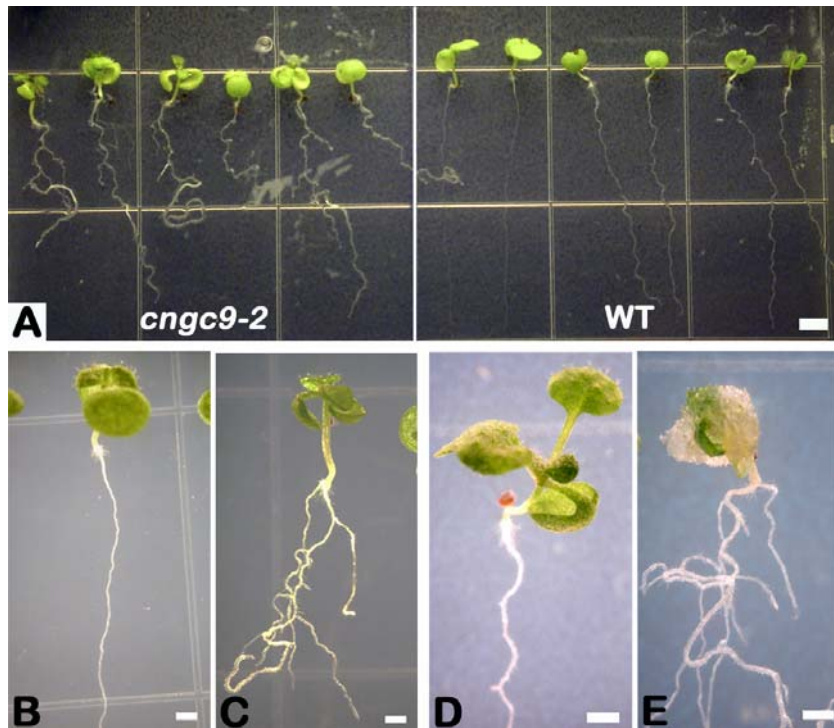


**Figure 13: *cngc9-2* plants show altered shoot and root morphologies when grown under  $\text{CaCl}_2$  stress.** (A) 10 days old wild-type and *cngc9-2* seedlings grown on  $\frac{1}{2}$  MS media supplemented with 20 mM  $\text{CaCl}_2$  under 8-h-light/16-h-dark conditions. Close up view of a representative 10 days old wild-type (B) and *cngc9-2* (C) seedling. 8 days later, the *cngc9-2* plant (E) developed callus-like tissue in contrast to wild-type (D). The size marker in A corresponds to 3 mm, while the markers in B-E represent 1 mm.

To test the relationship between  $\text{CaCl}_2$  and the observed phenotypes, *cngc9-2* plants were subjected to standard  $\frac{1}{2}$  MS media supplemented with 0 to 50 mM  $\text{CaCl}_2$ . In contrast to the initial experiments, these plants were kept under a 16-h-light/8-h-dark regime at 28°C to accelerate the development. Under these conditions 20 mM  $\text{CaCl}_2$  had a much milder effect, while plants grown at 30 mM  $\text{CaCl}_2$  displayed a comparable phenotype (Fig. 14B, C). At 40 and 50 mM, callus-like tissue formation was observed much earlier in the development of the seedlings (around formation of first true leaves), subsequently leading to earlier death of the plants (Fig. 14D, E). Interestingly, not all of the plants showed the same level of callus-like tissue formation, however the root response was observed for all the *cngc9-2* plants tested.

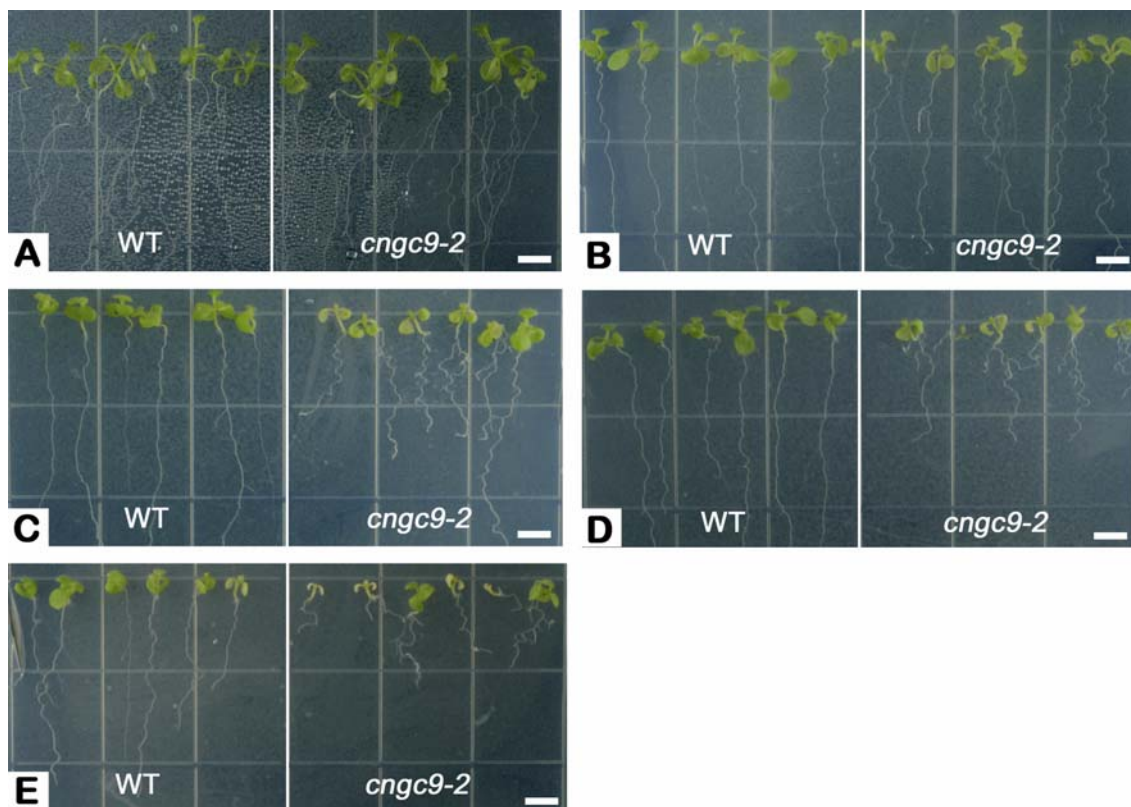


**Figure 14: Responses of wild-type and *cngc9-2* plants to increased  $\text{CaCl}_2$  levels.** 10 days old wild-type and *cngc9-2* seedling were grown under 16-h-light/8-h-darkness on standard  $\frac{1}{2}$  MS media supplemented with (A) 0 mM, (B) 20 mM, (C) 30 mM, (D) 40 mM, and (E) 50 mM  $\text{CaCl}_2$ .  $\text{CaCl}_2$  was added to the media after autoclaving.

Closer investigation of the root and shoot tissue of  $\text{Ca}^{2+}$  grown plants revealed abnormal morphologies on the cellular level for *cngc9-2* plants in both root and shoot (Fig. 15). Tissue without any clear organization was frequently observed which strongly reminded of callus or crown gall.

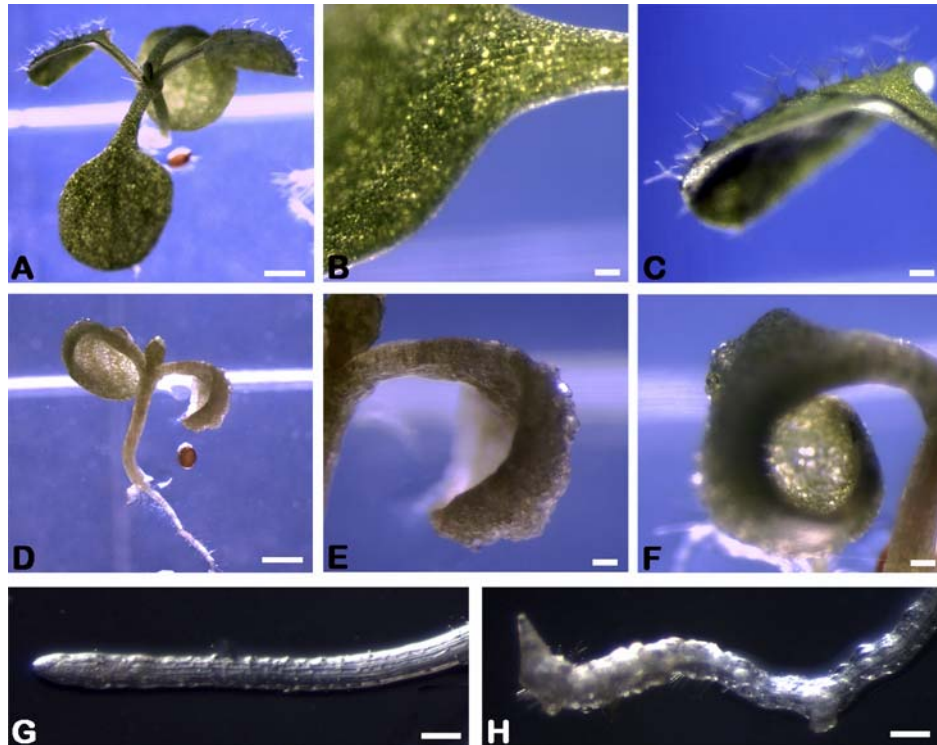


**Figure 15:  $\text{Ca}^{2+}$  responses of *cngc9-2* seedling.** Plants were grown on 40 mM  $\text{CaCl}_2$  at a 16-h-/8-h-dark regime at 28°C. The image illustrates representative examples of (A) a wild-type seedling and (D) a side-by-side grown *cngc9-2* mutant. Close up image of  $\text{Ca}^{2+}$ -grown wild-type leaves (B, C) and root (G). Altered tissue structures in leaves (E, F) and root (H) of *cngc9-2* plants that were grown on high  $\text{Ca}^{2+}$  media.

### 3.3.2 Different CNGC9 expression levels in two independent T-DNA disruption lines causes different $\text{Ca}^{2+}$ sensitivity

To test if the observed phenotype was linked to disruption of *CNGC9* (At4g30560), a second site insertion was isolated by PCR diagnostics and a complementation approach was initiated. Sequencing of the *CNGC9*/T-DNA-left border fragment revealed that *cngc9-2* (SAIL\_736\_D02) is located 35bp

upstream of the start codon, while *cngc9-4* (SALK\_026086) disrupts intron 5 of the CNGC9 open reading frame (Fig. 16).

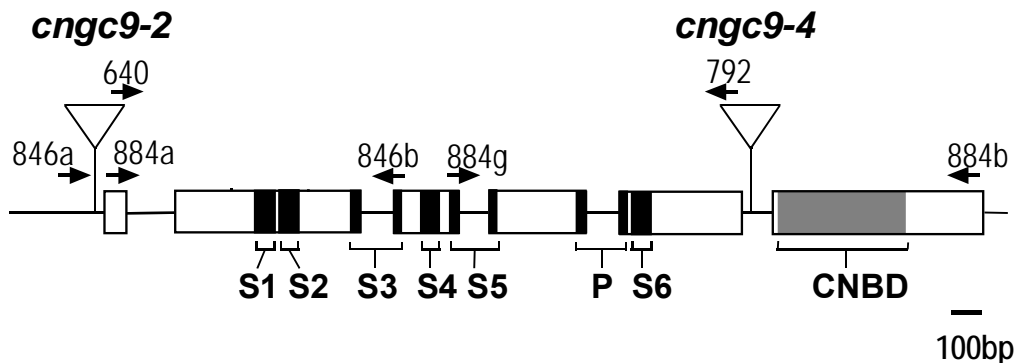


**Figure 16: Diagram showing CNGC9 T-DNA insertions.** The diagram illustrates the genomic structure of CNGC9 (At4g30560) including the T-DNA insertion sites (triangles) of *cngc9-2* and *9-4*, located 35 bp upstream and 1965 bp downstream of the start codon respectively. □ = exons, - = introns, ■ = trans-membrane domains (S1-6) and pore domain (P), ■ = cyclic nucleotide binding domain (CNBD), → = position of the primers.

When *cngc9-4* was tested under high  $\text{Ca}^{2+}$  conditions, no  $\text{Ca}^{2+}$  hypersensitivity phenotype comparable to *cngc9-2* was observed. To test whether a potentially truncated protein in either of the mutants was responsible for the differences between the two alleles, total RNA was isolated from inflorescence and root tissue, where CNGC9 is expected to be expressed (compare section 3.3.4). RT-PCR diagnostics revealed increased transcript levels in *cngc9-2* mutants, while CNGC9 transcripts were not detect in roots of *cngc9-4* plants (Fig. 17). RT-PCR from RNA of *cngc9-4* flowers resulted in a very faint product at 30 PCR cycles, indicating leaky expression. These results suggest that elevated transcript levels in *cngc9-2* might cause the observed phenotypes on high  $\text{Ca}^{2+}$  media, while loss or strong reduction of CNGC9 do not result in a noticeable change in *cngc9-4* plants.

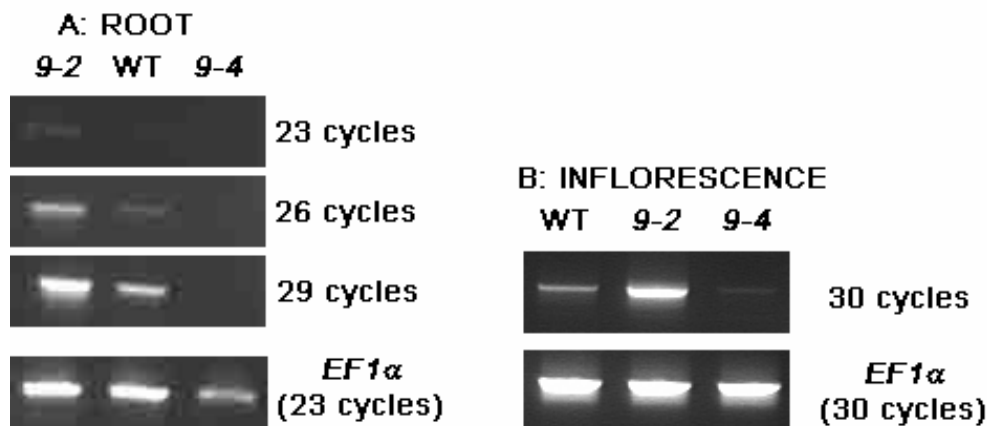


**Figure 17: Analysis of the CNGC9 expression levels by RT-PCR diagnostics.** RNA for the RT-PCR analysis was extracted from root tissue (A) and inflorescences (B) of wild-type (WT), *cngc9-2* (9-2) and *cngc9-4* (9-4) plants.

Increased transcript levels in *cngc9-2* plants can also explain the results of a complementation approach, which was started prior to the isolation of the second allele. In this approach, a 5.27 kb genomic construct (ps# 633, Fig. A2, A8) subcloned from the BAC clone *F17I23* (Mozo et al., 1998) containing the predicted open reading frame of CNGC9 (At4g30560), as well as a 1452 bp upstream and 1108 bp downstream untranslated region did not complement the observed phenotypes of *cngc9-2* plants.

### 3.3.3 *cngc9-2* plants accumulate more Ca<sup>2+</sup> when grown under high Ca<sup>2+</sup> conditions

In plants and animals CNGCs are unspecific channels whose physiological function depends on Ca<sup>2+</sup> permeability (Very and Sentenac, 2002; Kaupp and Seifert, 2002; Talke et al., 2003). To study whether the increased transcript levels of CNGC9 change the ion homeostasis in *cngc9-2* mutants, the ion accumulation profile was determined by inductively coupled plasma spectroscopy (ICP). In this experiment, wild-type and *cngc9-2* mutants were grown on ½ MS media supplemented with 0, 10, and 20 mM CaCl<sub>2</sub>. Figure 18 shows the average ion accumulation of 10 samples (shoots and root of 10 plants each) for Ca, K, Na, P

and S. Out of the 30 elements (mainly metals) that were spectroscopically analyzed by ICP-analysis, Ca, K, and Na were selected based on electrophysiological studies in plant and animals that suggest that CNGCs are mainly permeable to  $\text{Ca}^{2+}$ ,  $\text{K}^+$ , or  $\text{Na}^+$ . To demonstrate that there are no irregularities in the samples, the relative P and S content are indicated. Comparison of the ion profile of wild-type and mutant plants revealed that *cngc9-2* plants specifically accumulate more  $\text{Ca}^{2+}$  (but not  $\text{K}^+$  or  $\text{Na}^+$ ) when grown on media supplemented with 20 mM  $\text{CaCl}_2$  ( $p$ -value 0.03). These findings suggest that the elevated CNGC9 transcript levels in *cngc9-2* plants result in increased  $\text{Ca}^{2+}$  accumulation when grown on high  $\text{Ca}^{2+}$ . Further ICP analysis of plants grown under abiotic stress conditions such as non-physiological  $\text{K}^+$ ,  $\text{Na}^+$  or  $\text{Mg}^{2+}$  level is needed to determine if this increased accumulation is specific to  $\text{Ca}^{2+}$ .

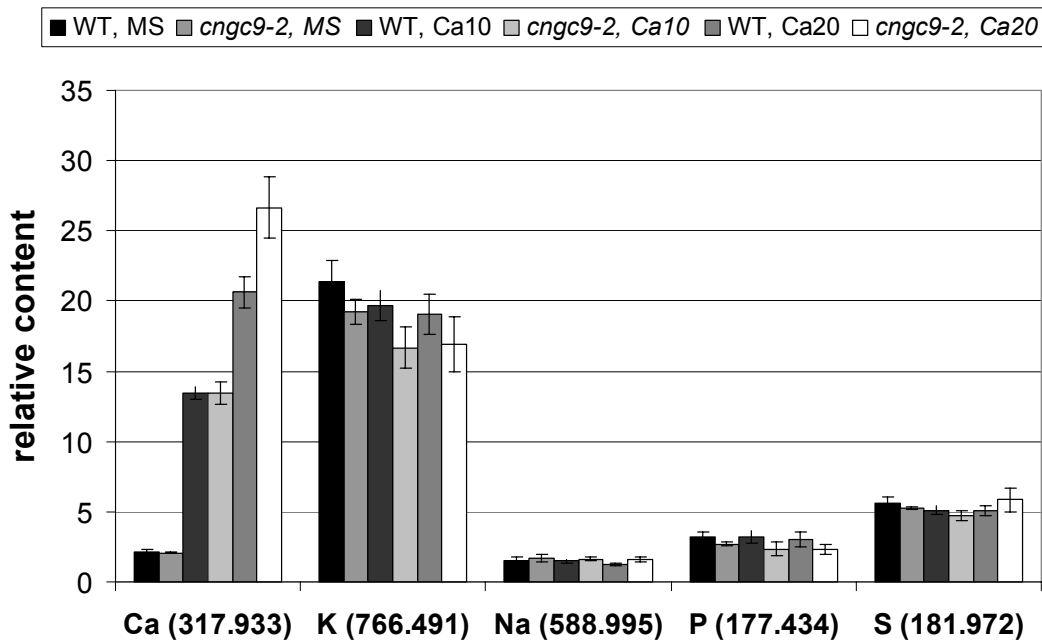


**Figure 18: Relative cation content in wild-type and *cngc9-2* plants grown under  $\text{Ca}^{2+}$  stress.** Wild-type and *cngc9-2* plants were grown side by side on standard  $\frac{1}{2}$  MS media supplemented with 0 mM (MS), 10 mM (Ca10), and 20 mM  $\text{CaCl}_2$  (Ca20). The root and shoot material of 10 plants each were combined and the relative ion content was determined by Inductively Coupled Plasma Spectroscopy (ICP) analysis. The diagram shows the average Ca, K, Na, P and S content of 10 samples each including the standard error, as determined by spectral analysis at 317.933 nm (Ca), 766.491 nm (K), 588.995 nm (Na) 177.434 nm (P) and 181.972 nm (S). Based on previous studies that demonstrated that the  $\text{Mg}^{2+}$  content is in direct proportional to the amount of sample used in the experiment, the data was normalized to the  $\text{Mg}^{2+}$  level in each sample (Lahner et al., 2003).

### 3.3.4 Expression pattern of CNGC9

To study the expression pattern of *CNGC9* in *planta*, a 1.04 kb *CNGC9*-promotor was fused to a  $\beta$ -glucuronidase gene (ps# 826, Fig. A9). Initial analysis of the expression pattern in the T1 generation after transformation revealed expression in the pistil and anthers in 50% of the tested lines (Fig. 19A-B). These findings are consistent with an analysis of 2190 publicly available microarray expression datasets through the Genevestigator website (Zimmermann et al., 2004). However, in depth analysis of seedlings of the next generation of plants expressing *CNGC9*promoter::*GUS* (T2) are required to confirm *CNGC9* expression in roots as implicated by RT-PCR experiments (section 3.3.2) and profiling through the Genevestigator website(Fig. 19C).

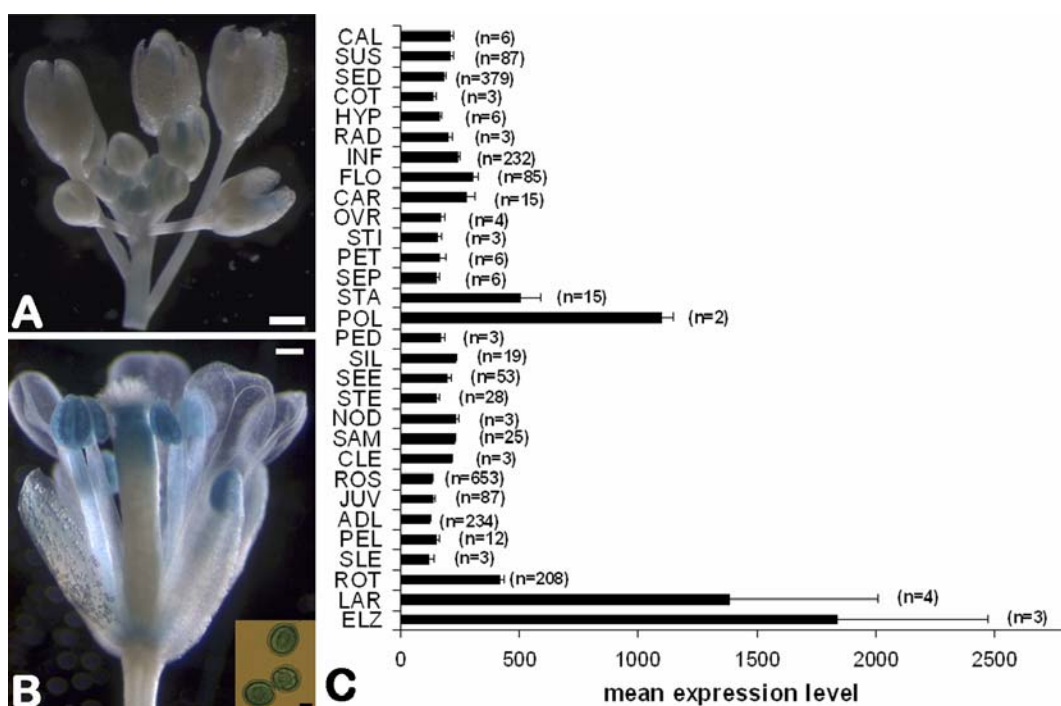


**Figure 19: Expression analysis of CNGC9.** (A, B) Floral tissue with expression of *CNGC9*promoter::*GUS*. (C) Expression pattern of *CNGC9* determined by the Meta-Analyzer algorithm from the Genevestigator database (<https://www.genevestigator.ethz.ch/at/index.php?page=7>). n= number of microarray datasets per tissue type.

Abbreviations: CAL= callus, SUS= cell suspension culture, SED= seedling, COT= cotyledons, HYP= hypocotyls, RAD= radicle, INF= inflorescence, FLO= flower, CAR= carpel, OVR=ovary, STI= stigma, PET= petal, SEP= sepal, STA= stamen, POL= pollen, PED= pedicel, SIL= siliques, SEE= seeds, STE= stem, NOD= node, SAM= shoot apical meristem, CLE= cauline leaf, ROS= rosette, JUV= juvenile leaf, ADL= adult leaf, PEL= petiole, SLE= senescent leaf, ROT= root, LAR= lateral root, ELZ= elongation zone.

## 4 Discussion

The studies present in this thesis provide evidence that a number of CNGCs are involved in plant development and responses to abiotic stress. An initial phenotypic analysis of gene disruptions in 10 different CNGCs resulted in the identification of 7 mutants with altered response to abiotic stress or general changes in the plant development (Tab. 3). The male sterile phenotype of *cngc18* and the Ca<sup>2+</sup> hypersensitivity of *cngc9-2* lines were chosen to study the function of CNGCs in detail and reveal further insight into ion signaling in plants.

It is important to note that a late germination phenotype for *cngc3* lines was also observed by another group when germinated on media with high Na<sup>+</sup> levels (Gobert et al., 2006). However, in this screen, late germination was observed for *cngc3* lines grown under K<sup>+</sup> starvation but not under Na<sup>+</sup> stress. It is not clear if possible explanations for this discrepancy are the different light and growth conditions used in each experiment or if the sample size in this screen was too small to detect an effect of Na<sup>+</sup>. More studies with different K<sup>+</sup>, Na<sup>+</sup> and Ca<sup>2+</sup> ratios are necessary to investigate the channels permeability and specificity of the effects of abiotic stresses.

### 4.1 Is CNGC9 a Ca<sup>2+</sup> permeable channel involved in plant hormone signaling?

When responses of *cngc9-2* plants to abiotic and biotic stress were tested, two distinct phenotypes were discovered. While *cngc9-2* plants appeared to be more resistant to osmotic stress as evident by longer roots (Fig. 12), high levels of Ca<sup>2+</sup> altered the plants morphology dramatically leading to callus-like structure and subsequent death (Fig. 13-15).

Formation of callus is a natural phenomenon initiated by bacteria or insects through changes to the physiological ratios of the plant hormones auxin and cytokinin. Callus formation is also observed when tissue explants are incubate on media containing auxins and cytokinins in a 5:1 ratio (Mathur and Koncz, 1998).

The development of callus-like tissue in *cngc9-2* plants suggests that either the internal ratio of auxin and/or cytokinin is changed or the signal perception of one or both of these hormones is altered upon  $\text{Ca}^{2+}$  stress. Crosses with plants expressing the auxin reporter DR5::GUS and the cytokinin reporter ARR5::GUS (Ulmasov et al., 1997; D'Agostino et al., 2000) are underway to investigate these hypotheses. Tests with leaf explants on media with different auxin/cytokinin ratios are necessary to determine if auxin or cytokinin responses (or both) are perturbed in *cngc9-2* plants (Inoue et al., 2001).

RT-PCR analysis revealed increased CNGC9 transcript levels in *cngc9-2* plants with T-DNA disruption in the promoter region (Fig. 17). In contrast, the CNGC9 transcript levels are strongly reduced in *cngc9-4* plants with wild-type-like phenotype. Studies to test whether the observed phenotype for *cngc9-2* is clearly linked to overexpression of CNGC9 are underway. In the course of this thesis two GFP-cDNA fusion constructs (N-and C-terminal fusion, ps# 791 and 776 respectively) controlled by a *CaMV-35S* promoter have been cloned and transformed into plants (Fig. A2, A10, and A11). The isolated N-TAP-GFP-CNGC9 and CNGC9-GFP over-expressing lines will be used to study a potential  $\text{Ca}^{2+}$  hypersensitivity phenotype and the subcellular localization pattern of CNGC9. In addition, three backcrosses of *cngc9-2* lines have been generated and homozygous lines currently processed for subsequent phenotypic analysis.

ICP profiling revealed that *cngc9-2* plants specifically accumulate more  $\text{Ca}^{2+}$  than wild-type plants when grown on media supplemented with 20 mM  $\text{CaCl}_2$ . These findings support the working hypothesis that  $\text{Ca}^{2+}$  induced callus formation in *cngc9-2* might be a consequence of increased  $\text{Ca}^{2+}$  uptake due to CNGC9 over-expression. ICP studies with higher  $\text{Ca}^{2+}$  levels as well as different  $\text{Ca}^{2+}$ ,  $\text{K}^+$  and  $\text{Na}^+$  ratios in the media (including *cngc9-4* as negative control) are necessary to further investigate the ion accumulation phenotype of *cngc9-2* plants. However, these initial studies provide *in planta* indications that CNGCs are  $\text{Ca}^{2+}$  permeable channels.

## 4.2 CNGC18 is essential for polarized tip growth

Genetic evidence presented here identifies one of the 20 CNGCs encoded in *Arabidopsis* as essential for the plant's life cycle. A lethal defect in the male gametophyte was observed for two independent T-DNA gene disruptions in CNGC18, as shown by the inability of mutant genes to be transmitted through pollen (Tab. 4). This defect was reversed by the expression of a wild-type CNGC18 under the control of its native promoter, indicating that the defect was the result of a loss of function mutation. The pollen defect is consistent with expression profiling and promoter-GUS reporter analyses that indicate that CNGC18 is expressed primarily in pollen, with no significant expression in any other cell types (Fig. 6, 7). Although two published expression profiling datasets (Honys and Twell, 2004; Pina et al., 2005) reveal significant expression in mature pollen of at least 6 other CNGCs, the observation of a *cngc18* male sterility phenotype indicates that these five additional isoforms are not functionally redundant with CNGC18.

While mutations in other CNGCs have been reported in plants and animals, none have been shown to result in a lethal defect. In animals, multiple CNGCs (subunits/isoforms A3, B1 and B3) have been found to be expressed in mammalian sperm suggesting a role in male reproduction in animals (Kaupp and Seifert, 2002). However, mice with a gene disruption of isoform A3 are fertile (Biel et al., 1999). Whether the two additional sperm expressed isoforms provide functional redundancy is not known (Kaupp and Seifert, 2002).

## 4.3 *cngc18* defines a unique pollen tube growth phenotype

Two lines of evidence indicate that the underlying cause of pollen sterility in *cngc18* loss-of-function mutants is the failure of pollen tubes to grow into the transmitting tract of the pistil. First, when germinated *in vitro*, *cngc18* pollen appeared to develop as "kinky" pollen tubes, always short, often thin, and frequently terminated with a bursted tip (Fig. 8B-D). Second, staining of a GUS marker linked to the *cngc18-1* mutation demonstrated that *cngc18* mutant pollen tubes are not capable of growing into the transmitting tract (Fig. 9). Thus, both *in*

*vitro* and *in vivo* experiments support the contention that the primary defect is a failure of pollen tubes to undergo normal directional tip growth.

A reasonable expectation is that more than 13,900 genes could be involved in controlling the many aspects of pollen development (Honys and Twell, 2004), including a large number of genes encoding components necessary for directional growth. While many pollen development mutations have been isolated, relatively few have been characterized that affect pollen tube growth. For example, in a mutant screen of more than 10,000 T-DNA mutant plants, 30 mutations called *hapless* (*hap*) were identified that disrupted some aspect of the male gametophyte (Johnson et al., 2004). Among these, 12 mutants were found to produce pollen that failed to grow into the transmitting tract, as observed here for *cngc18-1* (Fig. 4). However, within this category of mutants, there can be multiple causes, including a failure of the pollen to germinate or undergo directional growth.

The potassium channels SPIK1 (AKT6) and TPK4 are the only channels from pollen that have been characterized to date (Mouline et al., 2002; Becker et al., 2004). Homozygous *spik1* and *tpk4* mutants both exhibit significant reduction in potassium influx in pollen, but only *spik1* pollen displays reduced pollen tube growth and fitness. While some of the *spik1* pollen tubes do not grow properly, more than 60% of the pollen grains germinate to healthy fully elongated pollen tubes (Mouline et al., 2002). In contrast, *in vitro* and *in vivo* studies presented here demonstrate that *cngc18* pollen never develops healthy pollen tubes that can enter the transmitting tract for fertilization (Fig. 8 and 9).

Another category of pollen mutants are those with a defect in some aspect of directional growth or fertilization, but unlike *cngc18* pollen, are otherwise still capable of growing tubes into the transmitting tract. For example, a knockout of an amino acid γ-amino butyric acid (GABA) transaminase, POP2, results in pollen tubes with a severe defect in locating ovules (Palanivelu et al., 2003). In contrast, a knockout of the Ca<sup>2+</sup> pump ACA9 results in pollen tubes that can still undergo directional growth and locate ovules, but exhibit a partial male sterility phenotype due to reduced pollen tube growth and a defect in discharging sperm.

Within this second category of pollen mutants, the most relevant ones to the *cngc18* phenotype are those with apparent defects in tip growth morphologies. For example, similar “kinky” pollen tubes have been described for *kinky pollen (kip)*, which encodes a “SABRE-like” protein, *vanguard1 (vdg1)* which encodes a pectin methyl esterase, and *crinkle (crk)*, an EMS mutant selected for its root hair defect that disrupts nodulation in *Lotus japonicus* (Procissi et al., 2001; Tansengco et al., 2004; Jiang et al., 2005). However, in contrast to *cngc18*, which appears to cause complete male sterility, pollen from these other mutants can all still grow into the transmitting tract and fertilize ovules.

#### 4.3.1 A calcium signaling CNGC paradigm

Research on plant and animal CNGCs provides a strong precedent for hypothesizing that the channel activity of CNGC18 is: 1) activated by cAMP and/or cGMP, 2) suppressed by  $\text{Ca}^{2+}/\text{CaM}$ , and 3) provides a pathway for  $\text{Ca}^{2+}$  influx.

In animals, CNGCs are considered non-specific cation channels, whose physiological functions, for example in photoreceptors and olfactory nerves, are dependent on their ability to carry an inward  $\text{Ca}^{2+}$  current (Zufall et al., 1997; Kaupp and Seifert, 2002). CNGCs provide one of the three major sources of  $\text{Ca}^{2+}$  influx in animal cells (Zufall et al., 1997). Despite involvement in different signal transduction mechanisms, CNGCs all share activation through cNMP and deactivation through  $\text{Ca}^{2+}/\text{CaM}$  (Zufall et al., 1997; Kaupp and Seifert, 2002).

In plants, electrophysiological studies provide evidence for CNGC activation by cAMP and cGMP (Leng et al., 1999; Leng et al., 2002; Balague et al., 2003). High affinity binding of  $\text{Ca}^{2+}/\text{CaM}$  has the opposite effect and blocks cNMP induced transport in a  $\text{Ca}^{2+}$  dependent manner (Kohler and Neuhaus, 2000; Arazi et al., 2000; Hua et al., 2003b). Similar to animals, CNGCs in plants have been correlated with  $\text{Ca}^{2+}$ ,  $\text{K}^+$  and in some cases  $\text{Na}^+$  influx in electrophysiological experiments and heterologous expression in yeast mutants (Leng et al., 1999; Arazi et al., 1999; Leng et al., 2002; Balague et al., 2003; Hua et al., 2003a). Although further studies are needed to confirm ion conductance properties of

CNGCs in plant cells, the current paradigm supports a working model for CNGC18 as a cNMP and  $\text{Ca}^{2+}$ /CaM regulated unspecific cation channel with  $\text{Ca}^{2+}$  permeability.

#### 4.3.2 Asymmetric subcellular localization of CNGC18

Confocal microscopy of a GFP-tagged CNGC18 in pollen revealed two distinctive features of its subcellular localization. First, most of the fluorescent GFP signal was observed at the cell perimeter (Fig. 10C), consistent with a plasma membrane localization, but distinct from previously reported ER or Golgi localization (Parton et al., 2003). Second, for the plasma membrane associated GFP-CNGC18, the primary site of accumulation was at the growing tip in pollen tubes and germinating pollen grains (Fig. 10C, F, and G). This asymmetric pattern was very distinct from a more uniform distribution of the YFP-tagged plasma membrane  $\text{Ca}^{2+}$  pump, ACA9 (Fig. 10B, D and E) (Schiott et al., 2004). The polarized distribution of GFP-CNGC18 in germinating pollen grains and tubes implies a localized function of CNGC18 in the vicinity of the growing tip, as opposed to a general cellular function associated with regulating the membrane potential or nutritional uptake of cations.

A caveat to using a GFP-tag for subcellular localization is that targeting artifacts may arise from either over-expression, or the tag itself. While such artifacts cannot be ruled out completely, it is important to note that the distinctive features noted above were evident even in transgenic plant lines for which the level of GFP fluorescence was at its lower limits of detection. Thus, at the lower limits of sensitivity for a GFP imaging strategy, the localization appears as presented in Figure 10 and 11. It is also important to note that the *GFP-CNGC18* construct provided complementation in 41 of 42 independent transgenic lines. These findings suggest that at least some of the observed GFP-tagged CNGC18 was targeted to a functionally correct location.

A resulting working hypothesis is that the plasma membrane represents the primary functional location of CNGC18. Such a plasma membrane localization is consistent with observations supporting the same location for two other plant

CNGCs (HvCBT1, NtCBP4) (Schuurink et al., 1998; Arazi et al., 1999). Nevertheless, significant levels of fluorescence were also observed associated with vesicles. While it is possible that the abundance of the plant GFP-CNGC18 in non-plasma membrane locations is an artifact of over-expression, it is also possible that such vesicles normally harbor a small amount of CNGC18, and function in 1) the trafficking of proteins into and out of the plasma membrane to create a tip localized distribution of CNGC18, or as 2) an internal source of  $\text{Ca}^{2+}$  that can be released by a cNMP signal and used to trigger a downstream  $\text{Ca}^{2+}$  signaling pathway.

The asymmetric localization of GFP-CNGC 18 at the point of tip growth also correlates with the location of a tip-focused cytosolic  $\text{Ca}^{2+}$  gradient (Obermeyer and Weisenseel, 1991; Rathore et al., 1991; Pierson et al., 1994). Tip-focused  $\text{Ca}^{2+}$  signaling has been found to be crucial for polarized growth in many systems, including pollen tubes, root hairs, fungal hyphae, polar axis formation of the zygote and rhizoid growth in the brown algae *Fucus*, and neuronal growth cones (Miller et al., 1992; Jackson and Heath, 1993; Pierson et al., 1996; Taylor et al., 1996; Pu and Robinson, 1998; Very and Davies, 2000; Zheng, 2000; Carol and Dolan, 2002; Nishiyama et al., 2003). In several systems, putative  $\text{Ca}^{2+}$  channels have been localized to the region of tip growth or bud emergence (such as yeast budding) (Fischer et al., 1997; Paidhungat and Garrett, 1997), and *Fucus* rhizoid (Shaw and Quatrano, 1996). While it is worth considering the possibility that CNGC18 activity contributes to the tip focused  $\text{Ca}^{2+}$  gradient in pollen, no comparisons are yet possible with the locations and functions of many other putative  $\text{Ca}^{2+}$  channels expected to function in pollen.

#### 4.3.3 A model for CNGC18 in polarized tip growth

Once pollen grains have germinated and initiated tip growth, their continued directional growth is a dynamic process that is sensitive to tropism signals that ultimately guide the pollen tube to the ovule for fertilization. An emerging model of pollen tube growth includes the following features. 1) Growth involves the insertion of new membrane at the growing tip. 2) A change in growth direction

occurs when a tropism signal elicits a localized increase in a cyclic nucleotide (cNMP) (Moutinho et al., 1998; Holdaway-Clarke and Hepler, 2003). 3) cNMP signals trigger a localized cytosolic  $\text{Ca}^{2+}$  increase (Malho et al., 2000) that results in a localized disruption of F-actin (Geitmann et al., 2000; Fan et al., 2004; Gu et al., 2005). 4) Although the mechanism is unclear, a localized disruption of F-actin changes membrane vesicle trafficking dynamics resulting in a tip that bends in the direction of the tropism signal (Smith and Oppenheimer, 2005), perhaps by blocking vesicle delivery to one side of the growing tip.

A critical regulator of actin dynamics during pollen tube growth is the ROP1 GTPase and its downstream targets RIC3 & 4 (Fu et al., 2001; Gu et al., 2005). RIC4 stabilizes F-actin cables, while RIC3 mediates  $\text{Ca}^{2+}$  induced F-actin disassembly (Gu et al., 2005). However, it remains an open question whether the ROP/RIC signaling pathway is independent or somehow connected to cNMP signaling and CNGC18.

Regardless of the precise mechanism by which the cytoskeleton and secretory machinery are regulated, there is strong experimental evidence that at least some “upstream” tropism signals can generate a localized increase in a cNMP, which then triggers a growth-altering  $\text{Ca}^{2+}$  release (Malho et al., 1994; Malho and Trewavas, 1996; Malho et al., 2000; Moutinho et al., 2001). One of many potential consequences of a  $\text{Ca}^{2+}$  release is the activation of CaM, which has been implicated as important regulator during pollen tube orientation, possibly providing negative feedback regulation of  $\text{Ca}^{2+}$  channel activity (Rato et al., 2004). Experiments with caged  $\text{Ca}^{2+}$  have repeatedly shown that a localized increase of  $\text{Ca}^{2+}$  alone can trigger a directional change in several tip growth systems, such as nerve growth cones, root hairs and pollen tubes (Malho and Trewavas, 1996; Bibikova et al., 1999; Zheng, 2000; Gomez et al., 2001). Based on the above observations, Malho and others have speculated that one of the plant CNGCs could regulate the  $\text{Ca}^{2+}$  release that controls directional tip growth in pollen (e.g. Trewavas et al., 2002; Hetherington and Brownlee, 2004).

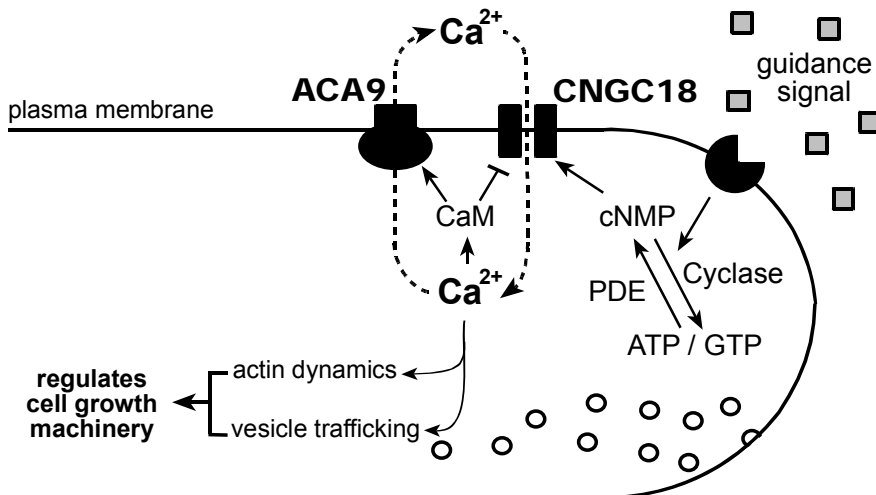


**Figure 20: A model for CNGC18 function in polarized tip-growth of pollen based a  $\text{Ca}^{2+}$  channel paradigm.** Triggered by the binding of a guidance factor with a putative receptor, a localized cytosolic increase in cyclic nucleotide (cNMP) triggers a  $\text{Ca}^{2+}$  influx by activating CNGC18.  $\text{Ca}^{2+}$  binds many downstream effectors including regulators of actin dynamics and vesicle trafficking as well as calmodulin (CaM). Calmodulin terminates the calcium signal by activating  $\text{Ca}^{2+}$  pumps and exchangers (e.g. ACA9) and a blocking CNGC18 activity trough a negative feedback loop.

Consistent with emerging pollen tip growth models, the work presented in this thesis provides evidence for a tip focused localization of a CNGC that could integrate cNMP and  $\text{Ca}^{2+}$  signals to modulate the tip growth machinery (Fig. 20). In support of this function for CNGC18, the corresponding loss-of-function mutants show defective pollen tubes that are short, “kinky”, and often thin. Pollen tube growth and guidance has frequently been compared to directional growth of neurons during animal development (Palanivelu and Preuss, 2000; Lord, 2000; Zheng and Yang, 2000). In support of this analogy, missense mutations in two CNGCs in *C. elegans* (TAX2+4) also results in a neuron tropism defect (Komatsu et al., 1996; Coburn and Bargmann, 1996; Coburn et al., 1998; Kaupp and Seifert, 2002). In contrast to the *cngc18* null mutations, which block polarized growth, the *tax2* and 4 mutations appear to allow neurons to grow beyond their normal termination point. However, not all directional growth mechanisms utilize CNGCs, as fungal systems without obvious CNGC orthologs still engage in directional tip growth, perhaps using alternative  $\text{Ca}^{2+}$  channels such as CCH1 (Fischer et al., 1997). Regardless, the identification of CNGC18’s role in pollen tip growth emphasizes the potential widespread role of CNGCs in the control of other polarized growth processes in both plants and animals, such as tip growth

in root hairs, the development of leaf trichomes, the elongated growth expansion of cells in e.g. the root epidermis, or the variety of cell morphologies observed in animal systems.

## 5 Summary

Dynamic ion fluxes are critical to regulating many major signaling pathways in eukaryotes. In plants, the underlying ion transporters and their physiological function remain largely unknown. Using *Arabidopsis thaliana* as a model system, seven mutants with gene disruption in a Cyclic Nucleotide-Gated Channel (CNGC) have been identified with altered responses to abiotic stress. The male sterility of *cngc18* and Ca<sup>2+</sup> hypersensitivity of *cngc9-2* mutants were studied in detail.

Genetic analysis of two independent gene disruptions in CNGC18 demonstrates male sterility thereby identifying the first CNGC in plants or animals that is essential for completion of an organism's life cycle. While *cngc18* pollen can germinate, the mutant pollen tubes appear to be short, "kinky", and often thin growing without a clear direction. *In vivo* histochemical staining of a pollen-expressed GUS-reporter linked to *cngc18-1* revealed that mutant pollen fail to grow into the transmitting tract of a pistil. While partial male sterility has been reported for other cation channels, this is the first example of a cation channel that is essential for regulation of polarized tip growth of pollen. Analysis of the subcellular localization of a GFP-tagged CNGC18 in complemented *cngc18* mutants reveals asymmetric localization consistent with the plasma membrane at the growing pollen tip. The polarized distribution of GFP-CNGC18 was observed to develop during pollen grain germination at the stage of the initiation of tip growth. Thus, this tip-focused localization of CNGC18 could provide a mechanism to directly transduce a cNMP signal into Ca<sup>2+</sup>-signals that regulate the pollen tube tip growth machinery.

*cngc9-2* mutants are hypersensitive to increased Ca<sup>2+</sup> as evident by wavy looking root and callus-like tissue formation in root and shoot. Formation of callus-like structure is a natural occurring phenomenon initiated by bacteria or insects through changes to the normal physiological ratios of the plant hormones auxin and cytokinins. The development of callus-like structures in *cngc9-2* root and shoot tissue suggest altered auxin and/or cytokinins levels or a defect in signaling and perception of these hormones. RT-PCR and sequencing analysis

reveal that a T-DNA insertion in the promoter region of CNGC9 confers increased transcript levels in *cngc9-2* mutants. Elevated transcript levels can explain enhanced  $\text{Ca}^{2+}$  accumulation in comparison to wild-type plants when grown on high  $\text{Ca}^{2+}$  indicating that CNGC9 might be permeable to  $\text{Ca}^{2+}$ . Further analyses are required to determine a potential role of CNGC9 in plant hormone signaling as well as the ion accumulation profile.

The analyses presented in this thesis identify a crucial role of a CNGC in regulation of polarized tip growth and suggest involvement of another CNGC in plant hormone responses. Together these findings suggest a much more widespread role of CNGCs in regulating plant growth and development than previously thought.

## 6 Future outlook

Several mutant studies in the recent years revealed a first glance about the diverse roles of plant CNGCs in responses to biotic and abiotic stresses. The studies presented in this thesis further suggest a potential role of a CNGC in plant hormone responses and identify the first CNGC that is essential for a plants life cycle. However, little is known about the molecular properties of CNGCs such as ion conductivity, interacting partners, regulation or downstream components.

### 6.1 What is the ion conductivity of a plant CNGC?

Despite electrophysiological studies in heterologous system that suggest K<sup>+</sup>, Ca<sup>2+</sup> and in some cases Na<sup>+</sup> permeability of plant CNGCs, the most pertinent remaining open question is the ion conductivity of these channels. The studies in heterologous systems have not provided sufficient answers to this question for two reasons. First, the potential Ca<sup>2+</sup> permeability of plant CNGCs has been neglected in most studies. There is a reasonable expectation that the function of a plant CNGC might depend on its ability to carry Ca<sup>2+</sup> based on first electrophysiological experiments in plants and the paradigm from animals, where the Ca<sup>2+</sup> fraction of the current (even if it is as low as 20%) determines the channels physiological function and regulation (Very and Sentenac, 2002; Kaupp and Seifert, 2002; Trewavas et al., 2002; Talke et al., 2003). Second the present studies do not take into account that CNGCs might be hetero-tetramers consisting of several CNGC isoforms as their animal counter parts (Kaupp and Seifert, 2002). The genomes of animals encode less CNGC isoforms than plants (i.e. 6 isoforms in vertebrates) (Kaupp and Seifert, 2002). The specificity of animal CNGCs that are expressed in many excitatory and non-excitatory tissues is given by different CNGC isoform composition and stoichiometry in the tetrameric channels (Kaupp and Seifert, 2002). The consistence of a functional CNGC tetramer has profound effects on the permeability of a CNGC channel. For example, the fraction of the CNGC dark current carried by Ca<sup>2+</sup> is about two fold higher in vertebrate cone than rod photoreceptors (Kaupp and Seifert, 2002).

In plants, it is not known if CNGCs form heteromeric and/or homomeric tetramers. *In planta* studies are necessary to study the composition and ion conductance of CNGCs. While protein interaction studies to determine the composition of a CNGC tetramer are hardly possible in pollen due to its size and abundance, three approaches have been started in the course of this thesis to investigate the permeability of a CNGC tetramer consisting at least partially of CNGC18. It is important to note that a cDNA of *CNGC18* did not complement the K<sup>+</sup> and Ca<sup>2+</sup> deficient yeast strains *trk1,2*, *mid1*, and *cch1* when tested during this thesis, suggesting no functional expression in yeast.

First, electrophysiological analyses of the ion conductivity of *cngc18* pollen protoplasts have been started in a collaborative effort with Dr. Yongfei Wang, a specialist in patch clamp analysis in the laboratory of Prof. Dr. Julian I. Schroeder at the University of California, San Diego, USA. While it is already very challenging to measure Ca<sup>2+</sup> currents in wild-type pollen protoplasts, the lack of homozygous *cngc18* plants only allows investigation of a mixed population of mutant and wild-type pollen from a heterozygous plant. A single cell PCR analysis of pollen grains based on a nested approach was developed to genotype the pollen protoplast after patch clamp analysis. With this approach we hope to determine the ion permeability of a CNGC18 channel in pollen grains in the whole cell configuration.

In a second approach, pollen tube growth of pollen expressing GFP-CNGC18 under the control of the *ACA9* promoter is investigated under low K<sup>+</sup> and Ca<sup>2+</sup> conditions. Based on microarray profiling, the *ACA9* promoter is expected to exhibit an at least 3-4 times higher transcriptional activity than the native promoter of *CNGC18* providing over-expression in these lines. Preliminary studies with pollen from three independent over-expressing lines suggest that over-expression of *CNGC18* results in pollen with longer tubes when grown for 5h on basic pollen germination media and in particular under low Ca<sup>2+</sup> conditions. Further studies with different Ca<sup>2+</sup> and K<sup>+</sup> concentrations are underway to determine if *CNGC18* over-expression in pollen tubes conveys an advantage under low Ca<sup>2+</sup> and K<sup>+</sup> conditions thereby providing indirect evidence for the permeability of a CNGC18 channel.

In the third study, *cngc18* lines have been transformed with a new version of the  $\text{Ca}^{2+}$  reporter cameleon (cpvD3, kindly provided by Prof. Dr. Roger Tsien, University of California, San Diego) under the control of the ACA9 promoter (ps# 844). First ratiometric fluorescence experiments with wild-type pollen tubes show regular  $\text{Ca}^{2+}$  transients in growing pollen tip (Fig. 21). In the shaft of the pollen tube smaller changes in  $\text{Ca}^{2+}$  were detected. Pollen tubes that stopped growing did not exhibit any  $\text{Ca}^{2+}$  transients. Next, wild-type and mutant pollen tubes will be analyzed shortly after germination when a small bulge or tip is visible (compare pollen stage shown in Fig. 10F, G). This growth stage should allow direct comparison between the morphologically similar wild-type and mutant pollen, which is not possible in later stages when *cngc18* pollen tubes displays kinky structures and often burst at the tip (compare Fig. 8B-D). To differentiate between mutant and wild-type pollen of the heterozygous *cngc18-1* plants, histochemical staining of the T-DNA encoded *LAT52::GUS* construct in mutant pollen will follow the ratiometric  $\text{Ca}^{2+}$  analysis.

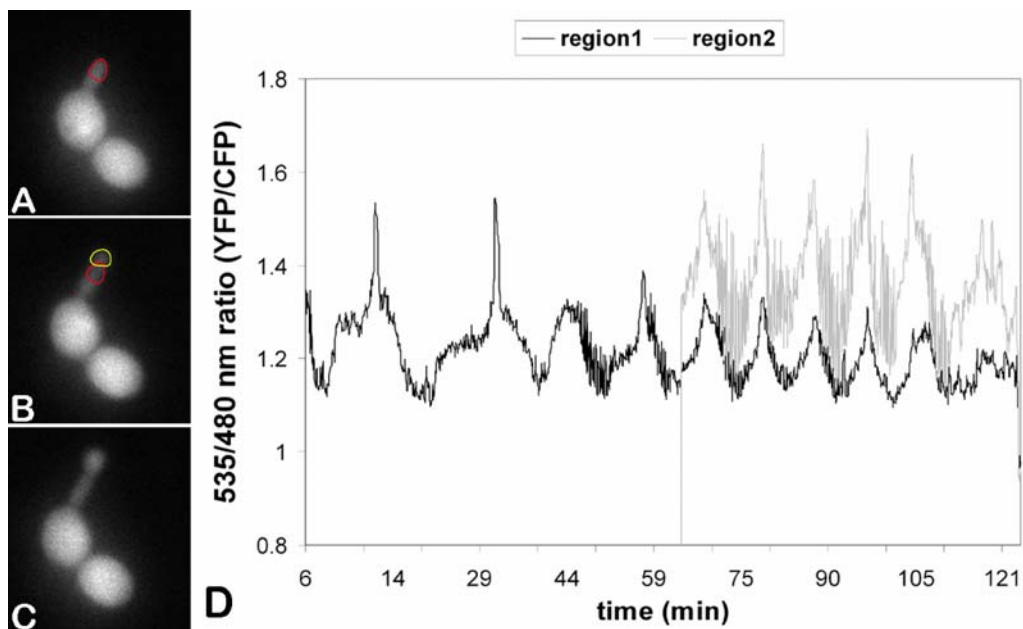


**Figure 21:  $\text{Ca}^{2+}$  transients in growing pollen tubes.** (A-C) Fluorescent images of a growing pollen tube that were taken after about 0, 60 and 105 min during the experiment shown in (D). The images show only the YFP image that was acquired. The red circle in A and B illustrate the initial region (region 1) that was used to determine the YFP/CFP ratio (535/480 nm), while the yellow region indicates a second region that was chosen after about 1 h of the experiment (region 2). (D) Diagram showing the ratio changes between YFP and CFP emission of a cameleon (cpvD3) expressing pollen tube representing changes in cytosolic  $\text{Ca}^{2+}$  levels. Region 1 and region 2 represent the growing tip of the pollen tube.

A major difficulty in many of these experiments is the lack of homozygous *cngc18* mutants. The GFP-CNGC18 construct under the control of an ethanol inducible promoter system (*A/cR/A/cA*) was transformed in *cngc18-1* plants. Positive transformants have been selected and first attempts to produce a homozygous *cngc18* lines have been started in the laboratory of Prof. Dr. Jeffrey F. Harper. Isolation of homozygous *cngc18* lines will allow electrophysiological studies as well as repressor studies with EMS mutagenized seeds thereby identifying potential up- or downstream components of the signaling cascade involving CNGC18.

## 6.2 The function of other CNGC isoforms expressed in pollen

As indicated above, plant CNGCs are expected to form tetramers consisting of several CNGC isoforms. To find out more about the role of CNGCs in plants, it is important to identify the different interaction partners in each tissue. While protein interaction studies based on protein pull down experiments are not feasible in pollen, the CNGCs forming a functional channel together with CNGC18 might be identified by interaction studies in yeast (split-ubiquitin) or Fluorescent Energy Transfer (FRET) studies between two fluorescent protein tagged CNGC isoforms.

Microarray profiling indicates expression of at least six CNGCs in mature pollen and ten CNGCs throughout pollen development (Fig. 22) (Honys and Twell, 2004). In the laboratory of Prof. Dr. Jeffrey F. Harper lab, the cDNAs of all six pollen expressed CNGCs have been fused to a red or green fluorescent protein (RFP or GFP) under the control of the ACA9 promoter. The constructs have been transformed into the *cngc18-1* background to analyze not only the subcellular localization pattern and potential colocalization with CNGC18, but also to investigate whether over-expression of another CNGC can complement the *cngc18* male sterility phenotype as it has been shown for other  $\text{Ca}^{2+}$  transporters (Schiott et al., 2004).

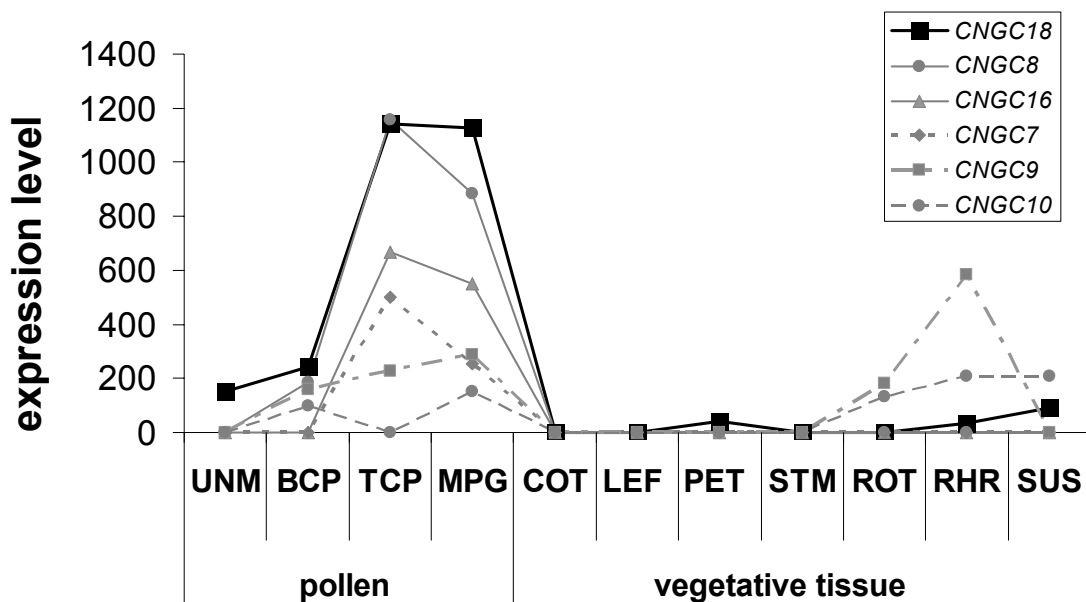


**Figure 22: Microarray profiling of CNGCs expressed in pollen.** The diagram shows the expression level of CNGC7, 8, 9, 10, 16 and 18 several different tissues (Honys and Twell, 2004): UNM= uninucleate microspore, BCP= bicellular pollen, TCP= tricellular pollen, MPG= mature pollen, COT= cotyledons, LEF= leaves, PET= petiole, STEM= stem, ROT= root, RHR= root hairs, SUS= suspension culture.

### 6.3 Structure function studies using the male sterile phenotype of *cngc18*

Little is known about the molecular properties of a plant CNGC. As a first step to investigate the structural properties of the cyclic nucleotide binding domain of CNGC18 a subset of EMS-mutants have been identified by the Arabidopsis Tilling Facility in Seattle, Washington, USA <http://tilling.fhcrc.org:9366/> (Tab. 5). The Arabidopsis Tilling Facility developed a high throughput screen that identified missense mutations based on recognition and cleavages of mismatch heteroduplexes between mutant and wild-type DNA through the endonuclease CEL1 (Till et al., 2003). Since EMS lines contain an average of 70-100 mutations, a series of backcrosses have been initiated and phenotypic analysis will follow.

<b>name</b>	<b>amino acid mutation</b>	<b>location</b>	<b>SIFT</b>	<b>PSSM difference</b>	<b>zygosity</b>	<b>ABRC stock</b>
<i>cngc18-4</i>	D386N	S6 - CNBD	0.11	7.8	hetero	CS94045
<b><i>cngc18-13</i></b> <sup>+</sup>	<b>V447I</b>	<b>CNBD</b>	<b>0.00</b>	<b>5.7</b>	hetero	<b>CS88015</b>
<i>cngc18-5</i>	S451F	CNBD	0.02	7.1	hetero	CS85437
<i>cngc18-6</i>	D454N	CNBD	0.00	10	hetero	CS92263
<i>cngc18-7</i>	L458F	CNBD	0.00	8	hetero	CS93689
<b><i>cngc18-14</i></b> <sup>+</sup>	<b>A460T</b>	<b>CNBD</b>	<b>0.02</b>	<b>9.8</b>	homo	<b>CS87224</b>
<i>cncg18-15</i> <sup>+</sup>	G463E	CNBD	1.00	-4.4	hetero	CS87652
<i>cngc18-8</i>	S470N	CNBD	0.18	2.7	hetero	CS92251
<b><i>cncg18-16</i></b> <sup>+</sup>	<b>R478H</b>	<b>CNBD</b>	<b>0.00</b>	<b>19</b>	hetero	<b>CS91067</b>
<i>cngc18-9</i>	G480S	CNBD	0.00	22.6	hetero	CS92119
<i>cngc18-9b</i> <sup>+</sup>	G480S	CNBD		22.6	homo	CS91057
<b><i>cngc18-17</i></b> <sup>+</sup>	<b>V483M</b>	<b>CNBD</b>	<b>0.00</b>	<b>16.8</b>	hetero	<b>CS90353</b>
<b><i>cngc18-18</i></b> <sup>+</sup>	<b>R491Q</b>	<b>CNBD</b>	<b>0.01</b>	<b>18.4</b>	homo	<b>CS91890</b>
<i>cngc18-19</i> <sup>+</sup>	G501E	CNBD	0.01	-	hetero	CS91540
<i>cngc18-10</i>	D516N	CNBD	0.17	5.4	hetero	CS86157
<i>cngc18-20</i> <sup>+</sup>	R540*	CNBD		-	hetero	CS90972
<i>cncg18-21</i> <sup>+</sup>	S546F	CNBD	0.03	8.8	homo	CS88060
<b><i>cngc18-12</i></b>	<b>E556K</b>	<b>CNBD</b>	<b>0.03</b>	<b>12.2</b>	homo	<b>CS92358</b>
<b><i>cngc18-22a</i></b> <sup>+</sup>	<b>R578K</b>	<b>C-term</b>	<b>0.00</b>	<b>19.3</b>	hetero	<b>CS87733</b>
<b><i>cngc18-22b</i></b> <sup>+</sup>	<b>R578K</b>	<b>C-term</b>		<b>19.3</b>	hetero	<b>CS90758</b>
<i>cngc18-23</i> <sup>+</sup>	R632K	C-term	1.00	-	homo	CS87703
<i>cngc18-24</i> <sup>+</sup>	G651R	C-term	0.28	1.2	hetero	CS85564
<i>cngc18-25</i> <sup>+</sup>	D288N	N-term	0.13	-	hetero	CS86276
<i>cngc18-26</i> <sup>+</sup>	R255K	N-term	1.00	-	hetero	CS87050
<i>cngc18-27</i> <sup>+</sup>	L260F	N-term	0.72	-	hetero	CS87178
<i>cngc18-28</i> <sup>+</sup>	G213R	N-term	0.00	-	hetero	CS87264
<i>cngc18-29</i> <sup>+</sup>	L284F	N-term	0.45	-	hetero	CS87681

**Table 5: EMS mutants identified by the Arabidopsis Tilling Facility.** The list includes the name of the line, amino acid mutation (\* indicates a Stop codon), the proximate location of the mutation (with: S6-CNBD = between the transmembrane domain S6 and the cyclic nucleotide binding domain; CNBD = cyclic nucleotide binding domain, C-term = C-terminus of the protein, and N-term = N-terminus of the protein), SIFT and PSSM scores, zygosity of the mutant (hetero= heterozygous and homo= homozygous), as well as the seed stock number at the Arabidopsis Biological Resource Center, Ohio, USA (ABRC). The lines that are highlighted in bold were classified as most interesting lines based on their SIFT and PSSM scores. Homozygous lines are still considered interesting because they might display a partial male sterility.

The mutations are classified by the SIFT and the PSSM difference score. SIFT is a homology based tool that sorts intolerant from tolerant amino acids (SIFT) based on the assumption that protein evolution and function are correlated ([http://blocks.fhcrc.org/sift/SIFT\\_help.html](http://blocks.fhcrc.org/sift/SIFT_help.html)). SIFT uses multiple alignment information to predict tolerant and deleterious mutations. A probability score lower than 0.05 is considered deleterious for the function of the protein. The PSSM scores (Position-Specific Scoring Matrix) gives each amino acid substitution a score based on its position in a protein multiple sequence alignment ([http://www.ncbi.nlm.nih.gov/Class/Structure/pssm/pssm\\_viewer.cgi](http://www.ncbi.nlm.nih.gov/Class/Structure/pssm/pssm_viewer.cgi)). PSSM scores are shown as positive or negative values. Positive scores indicate that a change occurs more frequently than expected by chance, while negative scores indicate that the corresponding amino acid is less variable than expected. Large positive scores often indicate important functional residues as for example an active site or an amino acid required for inter- or intramolecular interactions.

<sup>+</sup> = lines that have been identified recently but were not ordered yet

While these EMS lines can provide a first glimpse about the structural properties of the cyclic nucleotide binding domain of CNGC18, targeted site mutations are necessary to study this and other domains of the protein. For example, naturally occurring mutations in animal and human CNGCs leading to diseases such as blindness can be used to identify potentially critical amino acids. The *cngc18* phenotype provides an ideal tool for such structure function studies. To test the role of specific amino acids, mutated cDNA constructs can be transformed into *cngc18* mutants and tested for complementation of the male sterile phenotype.

## 7 References

- Alexander M.P. 1969. Differential staining of aborted and nonaborted pollen. *Stain Technol.* 44:117-122.
- Arazi T., Kaplan B., and Fromm H. 2000. A high-affinity calmodulin-binding site in a tobacco plasma-membrane channel protein coincides with a characteristic element of cyclic nucleotide-binding domains. *Plant Mol. Biol.* 42:591-601.
- Arazi T., Sunkar R., Kaplan B., and Fromm H. 1999. A tobacco plasma membrane calmodulin-binding transporter confers Ni<sup>2+</sup> tolerance and Pb<sup>2+</sup> hypersensitivity in transgenic plants. *Plant J.* 20:171-182.
- Balague C., Lin B., Alcon C., Flottes G., Malmstrom S., Kohler C., Neuhaus G., Pelletier G., Gaymard F., and Roby D. 2003. HLM1, an essential signaling component in the hypersensitive response, is a member of the cyclic nucleotide-gated channel ion channel family. *Plant Cell* 15:365-379.
- Barbier-Brygoo H., Vinauger M., Colcombet J., Ephritikhine G., Frachisse J.M., and Maurel C. 2000. Anion channels in higher plants: functional characterization, molecular structure and physiological role. *Biochim. Biophys. Acta* 1465:199-218.
- Becker D., Geiger D., Dunkel M., Roller A., Bertl A., Latz A., Carpaneto A., Dietrich P., Roelfsema M.R.G., Voelker C., Schmidt D., Mueller-Roeber B., Czempinski K., and Hedrich R. 2004. AtTPK4, an *Arabidopsis* tandem-pore K<sup>+</sup> channel, poised to control the pollen membrane voltage in a pH- and Ca<sup>2+</sup>-dependent manner. *Proc. Natl. Acad. Sci. U. S. A* 101:15621-15626.
- Bibikova T.N., Blancaflor E.B., and Gilroy S. 1999. Microtubules regulate tip growth and orientation in root hairs of *Arabidopsis thaliana*. *Plant J.* 17:657-665.
- Biel M., Seeliger M., Pfeifer A., Kohler K., Gerstner A., Ludwig A., Jaissle G., Fauser S., Zrenner E., and Hofmann F. 1999. Selective loss of cone function in mice lacking the cyclic nucleotide-gated channel CNG3. *Proc. Natl. Acad. Sci. U. S. A* 96:7553-7557.
- Carol R.J. and Dolan L. 2002. Building a hair: tip growth in *Arabidopsis thaliana* root hairs. *Philos. Trans. R. Soc. Lond B Biol. Sci* 357:815-821.
- Chan C.W., Schorrak L.M., Smith R.K., Jr., Bent A.F., and Sussman M.R. 2003. A cyclic nucleotide-gated ion channel, CNGC2, is crucial for plant development and adaptation to calcium stress. *Plant Physiol.* 132:728-731.
- Cherel I. 2004. Regulation of K<sup>+</sup> channel activities in plants: from physiological to molecular aspects. *J. Exp. Bot.* 55:337-351.
- Choi S., Creelman R.A., Mullet J.E., and Wing R.A. 1995. Construction and characterization of a bacterial artificial chromosome library for *Arabidopsis thaliana*. *Weeds World* 2:17-20.
- Clough S.J. and Bent A.F. 1998. Floral dip: a simplified method for *Agrobacterium*-mediated transformation of *Arabidopsis thaliana*. *Plant J.* 16:735-743.
- Clough S.J., Fengler K.A., Yu I.C., Lippok B., Smith R.K., Jr., and Bent A.F. 2000. The *Arabidopsis dnd1* "defense, no death" gene encodes a mutated cyclic nucleotide-gated ion channel. *Proc. Natl. Acad. Sci. U. S. A* 97:9323-9328.
- Coburn C.M., Mori I., Ohshima Y., and Bargmann C.I. 1998. A cyclic nucleotide-gated channel inhibits sensory axon outgrowth in larval and adult *Caenorhabditis elegans*: a distinct pathway for maintenance of sensory axon structure. *Development* 125:249-258.
- Coburn C.M. and Bargmann C.I. 1996. A putative cyclic nucleotide-gated channel is required for sensory development and function in *C. elegans*. *Neuron* 17:695-706.

- D'Agostino I.B., Deruere J., and Kieber J.J. 2000. Characterization of the response of the *Arabidopsis* response regulator gene family to cytokinin. *Plant Physiol.* 124:1706-1717.
- Fan L.M., Wang Y.F., Wang H., and Wu W.H. 2001. *In vitro* *Arabidopsis* pollen germination and characterization of the inward potassium currents in *Arabidopsis* pollen grain protoplasts. *J. Exp. Bot.* 52:1603-1614.
- Fan X., Hou J., Chen X., Chaudhry F., Staiger C.J., and Ren H. 2004. Identification and characterization of a  $\text{Ca}^{2+}$ -dependent actin filament-severing protein from lily pollen. *Plant Physiol.* 136:3979-3989.
- Feijo J.A., Costa S.S., Prado A.M., Becker J.D., and Certal A.C. 2004. Signalling by tips. *Curr. Opin. Plant Biol.* 7:589-598.
- Fischer M., Schnell N., Chattaway J., Davies P., Dixon G., and Sanders D. 1997. The *Saccharomyces cerevisiae* *CCH1* gene is involved in calcium influx and mating. *FEBS Letters* 419:259-262.
- Franklin-Tong V.E. 1999. Signaling and the modulation of pollen tube growth. *Plant Cell* 11:727-738.
- Fu Y., Wu G., and Yang Z. 2001. Rop GTPase-dependent dynamics of tip-localized F-actin controls tip growth in pollen tubes. *J. Cell Biol.* 152:1019-1032.
- Geitmann A., Snowman B.N., Emons A.M., and Franklin-Tong V.E. 2000. Alterations in the actin cytoskeleton of pollen tubes are induced by the self-incompatibility reaction in *Papaver rhoeas*. *Plant Cell* 12:1239-1252.
- Gobert A., Park G., Amtmann A., Sanders D., and Maathuis F.J.M. 2006. *Arabidopsis thaliana* cyclic nucleotide-gated channel 3 forms a non-selective ion transporter involved in germination and cation transport. *J. Exp. Bot.* 57:791-800.
- Golovkin M. and Reddy A.S.N. 2003. A calmodulin-binding protein from *Arabidopsis* has an essential role in pollen germination. *Proc. Natl. Acad. Sci. U. S. A* 100:10558-10563.
- Gomez T.M., Robles E., Poo M.m., and Spitzer N.C. 2001. Filopodial calcium transients promote substrate-dependent growth cone turning. *Science* 291:1983-1987.
- Griessner M. and Obermeyer G. 2003. Characterization of whole-cell  $\text{K}^+$  currents across the plasma membrane of pollen grain and tube protoplasts of *Lilium longiflorum*. *J. Membr. Biol.* 193:99-108.
- Gu Y., Fu Y., Dowd P., Li S., Vernoud V., Gilroy S., and Yang Z. 2005. A Rho family GTPase controls actin dynamics and tip growth via two counteracting downstream pathways in pollen tubes. *J. Cell Biol.* 169:127-138.
- Hellens R.P., Edwards E.A., Leyland N.R., Bean S., and Mullineaux P.M. 2000. pGreen: a versatile and flexible binary Ti vector for *Agrobacterium*-mediated plant transformation. *Plant Mol. Biol.* 42:819-832.
- Hepler P.K., Vidali L., and Cheung A.Y. 2001. Polarized cell growth in higher plants. *Annu. Rev. Cell Dev. Biol.* 17:159-187.
- Hetherington A.M. and Brownlee C. 2004. The generation of  $\text{Ca}^{2+}$  signals in plants . *Annu. Rev. Plant Biol.* 55:401-427.
- Holdaway-Clarke T.L., Feijo J.A., Hackett G.R., Kunkel J.G., and Hepler P.K. 1997. Pollen tube growth and the intracellular cytosolic calcium gradient oscillate in phase while extracellular calcium influx is delayed. *Plant Cell* 9:1999-2010.
- Holdaway-Clarke T.L. and Hepler P.K. 2003. Control of pollen tube growth: role of ion gradients and fluxes. *New Phytol.* 159:539-563.

- Honyo D. and Twell D.** 2004. Transcriptome analysis of haploid male gametophyte development in *Arabidopsis*. *Genome Biol.* 5:R85.
- Hua B.G., Mercier R.W., Leng Q., and Berkowitz G.A.** 2003a. Plants do it differently. A new basis for potassium/sodium selectivity in the pore of an ion channel. *Plant Physiol.* 132:1353-1361.
- Hua B.G., Mercier R.W., Zielinski R.E., and Berkowitz G.A.** 2003b. Functional interaction of calmodulin with a plant cyclic nucleotide-gated cation channel. *Plant Physiol. Biochem.* 41:945-954.
- Inoue T., Higuchi M., Hashimoto Y., Seki M., Kobayashi M., Kato T., Tabata S., Shinozaki K., and Kakimoto T.** 2001. Identification of CRE1 as a cytokinin receptor from *Arabidopsis*. *Nature* 409:1060-1063.
- Jackson S.L. and Heath I.B.** 1993. Roles of calcium ions in hyphal tip growth. *Microbiol. Rev.* 57:367-382.
- Jefferson R.A., Kavanagh T.A., and Bevan M.W.** 1987. GUS fusions: beta-glucuronidase as a sensitive and versatile gene fusion marker in higher plants. *EMBO J.* 6:3901-3907.
- Jiang L., Yang S.L., Xie L.F., Puah C.S., Zhang X.Q., Yang W.C., Sundaresan V., and Ye D.** 2005. Vanguard1 encodes a pectin methylesterase that enhances pollen tube growth in the *Arabidopsis* style and transmitting tract. *Plant Cell* 17:584-596.
- Johnson-Brousseau S.A. and McCormick S.** 2004. A compendium of methods useful for characterizing *Arabidopsis* pollen mutants and gametophytically-expressed genes. *Plant J.* 39:761-775.
- Johnson M.A., von Besser K., Zhou Q., Smith E., Aux G., Patton D., Levin J.Z., and Preuss D.** 2004. *Arabidopsis* hapless mutations define essential gametophytic functions. *Genetics* 168:971-982.
- Johnson S.A. and McCormick S.** 2001. Pollen germinates precociously in the anthers of *raring-to-go*, an *Arabidopsis* gametophytic mutant. *Plant Physiol.* 126:685-695.
- Kaupp U.B. and Seifert R.** 2002. Cyclic nucleotide-gated ion channels. *Physiol. Rev.* 82:769-824.
- Kohler C. and Neuhaus G.** 2000. Characterisation of calmodulin binding to cyclic nucleotide-gated ion channels from *Arabidopsis thaliana*. *FEBS Lett.* 471:133-136.
- Komatsu H., Mori I., Rhee J.S., Akaike N., and Ohshima Y.** 1996. Mutations in a cyclic nucleotide-gated channel lead to abnormal thermosensation and chemosensation in *C. elegans*. *Neuron* 17:707-718.
- Lahner B., Gong J., Mahmoudian M., Smith E.L., Abid K.B., Rogers E.E., Guerinot M.L., Harper J.F., Ward J.M., McIntyre L., Schroeder J.I., and Salt D.E.** 2003. Genomic scale profiling of nutrient and trace elements in *Arabidopsis thaliana*. *Nat. Biotechnol.* 21:1215-1221.
- Lemtiri-Chlieh F. and Berkowitz G.A.** 2004. Cyclic adenosine monophosphate regulates calcium channels in the plasma membrane of *Arabidopsis* leaf guard and mesophyll cells. *J. Biol. Chem.* 279:35306-35312.
- Leng Q., Mercier R.W., Hua B.G., Fromm H., and Berkowitz G.A.** 2002. Electrophysiological analysis of cloned cyclic nucleotide-gated ion channels. *Plant Physiol.* 128:400-410.
- Leng Q., Mercier R.W., Yao W., and Berkowitz G.A.** 1999. Cloning and first functional characterization of a plant cyclic nucleotide-gated cation channel. *Plant Physiol.* 121:753-761.
- Li XL., Borsics T., Harrington H., and Christopher D.** 2005. *Arabidopsis* AtCNGC10 rescues potassium channel mutants of *E. coli*, yeast and *Arabidopsis* and is regulated by calcium/calmodulin and cyclic GMP in *E. coli*. *Funct. Plant Biol.* 32:643-653.
- Lord E.** 2000. Adhesion and cell movement during pollination: cherchez la femme. *Trends Plant Sci.* 5:368-373.

- Malho R. and Trewavas A.J.** 1996. Localized apical increases of cytosolic free calcium control pollen tube orientation. *Plant Cell* 8:1935-1949.
- Malho R., Camacho L., and Moutinho A.** 2000. Signalling pathways in pollen tube growth and reorientation. *Ann. Bot.* 85:59-68.
- Malho R., Read N.D., Pais M.S., and Trewavas A.J.** 1994. Role of cytosolic free calcium in the reorientation of pollen tube growth. *Plant J.* 5:331-341.
- Maser P., Thomine S., Schroeder J.I., Ward J.M., Hirschi K., Sze H., Talke I.N., Amtmann A., Maathuis F.J.M., Sanders D., Harper J.F., Tchieu J., Grabskov M., Persans M.W., Salt D.E., Kim S.A., and Guerinot M.L.** 2001. Phylogenetic relationships within cation transporter families of *Arabidopsis*. *Plant Physiol.* 126:1646-1667.
- Mathur J. and Koncz C.** 1998. Callus culture and regeneration. In: *Arabidopsis protocols*. Martinez-Zapater J. and Salinas J., editors. Humana Press, 31-34.
- McElver J., Tzafir I., Aux G., Rogers R., Ashby C., Smith K., Thomas C., Schetter A., Zhou Q., Cushman M.A., Tossberg J., Nickle T., Levin J.Z., Law M., Meinke D., and Patton D.** 2001. Insertional mutagenesis of genes required for seed development in *Arabidopsis thaliana*. *Genetics* 159:1751-1763.
- Messerli M. and Robinson K.R.** 1997. Tip localized  $\text{Ca}^{2+}$  pulses are coincident with peak pulsatile growth rates in pollen tubes of *Lilium longiflorum*. *J. Cell Sci.* 110:1269-1278.
- Messerli M.A. and Robinson K.R.** 2003. Ionic and osmotic disruptions of the lily pollen tube oscillator: testing proposed models. *Planta* 217:147-157.
- Miller D.D., Callaham D.A., Gross D.J., and Hepler P.K.** 1992. Free  $\text{Ca}^{2+}$  gradient in growing pollen tubes of *Lilium*. *J. Cell Sci.* 101:7-12.
- Mouline K., Very A.A., Gaynard F., Boucherez J., Pilot G., Devic M., Bouchez D., Thibaud J.B., and Sentenac H.** 2002. Pollen tube development and competitive ability are impaired by disruption of a Shaker  $\text{K}^+$  channel in *Arabidopsis*. *Genes Dev.* 16:339-350.
- Moutinho A., Hussey P.J., Trewavas A.J., and Malho R.** 2001. cAMP acts as a second messenger in pollen tube growth and reorientation. *Proc. Natl. Acad. Sci. U. S. A* 98:10481-10486.
- Moutinho A., Trewavas A.J., and Malho R.** 1998. Relocation of a  $\text{Ca}^{2+}$ -dependent protein kinase activity during pollen tube reorientation. *Plant Cell* 10:1499-1510.
- Mozo T., Fischer S., Shizuya H., and Altmann T.** 1998. Construction and characterization of the IGF *Arabidopsis* BAC library. *Mol. Gen. Genet.* 258:562-570.
- Nishiyama M., Hoshino A., Tsai L., Henley J.R., Goshima Y., Tessier-Lavigne M., Poo M., and Hong K.** 2003. Cyclic AMP/GMP-dependent modulation of  $\text{Ca}^{2+}$  channels sets the polarity of nerve growth-cone turning. *Nature* 423:990-995.
- Obermeyer G. and Weisenseel M.H.** 1991. Calcium channel blocker and calmodulin antagonists affect the gradient of free calcium ions in lily pollen tubes. *Eur. J Cell Biol.* 56:319-327.
- Paidhungat M. and Garrett S.** 1997. A homolog of mammalian, voltage-gated calcium channels mediates yeast pheromone-stimulated  $\text{Ca}^{2+}$  uptake and exacerbates the *cdc1* (Ts) growth defect. *Mol. Cell. Biol.* 17:6339-6347.
- Palanivelu R., Brass L., Edlund A.F., and Preuss D.** 2003. Pollen tube growth and guidance is regulated by *POP2*, an *Arabidopsis* gene that controls GABA levels. *Cell* 114:47-59.
- Palanivelu R. and Preuss D.** 2000. Pollen tube targeting and axon guidance: parallels in tip growth mechanisms. *Trends Cell Biol.* 10:517-524.

- Parton R.M., Fischer-Parton S., Trewavas A.J., and Watahiki M.K.** 2003. Pollen tubes exhibit regular periodic membrane trafficking events in the absence of apical extension. *J. Cell Sci.* 116:2707-2719.
- Pierson E.S., Miller D.D., Callaham D.A., Shipley A.M., Rivers B.A., Cresti M., and Hepler P.K.** 1994. Pollen tube growth is coupled to the extracellular calcium ion flux and the intracellular calcium gradient: effect of BAPTA-type buffers and hypertonic media. *Plant Cell* 6:1815-1828.
- Pierson E.S., Miller D.D., Callaham D.A., van Aken J., Hackett G., and Hepler P.K.** 1996. Tip-localized calcium entry fluctuates during pollen tube growth. *Dev. Biol.* 174:160-173.
- Pina C., Pinto F., Feijo J.A., and Becker J.D.** 2005. Gene family analysis of the *Arabidopsis* pollen transcriptome reveals biological implications for cell growth, division control, and gene expression regulation. *Plant Physiol.* 138:744-756.
- Preuss D., Rhee S.Y., and Davis R.W.** 1994. Tetrad analysis possible in *Arabidopsis* with mutation of the quartet (*qrt*) genes. *Science* 264:1458-1460.
- Procissi A., de Laissardiere S., Ferault M., Vezon D., Pelletier G., and Bonhomme S.** 2001. Five gametophytic mutations affecting pollen development and pollen tube growth in *Arabidopsis thaliana*. *Genetics* 158:1773-1783.
- Pu R. and Robinson K.R.** 1998. Cytoplasmic calcium gradients and calmodulin in the early development of the fucoid alga *Pelvetia compressa*. *J. Cell Sci.* 111:3197-3207.
- Rathore K.S., Cork R.J., and Robinson K.R.** 1991. A cytoplasmic gradient of  $\text{Ca}^{2+}$  is correlated with the growth of lily pollen tubes. *Dev. Biol.* 148:612-619.
- Rato C., Monteiro D., Hepler P.K., and Malho R.** 2004. Calmodulin activity and cAMP signalling modulate growth and apical secretion in pollen tubes. *Plant J.* 38:887-897.
- Robertson W.R., Clark K., Young J.C., and Sussman M.R.** 2004. An *Arabidopsis thaliana* plasma membrane proton pump is essential for pollen development. *Genetics* 168:1677-1687.
- Rosso M.G., Li Y., Strizhov N., Reiss B., Dekker K., and Weisshaar B.** 2003. An *Arabidopsis thaliana* T-DNA mutagenized population (GABI-Kat) for flanking sequence tag-based reverse genetics. *Plant Mol. Biol.* 53:247-259.
- Sambrook J., Fritsch E.F., and Maniatis T.** 1989. Molecular Cloning: a laboratory manual. Cold Spring Harbor Laboratory Press, Plainview, New York, U.S.A.
- Sanders D., Pelloux J., Brownlee C., and Harper J.F.** 2002. Calcium at the crossroads of signaling. *Plant Cell* 14:S401-S417.
- Schiott M., Romanowsky S.M., Baekgaard L., Jakobsen M.K., Palmgren M.G., and Harper J.F.** 2004. A plant plasma membrane  $\text{Ca}^{2+}$  pump is required for normal pollen tube growth and fertilization. *Proc. Natl. Acad. Sci. U. S. A* 101:9502-9507.
- Schroeder J.I., Allen G.J., Hugouvieux V., Kwak J.M., and Waner D.** 2001. Guard cell signal transduction. *Annu. Rev. Plant Physiol. Plant Mol. Biol.* 52:627-658.
- Schuurink R.C., Shartzer S.F., Fath A., and Jones R.L.** 1998. Characterization of a calmodulin-binding transporter from the plasma membrane of barley aleurone. *Proc. Natl. Acad. Sci. U. S. A* 95:1944-1949.
- Shaw S.L. and Quatrano R.S.** 1996. Polar localization of a dihydropyridine receptor on living *Fucus* zygotes. *J. Cell Sci.* 109:335-342.
- Smith L.G. and Oppenheimer D.G.** 2005. Spatial control of cell expansion by the plant cytoskeleton. *Annu. Rev. Cell Dev. Biol.* 21:271-295.

- Smyth D.R., Bowman J.L., and Meyerowitz E.M.** 1990. Early flower development in *Arabidopsis*. *Plant Cell* 2:755-767.
- Sunkar R., Kaplan B., Bouche N., Arazi T., Dolev D., Talke I.N., Maathuis F.J., Sanders D., Bouchez D., and Fromm H.** 2000. Expression of a truncated tobacco NtCBP4 channel in transgenic plants and disruption of the homologous *Arabidopsis* CNGC1 gene confer Pb<sup>2+</sup> tolerance. *Plant J.* 24:533-542.
- Talke I.N., Blaudez D., Maathuis F.J.M., and Sanders D.** 2003. CNGCs: prime targets of plant cyclic nucleotide signalling? *Trends Plant Sci.* 8:286-293.
- Tansengco M.L., Imaizumi-Anraku H., Yoshikawa M., Takagi S., Kawaguchi M., Hayashi M., and Murooka Y.** 2004. Pollen development and tube growth are affected in the symbiotic mutant of *Lotus japonicus*, crinkle. *Plant Cell Physiol.* 45:511-520.
- Taylor A.R., Manison N.F.H., Fernandez C., Wood J., and Brownlee C.** 1996. Spatial organization of calcium signaling involved in cell volume control in the *Fucus* rhizoid. *Plant Cell* 8:2015-2031.
- Till B.J., Reynolds S.H., Greene E.A., Codomo C.A., Enns L.C., Johnson J.E., Burtner C., Odden A.R., Young K., Taylor N.E., Henikoff J.G., Comai L., and Henikoff S.** 2003. Large-scale discovery of induced point mutations with high-throughput tillering. *Genome Res.* 13:524-530.
- Trewavas A.J., Rodrigues C., Rato C., and Malho R.** 2002. Cyclic nucleotides: the current dilemma. *Curr. Opin. Plant Biol.* 5:425-429.
- Ulmasov T., Murfett J., Hagen G., and Guilfoyle T.J.** 1997. Aux/IAA proteins repress expression of reporter genes containing natural and highly active synthetic auxin response elements. *Plant Cell* 9:1963-1971.
- Van der Veen J.H. and Wirtz P.** 1968. EMS-induced genetic male sterility in *Arabidopsis thaliana*: a model selection experiment. *Euphytica* 17:371-377.
- Very A.A. and Davies J.M.** 2000. Hyperpolarization-activated calcium channels at the tip of *Arabidopsis* root hairs. *Proc. Natl. Acad. Sci. U. S. A* 97:9801-9806.
- Very A.A. and Sentenac H.** 2002. Cation channels in the *Arabidopsis* plasma membrane. *Trends Plant Sci.* 7:168-175.
- Ye G.N., Stone D., Pang S.Z., Creely W., Gonzalez K., and Hinchee M.** 1999. *Arabidopsis* ovule is the target for *Agrobacterium in planta* vacuum infiltration transformation. *Plant J.* 19:249-257.
- Yoshioka K., Moeder W., Kang H.G., Kachroo P., Masmoudi K., Berkowitz G., and Klessig D.F.** 2006. The chimeric *Arabidopsis* cyclic nucleotide-gated ion channel 11/12 activates multiple pathogen resistance responses. *Plant Cell* 18:747-763.
- Zheng J.Q.** 2000. Turning of nerve growth cones induced by localized increases in intracellular calcium ions. *Nature* 403:89-93.
- Zheng Z.L. and Yang Z.** 2000. The Rop GTPase switch turns on polar growth in pollen. *Trends Plant Sci.* 5:298-303.
- Zimmermann P., Hirsch-Hoffmann M., Hennig L., and Gruissem W.** 2004. Genevestigator. *Arabidopsis* microarray database and analysis toolbox. *Plant Physiol.* 136:2621-2632.
- Zufall F., Shepherd G.M., and Barnstable C.J.** 1997. Cyclic nucleotide gated channels as regulators of CNS development and plasticity. *Curr. Opin. Neurobiol.* 7:404-412.

## 8 Acknowledgements

First I would like to thank my Ph.D. advisor Prof. Dr. Jeffrey F. Harper for giving me the opportunity to join his lab and work on such an exciting project. Jeff, I would like to thank you for all your advice and extraordinary support over the entire thesis. Thank you for your guidance and sharing your tremendous expertise. I especially appreciate your understanding and support during my time at UCSD and the warm welcome to your family during my stays in Reno.

I am very thankful to my second advisor PD Dr. Stefan Binder for supporting a Ph.D. thesis in the United States. Stefan, without you it would never have been possible for me to start a Ph.D. research project in the US. I truly appreciate your support and advice over the past years.

I would like to thank Prof. Dr. Julian I. Schroeder to give me the opportunity to finish my thesis in his lab at the University of California, San Diego after the relocation of the laboratory of Prof. Harper to the University of Nevada, Reno. Julian, thank you so much for your advice and generous support as well as for opening a door to electrophysiological experiments and cameleon imaging.

I am very grateful to my entire thesis committee. My special thanks go to Prof. Dr. Axel Brennicke for revising this thesis and for our wonderful meetings in Ventura.

I would like to thank all my collaborators: Dr. Yongfei Wang for his tedious and never ending new ideas on how to measure a  $\text{Ca}^{2+}$  current in pollen; Matthias Gehl and Chris Sladek for running the ICP and helping with the analysis of the ion profiling results; Lisbeth Rosagar, Dr. Nadia Robert and Dr. Catherine Chan for providing some of the *cngc* gene disruption lines; Dr. Josef Kuhn for helping with the yeast complementation assay. For technical support, I would like to thank the : Greta Granstedt, Kathy Truong, Citlali Villalobos and Cyrus Dadachanji.

A big thank you goes to all present and former members of the Harper and Schroeder labs for creating such a friendly and funny lab environment. Thank you for all the exciting scientific discussions and for sharing your little tricks that make the bench work so much easier. Especially, I would like to acknowledge Shawn Romanowsky for insights on his view on pollen biology and for helping me taking my first steps in the “world of pollen”. Also, I would like to thank our lunch groups both at Scripps and UCSD for the great time together that gave me the perfect balance to the work in the lab.

I would like to thank Prof. Dr. Laurie Smith and her lab for sharing their knowledge on confocal microscopy as well as Prof. Dr. Yunde Zhao for providing a darkfield stereomicroscope.

Josef, I would like to thank you for going on this journey to San Diego together with me and for giving me strength and support in any situation. I highly evaluate not only your scientific advice. I'm in deep thank for your understanding and putting up with me during this thesis. Josef, I would like to dedicate this thesis to you.

I'm also very indebted to family, who awakened my scientific curiosity by showing me the wonders of nature. Thank you for your personal and financial support over all these years that finally made it possible to pursue a Ph.D. thesis in San Diego.

My final thanks go to Boehringer Ingelheim Fonds not only for the generous financial support but also for welcoming me to the “BIF-family”.

## 9 Appendix

### 9.1 Abbreviations

ABA	abscisic acid
ACA9	autoinhibited calcium ATPase 9
AKT1	<i>Arabidopsis</i> K <sup>+</sup> transporter
ARR5	<i>Arabidopsis</i> response regulator 5
AlcA	ethanol responsive element
AlcR	ethanol inducible transcriptional activator
BAC	bacterial artificial chromosome
CaM	calmodulin
cAMP	cyclic adenosine monophosphate
cDNA	copy DNA
cGMP	cyclic guanosine monophosphate
CNGC	cyclic nucleotide-gated channel
cNMP	cyclic nucleotides
crk	crinkle
DIC	differential interference contrast microscopy
DR5	mutations in the 5' end of the smallest composite (D1-4) of the auxin response promoter element
ER	endoplasmatic reticulum
EMS	ethane methyl sulfonate
FRET	Fluorescent Energy Transfer
GABA	γ-amino butyric acid
GFP	green fluorescent protein
GUS	β-glucuronidase
hap	hapless mutants
ICP	inductively coupled plasma spectroscopy
KAT1	K <sup>+</sup> channel from <i>Arabidopsis thaliana</i>
kip	kinky pollen
LAT52	anther specific gene from tomato ( <i>Lycopersicon esculentum</i> )
mRNA	messenger RNA

---

MS	Murashige and Skoog
PCR	polymerase chain reaction
POP2	unknown name, gene encodes a GABA transaminase
ps#	plasmid stock number
<i>qrt</i>	<i>quartet</i>
RIC	ROP-interactive CRIB-containing proteins
RFP	red fluorescent protein
ROP	Rho family GTPase
RT-PCR	reverse transcription polymerase chain reaction
SPIK1	Shaker Pollen Inward K <sup>+</sup> channel
ss#	seed stock number
TPK4	tandem pore K <sup>+</sup> channel
TL#	seed line number in the laboratory of Prof. Dr. Jeffrey Harper
T-DNA	portion of the Ti (tumor-inducing) plasmid that is transferred to plant cells
T1	first generation after transformation
T2	second generation after transformation
<i>vgd</i>	<i>vanguard1</i>
WT	wild-type
X-Gluc	5-bromo-4-chloro-3-indolyl β-D-glucuronide cyclohexylamine salt
YFP	yellow fluorescent protein
(-/+)	heterozygous
(-/-)	homozygous
(-?)	T-DNA border confirmed

## 9.2 Isolated T-DNA disruption lines

Name	AGI	T-DNA number	ss#	eco-type	insertion site	LB	primers
<i>cngc1-1*</i>	At5g53130	SAIL_443_B11	94 (-/-)	Col	unknown	unknown	680a,b; 638-640
<i>cngc2-2<sup>t</sup></i>	At5g15410	WISC collection	57 (-/-)	WS	intron 4	unknown	797a,b LB
<i>cngc2-3</i>	At5g15410	SALK_018387	190 (-/-), 601 (-/-)	Col	intron 1	3'→5'	930, 797b, 792
<i>cngc2-4</i>	At5g15410	SALK_028773	145 (+/-)	Col	350bp upstream of ATG	5'→3'	930, 797b, 792
<i>cngc3-1</i>	At2g46430	SALK_056832	318 (-/-)	Col	exon 3	5'→3'	798a,b; 792
<i>cngc3-2</i>	At2g46430	SALK_066634	319 (-/-)	Col	intron 3	5'→3'	798a,b; 792
<i>cngc4-1<sup>+</sup></i>	At5g54250	SALK collection	602 (-/-)	Col	intron 6	5'→3'	865a,b; 792
<i>cngc4-2</i>	At5g54250	SALK_081369	in progress, TL#9022-30	Col	intron 2	3'→5'	865a,b; 792
<i>cngc5-2</i>	At5g57940	SALK_014991	143 (-/-)	Col	50bp upstream of ATG	3'→5'	794, 681b, 792
<i>cngc5-4</i>	At5g57940	SALK_149893	859 (-/-), 866 867 (-/+)	Col	exon 5	5'→3'	703e, 681b, 792
<i>cngc6-1</i>	At2g23980	SALK_042207	144 (-/-)	Col	intron 2	3'→5'	796a,b; 792
<i>cngc6-2</i>	At2g23980	SALK_064702	320 (-/-)	Col	last exon	5'→3'	854a,b; 792
<i>cngc7-1</i>	At1g15990	SAIL_59_F03	831 (-/-), 832 833 (-/+)	Col	exon 1	5'→3'	682a,b, 638, 682b
<i>cngc7-3</i>	At1g15990	SALK_060871	860 (-/-), 864 865 (-/+)	Col	exon 1	3'→5'	929, 682b, 792
<i>cngc8-1</i>	At1g19780	Gabi 101	600 (-/-)	Col	intron 3	3'→5'	960a,b; 958
<i>cngc9-1</i>	At4g30560	SAIL_309_D03	604	Col	exon 6	5'→3'	679a,b; 640
<i>cngc9-2</i>	At4g30560	SAIL_736_D02	187 (-/-), 577 (-/+ 3x backcross.)	Col	35 bp upstream of ATG	5'→3'	846a,b; 640
<i>cngc9-4</i>	At4g30560	SALK_026086	574 (-/-)	Col	intron 5	3'→5'	884g,b; 792
<i>cngc10-1</i>	At1g01340	SALK_015952	321 (-/-)	Col	exon 7	5'→3'	855a,b; 792
<i>cngc11-1*</i>	At2g46440	JP72_0E08L	124 (-/-)	Col	unknown	unknown	678a,b, 792
<i>cngc11-2</i>	At2g46440	SAIL_165_A02	189 (-/-)	Col	intron 3	5'→3'	678a,b, 638
<i>cngc11-3*</i>	At2g46440	SALK_048183	146 (-/-)	Col	intron 1	5'→3'	795, 678b, 792
<i>cngc11-4</i>	At2g46440	SALK_026568	606 (-/-)	Col	intron 7	3'→5'	678a,b; 792
<i>cngc12-2</i>	At2g46450	SALK_092657	607 (-/-)	Col	intron 4	5'→3'	718a,b; 792
<i>cngc12-3</i>	At2g46450	SALK_092622	608 (-/-)	Col	exon 7	5'→3'	718a,b; 792
<i>cngc13-1*</i>	At4g01010	SALK_013536	133 (-/-), 327 (-/-), 580 (-/-)	Col	intron 3	5'→3'	762a,b; 792
<i>cngc13-2</i>	At4g01010	SALK_060826	322 (-/-), 598 (-/-)	Col	exon 3	3'→5'	762a,b; 792
<i>cngc14-2</i>	At2g24610	DsLox437E09	669-671 (-/-), 672 (-/+)	Col	intron 1	3'→5'	998b,c; P745
<i>cngc15-3<sup>+</sup></i>	At2g28260	CS93507 (EMS)	768 (-/-)	Col er 105	438aa, Stop	n.a.	675a,b
<i>cngc16-1*</i>	At3g48010	SAIL_232_B12	95 (-/-), 96 (-/+)	Col	exon 3	3'→5'	676a,b; 640
<i>cngc16-2*</i>	At3g48010	SAIL_726_B04	91 (-/-) 92 (-/+)	Col	exon 3	3'→5'	676a,b; 640
<i>cngc17-2*</i>	At4g30360	SALK_041923	147 (-/-)	Col	exon 6	5'→3'	785a,b; 792

Name	AGI	T-DNA number	ss#	eco-type	insertion site	LB	primers
<i>cngc18-1</i>	At5g14870	SAIL_191_H04	130 (-/+), 578 (-/+, 2x backcross.)	Col	exon 5	5'→3'	886g,hr; 640
<i>cngc18-2</i>	At5g14870	GABI_052_H11	599 (-/+), 656 (-/+), 760 (-/+, 2x backcross.)	Col	exon 1	3'→5'	g: 886a,dr; 958
<i>cngc19-1</i>	At3g17690	SAIL_757_E05	131 (-/-)	Col	exon 8	5'→3'	691a,b, 638- 640
<i>cngc19-2</i>	At3g17690	SALK_007105	188 (-/-)	Col	intron 2	3'→5'	691a,b; 792
<i>cngc19-3</i>	At3g17690	SALK_027306	564 (-/?), 861-863(-?)	Col	exon 10	3'→5'	691a,b; 793
<i>cngc20-1</i> <sup>+</sup>	At3g17700	SALK_129133	769 (-/-)	Col	exon 4	3'→5'	938a,b; 792
<i>cngc20-2</i>	At3g17700	SALK_074919	in progress, TL# 9031- 9038	Col	two left borders, intron 8 and exon 10	3'→5' (E8), 5'→3' (E10)	938a,b; 793

**Table A1: Isolated T-DNA disruption lines including:** The name of mutant line, AGI number of the disrupted gene, T-DNA number, seed stock number (ss#) and genotype (-/- = homozygous, -/+ = heterozygous, -/? = T-DNA border confirmed, TL# = seed line), ecotype, insertion site, direction of the left border relative to the open reading frame (LB, 5'→3' or 3'→5'), as well as the primers used to genotype the plants.

Lines that were provided by other people were indicated as follows:

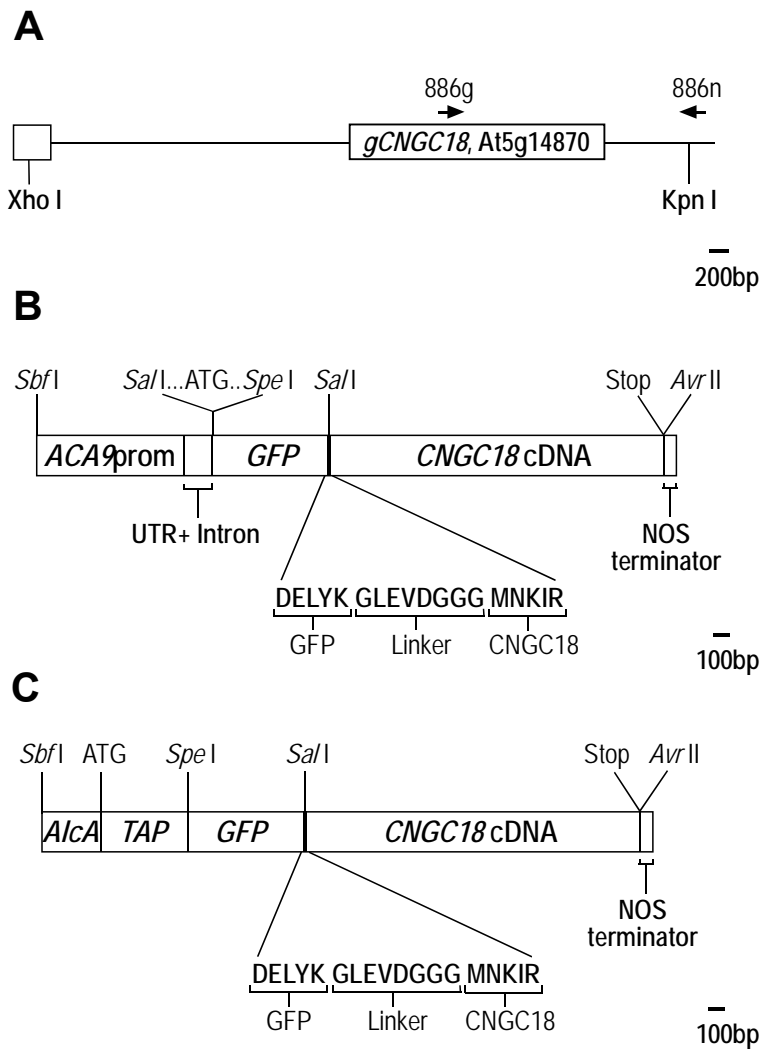
\* isolated by Lisbeth Rosagar prior to this thesis

<sup>+</sup> provided by Dr. Nadia Robert, University of California, San Diego, USA

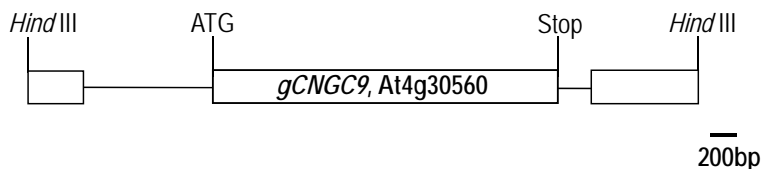
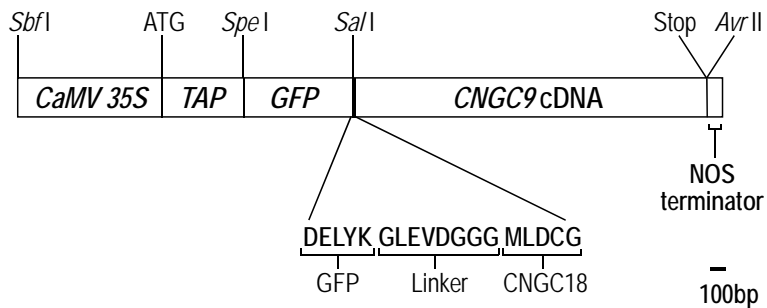
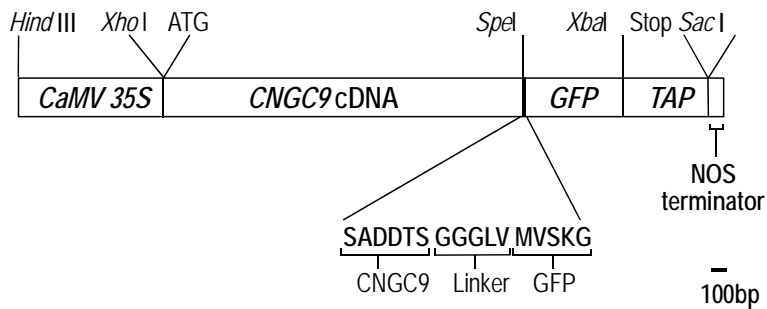
<sup>†</sup> provided by Dr. Catherine Chan, University of Wisconsin-Madison, Wisconsin, USA (Chan et al., 2003).

## 9.3 Plasmid maps and sequences

### 9.3.1 Maps of selected constructs



**Figure A1: Diagram of plasmid *gCNGC18*, *ACA9promoter::i-GFP-CNGC18* and *AlcA::TAP-GFP-CNGC18*.** (A) Diagram of the insert in *gCNGC18* (ps# 632) containing a 6.88 kb genomic fragment subcloned as a *Kpn* I and *Xho* I fragment from the Bacterial Artificial Chromosome (BAC) T9L3 (Choi et al., 1995). Complementation in *cngc18-1* mutants transformed with *gCNGC18* was analyzed by PCR-based genotyping of the F2 progeny using the primers 886g, 886n, and 640. □ = coding sequence, - = non-coding sequence, → = position of the primers used. (B) Diagram of the insert in *ACA9promoter::i-GFP-CNGC18* (ps# 855) including key restriction sites, the start (ATG) and stop codon. The protein sequence of a linker between *GFP* and the *CNGC18* cDNA is shown at the bottom. Complementation of *cngc18-1* mutants transformed with *GFP-CNGC18* was established in the F2 progeny after transformation by segregation and PCR analysis using the primers 886k, 886c, and 640. (C) Diagram of the insert in *AlcA::TAP-GFP-CNGC18* including key restriction sites, the start (ATG) and stop codon. The protein sequence of a linker is shown at the bottom. Plants transformed with *AlcA::TAP-GFP-CNGC18* require co-transformation with *LAT52promoter::AlcR* (ps# 845) to establish ethanol inducible expression of *TAP-GFP-CNGC18*.

**A****B****C**

**Figure A2: Diagram of plasmid *gCNGC9*, *N-TAP-GFP-CNGC9* and *CNGC9-GFP-TAP*.** (A) Diagram of the insert in *gCNGC9* (ps# 633) containing a 5.27 kb genomic fragment subcloned as *Hind* III fragment from the Bacterial Artificial Chromosome (BAC) *F23I17* (Mozo et al., 1998). □ = coding sequence, - = non-coding sequence. (B) Diagram of the insert in *N-TAP-GFP-CNGC9* (ps# 790) including key restriction sites, the start (ATG) and stop codon. The protein sequence of a linker between *GFP* and the *CNGC9* cDNA is shown at the bottom. (C) Diagram of the insert in *CNGC9-GFP-TAP* (ps# 776) including key restriction sites, the start (ATG) and stop codon. The protein sequence of a linker between *CNGC9* and *GFP* is shown at the bottom of the diagram.

### **9.3.2 Sequence information of the CNGC18 plasmids used provided as a fasta format text file**

### Figure A3: Plasmid gCNGC18 (ps# 632)

**Figure A4: Plasmid CNGC18promoter::GUS (ps# 827).**

```
> ACA9promoter::i-GFP-CNGC18
TTTATCCCGGAAAGCCTGGTAGAGGGTAGTTACGTGAAACCGCTAATGCCGAAAGCCTGATTACGGGCTTCGGCCGCTCCAAA
CTACCGCTGAAATCGCTAACGGTAGCTGAATCGCTAACGGTAGCTGAATCCATAAGCTCACGTAAATCGTAATCAAAAGGCACGTG
GAACGCTAACGCCCTTCAGATCAACAGCTGCAAACACCCCTCGCTCCGCAAGTAGTTACAGCAAGTAGTTACGCTTCATTAGCTTCA
ATTAGCTTAATTATGGTCGCCCTGGCTGGACAATGCGTCAGCGCACCCGCTGCCGGCTGGACAACCGCAAGCGGTTGCCACCGTCAG
GCCGCGCAGCTGGCCCAACGCCGGCCGCCGCCGCCAACAGATCTTATAAAATTTTTTTAAAGAAAAGAACGGCGAACCTCTGGCTTCTGG
ATTTGGCATCCCGGAATTAGAGATCTGGCAGGATATTGTTGTTGTAACGTTATCGATCTGGATTAGCTGGATTGTTAGGAATTAGAAATT
TTGTTAGAAGATTTACAAATACATAACTAAAGGGTTCTTATATGCTAACACATGAGCGAAACCTATAAGAACCTTAATTCCTGGAAACTACT
ACACATTATTGAGAAAAATAGAGAGATACTGGAGAGACTGGATTTGAGAGAGACTGGTAGCTGGCAGCTACGGAATTAACTCCGGCAGAC
GGCGAACCTGGCTGAGCTGGCAGAACCTGGCCACCAAGCTGAAGCCCTTCTCGCATTGGCTGGAGCTGGCTGGAGCCGCTTCGAATACG
CTCTGGTGGCTGGCATCTACTTCTTGGCCCTCGAGACTGGCTGGGGCTCGTGGTCTTCCATATGGCAGACTTCTACACGGCATCGTCCAG
GGCCGGCGCTTCTGGCCGGATTGGTAGCCGGCAGACTGGCTGGGGCTCGGATCGGACGATTGGCTGCCATGACCCCTGCGCCAAGCTGCAT
CTGGCTGCAACGACTCTGGTAGAGCTGGGAGACCACTATACGGGGAGACTACAGCCGGAGCTGGCAGCTGGCTGAGCTCTGGCTGCAAG
TAGCCGCTCTGGCTGCTCATCACAGCAACACGGCTTCAAGAAGATGGTAGCTGGCAGACTTCTGGCTGAGCTCTGGCTGCAAGCTGG
ACCGCTGTTATGGCCGATTGCTGGTAGGGAGCGGAATCTGGCTGCAAGCAGGTGGCCGACTTCTGGCTGGAGCTGGCTGCGCCAAG
CTCATCGAGACCTGGCTGGCAGACTGGCTGGAGCTGGCTGAGCTGGGAGACTACAGCTGGCTGGAGCTGGCTGGAGCTGGCTGCGCCA
TAGTGTGTTAGTGGCCGATTGCTGGTAGGGAGCTGGCTGAGCTGGCTGAGCTGGCTGGAGCTGGCTGGAGCTGGCTGGAGCTGGCTG
CTCATCGAGACCTGGCTGGCAGACTGGCTGGAGCTGGCTGAGCTGGCTGGAGCTGGCTGGAGCTGGCTGGAGCTGGCTGGAGCTGGCTG
CTCATCGAGACCTGGCTGGCAGACTGGCTGGAGCTGGCTGAGCTGGCTGGAGCTGGCTGGAGCTGGCTGGAGCTGGCTGGAGCTGGCTG
```

**Figure A5: Plasmid ACA9promoter::i-GFP-CNGC18 (ps# 855).**

**Figure A6: Plasmid *A/cApromoter-TAP-GFP-CNGC18* (ps# 831)**

```
> LAT52promoter::AlcR
TTTTCACCGGAAACGGCTTGATAGAGGGTAGTTACCGTAAACCGCTAATGCCCGAACGCCCTGATTACGGGGCTTCCGGCCGCTCCAAA
CTATCACCGTAAACGTCTAATCAGGGTACGTAAACGCTAATCGGAGTACGTGAATCGTAAATCGTAATAGGTACCGTAAATCGCTAATCAAAAGGCACGTG
GAACGCTAATAGCCCTTCAGATCAACGCTTGCACCCCTCGCTCCGGCAAGTAGTTACAGCAAGTAGTATGTTCAATTAGCTTCAATTATGAAATAT
ATATCAATTATGGTCGCCCTTGGTGGACAATGCGCTACGGCAGCCGGCTCCGGCGAACACGGCAGGGTCCGCCACCGTCGAGGCCAGC
CTTGGCCCAACACGGCGGCCGGCGGCCAACAGATCTTATAAATTTTTTTAAAGAAAAGAACGGCGAACCTCTGGCTTCTGGAT
TTGGATCCCCGGAAATTAGATCTGGCAGGATATTGGTGTAAACGTTACGATCTGGATTAGTTAGTCTGGATTGTTTGGATTAGAAATTATTTG
ATAGAAGTATTACAAATACACTAACTAGGGTTCTTATATGCTCAACCATGAGCGAACCCCTATAAGAACCCCTAATTCTCCCTATCGGGAAACTACT
ACACATTATTATGGAAAAAGAGAGAGATAGTTGAGAGAGAGACTGGTATTGCTACCGCTACCGAATTAATTCTCCCGGACCAAGCGAGCAGCTTAG
GCAACTGTGGCAGGAGAAACTGGCCACCAAGCTGAAGGCCCTTCCTCGCTTGGCTAGGCTCCGGCAGGTGGCTGAGGCGCTTCGGAAATCT
CCTCTTCTGGCGCATCTACTTATCTTCTGGCTCCGGCAGACTGGCTGGGGCGCTGGTTTCAACTGGCAGGACTACTCTACACGCGCATGGTCCAGA
```

**Figure A7: Plasmid *LAT52*promoter::*AlcR* (ps# 845)**

### 9.3.3 Sequence information of the CNGC9 plasmids provided as a fasta format text file

AACTACGGCTACACTAGAAGAACAGTATTTGGTATCTGGCTCTGCTGAAGCCAGTACCTTCGGAAGAAGAGTTGGTAGCTCTGTGATCCGGAAACAAACCA  
CGCCTGGTAGCGGGTTTTTTGGTGCAGCAGCACAGATTACCGCAGAAAAAAAAGGATCTCAAGAAGATCCTTGTATCTCGGGCTGACGCTCAG  
TGGAAACAAAATCAGCTTAAAGGATTTGGTCTAGGATATTCAAAAGGATCTTCACTTAAAGGATCTTCACTTAAATTTAAAGTAAAGTGTAACTTAAAGT  
TATATGTGTAACATTGGTCACTGGTATTAGAAAATCTCGAGCATCAATGAAACTGCAATTATTCAATCAGGATTCAATACCATATTTTGAAAAGCCG  
TTTCTGTAAAGGAGGAAAACCTACCGGAGCGATCTCATAGGTAGGAGATCCTGGTATCGGCTGATCCGCAACATACACATACAACTTAA  
ATTTCCCTGGTCAAATAAGGTTTCAAGTGAGAATACCATGAGTGCAGCTGATCCGGTGAAGAATGGCAAAAGATTGTGATCTTCTTCAGACTTTG  
CAACAGGCCAGCCTTACGGCTGTCAAAATCACTCGCATCAACCAAACCGTTATTCTGGTAGTTGGCCTGAGGGAGACGAAAATACCGCATCGCTGTTA  
AAAGGAACTTACAACAGGAATCGAATGCAACCGGCGCAGGAACACTGGCAGCAGTCAACAAATTTACCTGGTAACTCTTCAATGAGGATCTTCAATCCTGGAA  
TGGCTGTTTCCCAGGATCCAGTGAGTAACCTGATCATCGAGGATCGGATAAAATGCTTGTGTCGGAAAGGGCATAATTCGGCAGGGCAGTT  
AGCTTGACCATCTCATCTGAACAAACTGGCAACGGCTACCTTGGCATGTTGAGAACAAACTGGCAGCATGGGCTTCCCATAACTGGTAGATTCTGGC  
ACCTGTAGGGCCGACATTACGGCAGGCCATTACCTGGATCATGTTGAGAACAAACTGGCAGCATGGGCTTCCCATAACTGGTAGATTCTGGC  
GGCTCATAACACCCCTGTATTACTGTGAAAGCAGACAGTTTATTGTTGTGATGATATTTTATCTGTGCAATGTAACATCAGAGATTGAGACACA  
ACGTTGGCTTGTGAAATAATCGAACTTCTGCTGAGTTGAAGGATCAGATCAGCGATCTCCCGACACGCAGGCTTGGCAAGGCAAAAGCTTCAAAT  
CACCAACTGGTCACCTACACAAAGCTCATCACCGCTGGCTCCCTACTTCTGGATGATGGGGGATTAGGGCAGTCCCGATCCCCATCCAACAGCCCG  
CGTCGAGCGGGCT

**Figure A8: Plasmid gCNGC9 (ps# 633)**

TTGGCGCTGAGGGAGACGAAATACCGGATCCTGTGAAAAGGACAATTAAACAGGAATCTGAACCCGGCGCAGGAAACTCGGCCAGCGTCAACAAAT  
ATTTCACCTGAATCAGGATATTCTCTAATACCTGGATCTGTTTCCCCTGGATCAGCTGGTGAACCATGCATCATCAGGAGTCGGATAAAATGCTT  
GATGGTCTGGAGAGGAGCATTAATTCGGTACCGGAGCTGGTACCTGACCATCTCATCTGAAACACATTGGCAACCGTCACCTTGGCATGTTCAAGAACAACTCTG  
AATCGCAGCGCCTGGCTCCCATACATCTGGTAGATTGGCAGCCTGGTACCTGGCAGGACATTACCTGGATTAATACATCAGCATCTGGATTAATT  
AATCGCAGCGCCTGGACAGGACTTCCCTGGTGAATATTGCTCATACAAACCCCTTGATTACTGTTATGAAAGCAGACTTATTGTCATGATGATATT  
TATCTGTGCAATGTAACATCAGAGATTGGAGACACACCTGGCTTGTGAAATAATCGAACTTTGCTGAGTTGAAGGATCAGATCAGCATCTCCGACA  
ACCGACAGCCTTCCTGGCAAAAGCTTCAAACACCAACTGGCTTGTGAAATAATCGAACTTTGCTGAGTTGAAGGATCAGATCAGCATCTCCGACA  
TGGGGCATTCAGGGCATCCATCCAAACAGCCGGCGCTGCAGCGGGCT

**Figure A9: Plasmid CNGC9promoter::GUS (ps# 826)**

GGAAAGCCTGGCGCTTCTCATAGCTCACGGTGTAGGTTATCTCGTTCGGTGAGGTCTGGCTTCAGCGAACCCCCCGTTAGCCCG  
GACCCTGCGGCCATTACCGCTAACATCTCGTTCGGTCAAGCTGGCCAAACCCGGTAAGACAGCAGCTTATCGCCACTGGCAGCAGCTGGTAACAGGATTAGCAGAGCG  
AGGTATGAGGGCTGCTACAGAGTCTTGAAGTGTGGCCAACTACGGCTTACAGAAGAACAGTATTGGTATCTCGGCTCTGGTAAGGAGCTTACCT  
TCGGAAGAAGAGTGTGGCTTCTGATCCGCAAAACACCCGGCTGTGGCAGGGTTTTTTGTTGAAAGCAGCAGATTACCGCGAGAAAAAAAGGATC  
TCAGAAAGATCTTGTGATCTTCTACGGGGTCAAGGCTCACTGGTAAGGAGTTTGTCTAGTGGATGATGATCTTACAAAAGGGATCTTACACCA  
GATCTTAAATTTAAAGTAAAGTAAATCAATCTAAAGTATATGTGTAAACATTGGTAGTGTGATTAGGAAACACTCATCGAGCATCAAATGAAACTGCAATT  
TATTCTATCATAGGATTATCAACATATTGGAAAGGGCTTCTGTAACTGAAGGAGAAACCTACGGCAGGCTTCATAAGGATGCCAGATCTGGTATC  
GGCTCGGATTCGGCTACCTGTCACATCAACAACTATTAACTTCTCTGGTCAAAATAAGGTTTATCAAGTGGAGAAACCATGATGCGACTGAATTC  
GGTGAGAATGGCAAAGTTATGCATTCTTCAGACTTGTCAACAGGCCAGCATTACGCTCGTCAAAATCACTCGCATCAACCAACCGTTATTCA  
CGTGTGGCTGAGGCCAGGAGCAGAACATCGCGATCTGGTAAAGGACAACTAACACCGAATCTGAATGGCAGGCGCAGGAACTCGGCCATCA  
ACAAATTTCTCTGGTCAACGGATATTCTTCAAACTGGGAATCTGGTGTGTTTCTCTGGATCTGGCAGTGGTAGTAAACCTGATCATCAGGAGTACGGATAAA  
TGTGTTGATGTCGGAAAGGGCATAAATTCTGGTCAACGGCAGCTTGTAGTCTGACCATCTCATCTGGTAACAAACATTGGCAACCTGACCTTCTGGCATGAAACAA  
CTCTGGCCATCGGGCTTCCATACATGGTAGATGTCGACCTGATTGGCCGACATTATCGCAGGCCATTATACCCATATAACGATCATCTGGTGG  
ATTTTATCGGGCTTCTGACCAAGGCTTCCGGTGTGGATATGGCTCAACACCCCTTGTGTTACTGTGTTATGAGCAGACGATTTTGTCTAGTGTATA  
ATTTTTATCTTGTGCAATGAAACATCAGAGATTGAGACACACAGTGGCTTGTGGTAATAATCAGAATTTGCTGAGTTGAAGGATCAGATCAGCGATCTTCC  
CGACAACGGCAGACGGCTGGCAAGGCAAAGGTCAAACCAACTGGTCACCTACACAAAGCTCATCAACCGTGGCTCCACTTCTGGCT  
GATGATGGGGGCGATTAGGGCATCCACAGCCGGCTGAGCGGGCT

**Figure A10: Plasmid *N-TAP-GFP-CNGC9* (ps# 790)**

**Figure A11: Plasmid CNGC9-GFP-TAP (ps# 776)**

## 9.4 Publications

### 9.4.1 Publications

**Sabine Frietsch**, 2002, Characterization of cyclic nucleotide gated channels regulating  $\text{Ca}^{2+}$  oscillations in *Arabidopsis*, *Boehringer Ingelheim Fonds Futura*, 17:225

Heven Sze, **Sabine Frietsch**, ·Xiyan Li, · Kevin W. Bock, Jeffrey F. Harper, 2006, Genomic and molecular analyses of transporters in the male gametophyte, *Plant Cell Monogr.*, Springer-Verlag Berlin Heidelberg, *in press*

**Sabine Frietsch**, Julian I. Schroeder, and Jeffrey F. Harper, 2006, A cyclic nucleotide-gated channel essential for polarized tip-growth of pollen, *manuscript in preparation*

### 9.4.2 Oral presentations

*13<sup>th</sup> International Workshop on Plasma Membrane Biology, 2004, Montpellier, France*, Genetic evidence for essential calcium transporters in pollen growth and fertilization.

*5<sup>th</sup> North America Meeting of Boehringer Ingelheim Fonds, 2004, Woods Hole, MA, USA*, Reverse genetics to characterize the role of cyclic nucleotide-gated channels (CNGC) in plant development.

*Science get it across, Communication Workshop, 2005, Cold Spring Harbor, USA*, Calcium signaling during pollen germination and fertilization in *Arabidopsis thaliana*.

*San Diego Center for Molecular Agriculture Meeting, 2006, San Diego, USA*, A cyclic nucleotide-gated channel essential for polarized tip-growth of pollen.

### 9.4.3 Posters

**Sabine Frietsch**, Morton Schiøtt, Shawn M. Romanowsky, Michael G. Palmgren and Jeffrey F. Harper: Genetic evidence for essential calcium transporters in pollen growth and fertilization. *13<sup>th</sup> International Workshop on Plasma Membrane Biology, 2004, Montpellier, France*.

**Sabine Frietsch**, Morton Schiøtt, Shawn M. Romanowsky, Michael G. Palmgren and Jeffrey F. Harper: Genetic evidence for essential calcium transporters in pollen growth and fertilization. *15<sup>th</sup> International Conference of Arabidopsis Research, 2004, Berlin, Germany*.

## 9.5 Deutschsprachige Zusammenfassung

Dynamische Änderungen der zytosolischen Ionenkonzentrationen sind wichtige Komponenten in einer Vielzahl von Signaltransduktionswegen in allen Eukaryoten. In Pflanzen sind die zu Grunde liegenden Ionentransporter und ihre physiologische Bedeutung jedoch weitestgehend unbekannt. In der Modellpflanze *Arabidopsis* gibt es über 350.000 Mutanten, in denen die genomische DNA und damit auch häufig codierende Bereiche von einer sogenannten T-DNA aus *Agrobacterium* unterbrochen wird. Im Rahmen dieser Arbeit wurden verschiedene T-DNA Insertions-Linien für alle 20 *Cyclic Nucleotide-Gated Channels (CNGC)* aus *Arabidopsis* isoliert. Verglichen mit Wildtyp Pflanzen zeigen sieben Mutanten unterschiedliche Phänotypen unter abiotischen Stressbedingungen. Der primäre Fokus der durchgeführten Analysen lag auf der Charakterisierung der männlich sterilen *cngc18* und der *cngc9* Mutanten, die hypersensitiv auf  $\text{Ca}^{2+}$  reagieren.

Genetische Analysen von zwei unabhängigen *cngc18* Mutanten zeigten, dass die T-DNA Insertion in *CNGC18* durch den männlichen Gametophyten nicht vererbt werden kann. Damit wurde zum ersten Mal ein CNGC aus Pflanzen oder Tieren identifiziert, dessen Funktion für die Vollendung des Lebenszyklus essentiell ist. Zellbiologische Analysen zeigten, dass Pollen von *cngc18* Pflanzen keimungsfähig sind, jedoch starke Wachstumsdefekte aufweisen. Diese Defekte äußerten sich durch kurze, stark gekrümmte, scheinbar orientierungslose Pollenschläuche, die oft nach kurzem Wachstum aufplatzen. Histochemische Analysen eines GUS- Reportergens, das in der T-DNA von *cngc18-1* Pflanzen kodiert ist, zeigten, dass *cngc18* Pollenschläuche nicht in das Griffelgewebe des weiblichen Gynoecium einwachsen können. Da andere bereits bekannte Mutationen in Ionentransportern wie *ACA9* oder *SPIK1* nur partielle Pollenwachstumsdefekte aufweisen, ist dies das erste Beispiel eines Kationenkanals mit einer essentiellen Funktion während der Regulation des Spitzenwachstums von Pollenschläuchen. Studien zur subzellulären Lokalisation eines GFP-CNGC18 Fusionsproteins in komplementierten *cngc18-1* Pflanzen

zeigten asymmetrische Lokalisation an der wachsenden Spitze des Pollenschlauches, die mit einer Plasmamembranlokalisierung korreliert. Diese polarisierte Lokalisation konnte auch unmittelbar nach der Pollenkeimung beobachtet werden, nachdem sich eine kleine Ausbuchtung bzw. kleine Pollenschlauchspitze am hydrierten Pollenkorn gebildet hatte. Aus diesen und vorherigen Beobachtungen ergibt sich die Arbeitshypothese, dass CNGC18 einen  $\text{Ca}^{2+}$  permeablen Kanal darstellen könnte, der von zyklischen Nukleotiden (cNMP) und  $\text{Ca}^{2+}$ /Calmodulin ( $\text{Ca}^{2+}/\text{CaM}$ ) reguliert wird und damit die beiden regulatorischen Signaltransduktionswege miteinander verbindet.

*cngc9-2* Mutanten reagieren auf eine erhöhte  $\text{Ca}^{2+}$  Konzentration im Wachstumsmedium, indem sie verglichen mit Wildtyp Pflanzen zunächst verzweigt, kurvige und desorientiert wirkende Wurzeln bilden. Wenige Tage später kann in *cngc9-2* Pflanzen die Entwicklung von Kallus-ähnlichem Gewebe in Spross und Wurzeln beobachtet werden. Die Bildung von kallösem Gewebe ist eine natürliche Entwicklung, die hauptsächlich durch Bakterien und Insekten durch lokale Veränderungen des Hormonhaushaltes von Auxin und Cytokininen, hervorgerufen werden. Die  $\text{Ca}^{2+}$ -induzierte Kallusbildung in *cngc9-2* Pflanzen deutet entweder auf veränderte Hormonspiegel hin oder auf einen Defekt in der Signaltransduktionskaskade der Pflanzenhormone Auxin und/oder Cytokinin. Die Sequenzierung des Überganges der T-DNA in das CNGC9 Leseraster und RT-PCR Experimente zeigen, dass die T-DNA Insertion in der Promotorregion in CNGC9 zu gesteigerten Transkriptmengen führt. Erhöhte CNGC9 Transkripte können auch eine  $\text{Ca}^{2+}$  Akkumulation in *cngc9-2* Pflanzen erklären, die  $\text{Ca}^{2+}$  Stress während ihres Wachstums ausgesetzt waren. Weitere Experimente sind notwendig, um die Rolle von CNGC9 während der pflanzlichen Entwicklung zu bestimmen.

Die im Rahmen dieser Arbeit erzielten Ergebnisse zeigen, dass ein Cyclic Nucleotide-Gated Channel essentiell für die Regulierung des Spitzenwachstums von Pollenschläuchen ist und legen eine physiologische Rolle eines anderen CNGC im Hormonhaushalt von Pflanzen nahe. Zusammenfassend weisen diese

Ergebnisse auf eine weitreichendere Rolle von CNGCs in der pflanzlichen Entwicklung hin als bisher angenommen.

### **Erklärung**

Ich versichere hiermit, dass ich die vorliegende Arbeit selbstständig angefertigt habe und keine anderen als die angegebenen Hilfsmittel und Quellen benutzt sowie wörtlich oder inhaltlich übernommene Stellen als solche kenntlich gemacht habe.

Ulm, den 13. März 2006



Sabine Frietsch